Stony Brook University

Thermal Homeostasis in Buildings (THiB):

Radiant conditioning of hydronically activated buildings with large fenestration and adequate thermal mass using natural energy for thermal comfort

A Dissertation Presented

by

Peizheng Ma

to

The Graduate School

in Partial Fulfillment of the

Requirements

for the Degree of

Doctor of Philosophy

in

Mechanical Engineering

(Thermal Sciences and Fluid Mechanics)

Stony Brook University

May 2013

Stony Brook University

The Graduate School

Peizheng Ma

We, the dissertation committee for the above candidate for the

Doctor of Philosophy degree, hereby recommend

acceptance of this dissertation.

Lin-Shu Wang – Dissertation Advisor
Associate Professor, Department of Mechanical Engineering

John M. Kincaid – Chairperson of Defense
Professor, Department of Mechanical Engineering

Jon P. Longtin
Professor, Department of Mechanical Engineering

David J. Hwang
Assistant Professor, Department of Mechanical Engineering

Thomas A. Butcher – Outside Member
Professor, Brookhaven National Laboratory

This dissertation is accepted by the Graduate School

Charles Taber
Interim Dean of the Graduate School

Abstract of the Dissertation

Thermal Homeostasis in Buildings (THiB):

Radiant conditioning of hydronically activated buildings with large fenestration and adequate thermal mass using natural energy for thermal comfort

by

Peizheng Ma

Doctor of Philosophy

in

Mechanical Engineering

(Thermal Sciences and Fluid Mechanics)

Stony Brook University

2013

"Living" buildings, like living bodies, seek to maintain stable internal environments while the external surroundings keep on changing. In biology, the "stable internal environment" is called homeostasis. This dissertation focuses on thermal homeostasis in buildings. In a homeostatic building, adequate thermal mass is applied to keep indoor temperature varying within a small range; natural energy is harnessed to maintain indoor temperature at a comfortable level using lower-power equipment (lowPE); hydronic radiant conditioning system is employed to distribute heat or coolness effectively to avoid

over-heating or over-cooling; and large fenestration is designed for aesthetics, natural lighting and solar gain.

The design of homeostatic buildings is approached in interdependent but distinguishable two steps: *archi.engineering building's indoor air-mass partially homeostatic to be within an acceptable temperature range* without equipment, and *maintaining the building fully homeostatic to be at a comfortable temperature level* with lowPE or off-peak mechanical equipment. This new process design philosophy replaces the conventional heat balance design philosophy of *engineering building's indoor air to be at a fixed temperature*.

The new design philosophy is applied to a TABS (thermally activated building systems)-equipped office building-room using an RC (resistor-capacitor) model built in Matlab/Simulink. Everyone intuitively knows that a building's thermal resistance and its mass are the most important passive elements of its thermal-control system. However, common building codes make no provision for its mass. This inconsistency results from the static heat balance design philosophy. In the dynamic RC model, indoor temperatures are allowed to float within a range. Systematic study of building's structural thermal mass requirement leads to a new dynamic definition of the thermal envelope, which sets limit in minimum thermal mass and maximum WWR (window-to-wall ratio) for partially homeostatic buildings.

The use of TABS and thermal mass makes a partially homeostatic building possible to harness natural energy with lowPE, such as cooling tower. The favorable climatic conditions of using cooling tower are investigated to achieve full homeostasis in buildings. It shows that in seven selected cities the most favorable location is Sacramento, which has a largest diurnal temperature variation derived from the strong micro-climatic process of sea breeze. This finding argues that the changing "external environment" is not only a challenge but also an opportunity—the opportunity in how a partially homeostatic building can harness natural energy with lowPE to achieve full homeostasis.

Better than Sacramento, Paso Robles has a larger diurnal temperature swing in summers, which makes it one of the most favorite locations for homeostatic buildings. A stand-alone one-story south-facing small commercial building in Paso Robles is designed. Simulation confirms that the building is a good partially homeostatic building even with a very high WWR.

Thermal homeostasis in buildings is an example of sustainable technologies. The homeostatic conception makes a building into a harnessing system for a new kind of renewable "energy." Homeostasis in buildings and how it is engineered offer an opportunity of creating a new kind of man-made systems with ecological sustainability — a perfect revolutionary form and content for getting the green architecture movement lifting off.

Keywords: Thermal Homeostasis; Homeostatic Building; Building Hydronic Radiant Cooling; Building Energy Modeling; Resistor-Capacitor Model; Thermal Comfort; TABS; Thermally Activated Building Systems; Thermal Mass; Low-power Equipment; Natural Energy; Cooling Tower; Building Design; Heat Transfer; Heat Storage

To

My Mother, My Father,

My Wife and My Son

Table of Contents

List of Figures

List of Tables

Acknowledgements

I would like to express my deepest gratitude to my Ph.D. advisor—Professor Lin-Shu Wang, who guided me to do the research on thermal homeostasis in buildings. I thank him for his help, motivation and encouragement in these past five years. His creative passion, broad knowledge and insightful suggestions are priceless to my research now and will benefit me greatly in the future.

Many thanks to the members of my dissertation committee—Professor John Kincaid, Professor Jon Longtin, Professor David Huang and Professor Thomas Butcher, who reviewed my work in a short time and gave me many professional and useful suggestions.

I am very grateful to the faculty and staff of the department of Mechanical Engineering for their suggestions, help and support.

Thanks to the department of Mechanical Engineering and Stony Brook University for giving me the opportunity and financial support for doing the research.

I need to say thanks to the Optical Engineering group in the Data Capture Solutions division in Motorola-Solutions Inc. In the past two and a half years, I really learned a lot in the group. Particularly, I must say thanks a lot to my boss, David Shi, who helped me at my hardest time and provided me the position in the group.

I would like to express my sincere gratitude for all of my friends (too many to list here but you know who you are!) both in China and the United States for providing support and friendship that I needed. When life is tough, their friendship, kindness and support always come in time to help me conquer difficulties.

I am also thankful to my relatives for their support. Although they are half-of-the-earth away, I can feel the familial affection stronger with time passing by.

Most of all, I would like to thank my beloved family, to whom I dedicate this work, for their forever love. The selfless sacrifice and support of my parents is always the motivity of my progress. The constant love, understanding and encouragement of my wife, Nianhua Guo, make the experience of studying abroad easier, more pleasure and more precious. Life abroad is much harder, but she accompanies me and takes care of me all the time without a word of complaint. Last but not the least, special thanks to my son, for the happiness, as well as the troubles, given by him.

Chapter 1: Introduction

Like living bodies, living buildings (see *living building challenge*, [1.1] which is an international sustainable building certification program created in 2006) seek to maintain stable internal environments while the external surroundings keep on changing. In the field of biology, the "stable internal environment" is called **homeostasis**, which is defined in the Merriam-Webster Dictionary as "a relatively stable state of equilibrium or a tendency toward such a state between the different but interdependent elements or groups of elements of an organism, population, or group." In this dissertation, the concept of **Thermal Homeostasis in Buildings (THiB)**, which is inspired by the biological homeostasis, will be investigated.

1.1 Concept of building thermal homeostasis

1.1.1 Machine vs. organism

"A house is a machine for living in," famously asserted by the Swiss-born architect Le Corbusier. A building is of course a man-made thing and machines are the best example of man-made things. Willis H. Carrier's invention of air conditioning in 1911 was a perfect example of the Machine Age's reliance on devices (HVAC devices) as the solution to a problem, the problem of building conditioning (including cooling and heating). The over-use of mechanical solutions, rather than the design of buildings themselves, for building's thermal conditioning led in the 20th century to profligate energy consumption.

The "modernist" machine conception of a building, ironically, failed to appreciate the systems nature of the building. In the machine conception, "environmental control systems

tend to be treated rather like the Cinderella of architecture; given only the plainest clothes to wear, they are relegated to a back room to do the drudgery that maintains the elegant life-style of the other sisters: light, form, structure, and so forth," wrote Lisa Heschong in *Thermal Delight in Architecture*. [1.2] The elegance was only surface deep.

True elegance can only be achieved by returning architecture to its architectonic core. Architects always knew that a building was a *system*; they just got the wrong system to be their guiding metaphor: instead as a machine, a building should be conceived as an "organism," i.e., a building as a homeostatic system thermally.

Machine can be "static" (i.e., deterministically dynamic) and structure-oriented. An organism can never be static or inclusively represented by its structure; an organism is homeostatic (or, homeodynamic) and must be process-oriented. [1.3] Cells, like all living organisms, have to be understood in terms of processes reflecting their dynamic organizational interaction involving feedback loops. When a machine breaks down, a single cause for the breakdown can usually be identified; a machine that was otherwise in reasonably good condition is as good as new immediately after a faulty single component is replaced. In contrast, an organism, when it became ill and after the cause of its illness has been successfully treated, needs time to recuperate back to health because its illness is not simply a matter of a single cause but also a matter of the interconnectedness of the whole system—it takes time for a whole to get all the feedback loops well again even after the key issue is addressed.

The idea of organism as the metaphor of a building is not new: Frank Lloyd Wright was the most prominent of many architects who advocated organic architecture in the past and the current interest in global sustainability has led to strong current of a new organic architecture movement. "Organic architecture" is, however, often predominately associated with organic form as evident in the beautiful creation of one of most intriguing architects, Antoni Gaudi. Whereas true homeostatic architecture must be process-oriented, organic architecture is often structure- or form-oriented following the "dictatorship of the

eye" [1.4] design tradition of mainstream architecture. We argue below that true organic architecture must give greater role to processes and greater attention on how a building can be engineered architectonically.

1.1.2 Non-equilibrium thermodynamic (NET) existence in an ecosystem

A step in this direction has taken place with the argument that a building should be a system that shares the same thermodynamic principle with a human body system, one of the defining features of which is that it is hydronic. [1.5] This makes it possible to create an internal milieu for both kinds that are "independent" of their external milieu and at the same time they both have *need* of the external environment. Their need of the external environment is critical: machines have no such need, not a need of environment in its totality but only a need of input in the form of fuel-air and lubricant for instance. This is another reason why machines are the wrong metaphor for buildings.

The fact that a building and a living body are "independent" of their external milieu means that they exist in non-equilibrium thermodynamic (NET) states. Another kind of NET systems has been introduced by the Brussels School of Thermodynamics. A thing (animate and inanimate) in non-equilibrium state must, first suggested by Schrodinger, [1.6] extract "negentropy" from its surroundings for its survival. This preliminary picture has been rounded out by Prigogine, [1.7] the leader of the Brussels School, who argued for a constructive role of irreversibility in the form of *dissipative structures*—an inanimate dissipative structure produces large amount of entropy internally to maintain its structural order and at the same time dissipates produced entropy as outflow to the environmental sink in order to keep its low-entropy existence: like a beautiful palace among a sea of slum, not a pretty ecological picture of sustainability. Dissipative structures like machines have no need of external milieu in its totality either, but only a need of its negentropy, or its resources which are then consumed and converted into wastes discharged to it as a dump ground.

Neither machines nor dissipative structures are conceived with their co-existence in an ecological community in mind. Collection of individual buildings does not create automatically a dwelling place. [1.8] This can happen only if each building, unlike a typical man-made object such as a machine or a dissipative structure, is conceived to be a part of a dwelling place as a whole. The proposed building systems are different kind of man-made objects defined by their thermodynamic or homeostatic relationship with their external surroundings.

The thermodynamic principle that is relevant with the idea of "buildings collectively forming an ecological system" consists of three elements: (1) the Schrodinger-Prigogine principle of the constructive role of irreversibility (the destructive-constructive duality); (2) the critical role of *action* or *management* in the efficient use of irreversibility for constructive purpose; (3) ongoing irreversibility such as "an external environment that is in constant flux across time and space" is both a challenge and opportunity.

1.1.3 The challenge and opportunity of weather and climate

The ASHRAE Research Strategic Plan for 2010-2015's *Overview and Vision* stated, in one of the Technical Challenges (Goal 2), "energy reduction methods, systems and operations are highly dependent on the climatic conditions in which the building is located; this increases the complexity of developing energy design guides that capture dependence on climate and weather variability." [1.9] The architect J.M. Fitch put the matter this way, "The central paradox [challenge] of architecture [is] how to provide a stable, predetermined internal environment in an external environment that is in constant flux across time and space…" [1.10] It is of greatest interest—in this context—to recall the definition of milieu intérieur (a concept became known as *homeostasis*) for biological organisms defined by Claude Bernard (1865) as

> The living body, though it has need of the surrounding environment, is nevertheless relatively independent of it. This independence, which the organism has of its external

environment, derives from the fact that in the living being, the tissues are in fact withdrawn from direct external influences and are protected by a veritable internal environment which is constituted, in particular, by the fluids circulating in the body. [1.11: 4]

Fitch's central architectural paradox has long been resolved by living bodies in their evolutionary adaptation! What needs to be done is to make buildings not like machines but "living" buildings: "an external environment that is in constant flux across time and space" is both a challenge and an opportunity—the challenge is in how to achieve partial homeostasis in a properly-engineered building itself (without mechanical equipment), and the opportunity is in how such a building can harness natural temporal and spatial energy-gradient in its ambient environment, with equipment that only consumes small (low) power in order to achieve full homeostasis.

1.2 Steps of achieving thermal homeostasis in buildings

1.2.1 Thermally activated building systems: from air conditioning to radiant conditioning

Since ancient time (9,000 years ago) [1.12] up to 1911, the design of the physical building had been integral to meet thermal comfort for building occupants. This becomes true again today even with all the advanced energy-using devices available. As L.D.D. Harvey [1.13] noted, "the energy use of buildings depends to a significant extent on how the various energy-use devices are put together as systems, rather than depending on the efficiencies of the individual devices. The saving opportunities at the system level are generally many times what can be achieved at the device level …" The system thinking raises the question of what kind of heat transfer medium is best for building energy management. In an air-conditioned building, it is the indoor air that is being conditioned, not the building itself. Air is a poor choice as a heat transfer medium when it is compared to water; water is two-order-of-magnitude more effective than air. In hindsight, the 20th

century choice of air as the medium for conditioning was irrational, not only because it is a poor heat transfer medium, but also because it is a poor medium for thermally activating building mass. Therefore, the first decisive step of the system thinking application is the separation of the ventilation function of air from its cooling & heating function. The latter (cooling & heating function) is accomplished by using water for thermally activating building elements.

Instead of limiting a building's conditioning to conditioning air and consequently achieving thermal comfort by convective means alone, the new method of conditioning a building is by thermally activating building elements and consequently achieving thermal comfort radiantly as well as convectively (with the indirectly conditioned air). This latter method is called *radiant conditioning*.

Homeostatic or homeodynamic conception of buildings necessitates an engineering change in the building heat transfer medium from air, which has been the predominate medium in the 20th century after the invention of air conditioning by Willis Carrier, to water. "The tissues are in fact withdrawn from direct external influence and are protected by a veritable internal environment which is constituted by the fluids circulating the body" (Claude Bernard [1865]). Like all organisms maintaining homeostasis with blood (a liquid fluid) in their self-regulating circulatory system, a building system can be regulated efficiently with a liquid-fluid activated self-regulating circulatory system. A successful way of using water to activate building mass as thermal mass and to control and regulate indoor temperature *radiantly* through water-activated mass-surface was proposed in 1993 by Meierhans, [*1.14*] a Swiss engineer. Typically, the building mass is a concrete slab of floor, or ceiling, or wall of about 0.25 m (10 inches) thick. PEX pipes, whose diameter varies between 17 and 20 mm, are embedded in the middle of the slab. The distance between pipes is in the range of 150 to 200 mm. The thermally activated slabs are known as *thermally activated building systems* (TABS) [*1.15*] for radiant conditioning, which with dedicated outdoor air systems (DOAS) for air-quality & moisture control is widely viewed

to be a best path toward carbon neutrality in building sector [1.15]. Numerous commercial buildings constructed on the design basis of the TABS concept since 1993 have proven the viability of the concept and that TABS achieves much lower life-cycle cost without high initial cost barrier. "In Switzerland and Germany… TABS have [even] become a kind of state of the art." [1.16]

Water carrying pipes embedded in slabs are part of TABS and serve as the core of the self-regulating circulatory network. During the summer time a sufficiently large TABS thermal mass enables the daytime indoor temperature to remain within comfortable range without having water to be continuously chilled. It is then possible to use off-peak power or natural energy gradient to cool water in the nighttime for recharging the thermal mass back to a desirable morning temperature.

The inclusion of TABS in a building is a necessary step towards homeostatic building. "The human body is a hydronic, thermally active surface system. Heat energy is transferred in and around a body through the hydronic circulatory system. The heart circulates heat through the blood back and forth between the core of the body to its skin, a thermally active surface. Its thermal system is decoupled from its ventilation system. Thermally active surfaces in buildings follow this logic, literally. This alters energy consumption and amends human comfort. Thermally active surfaces in buildings are not metaphors for the body and do not mimic a natural system. Rather, they share the same thermo-dynamical system," argued compellingly the architect Kiel Moe [1.5]. TABS in itself, however, is not sufficient for making a building homeostatic.

Two notable TABS-based buildings in North America are California Academy of Sciences completed in 2008 and Hearst Tower in New York City completed in 2006. They are outstanding examples of energy efficient, radiantly-conditioned buildings with water-activated mass, which replace air fan power with much smaller water pump power and use lower cost "off-peak power" for cooling and heating equipment. Both are examples of energy efficiency in equipment power. However, neither building seizes the

full opportunity of building design possibility that TABS-radiant conditioning offers in achieving energy efficiency in systems approach—to power the "self-regulatory circulatory system" with *natural energy gradient* in the environment such as day-night temperature variation and day-night solar insolation variation. Therefore, beautiful though these two buildings are, they are not the best cases to highlight homeostatic architecture in its best light.

1.2.2 Partial homeostasis: synergy of thermal mass and high-performance envelope

A common misconception is that radiant heating requires high temperature source, or radiant conditioning requires large temperature difference (or gradient). The fact is exactly the opposite: "The radiant heating and cooling system supply water temperature would typically operate at a temperature [set points of] *less* than 180 °F for heating and *greater* than 45 °F for cooling, which [180 °F, 45 °F] are typical supply water temperatures for a traditional forced air system. The central-plant heating and cooling equipment can operate more efficiently at these temperature set points." [*1.17*] This is because a radiantly conditioned space is enclosed by a large area of activated surfaces and the fact that heat exchange is dependent on the product of the area and the temperature difference — the latter can be small for meeting a required heat exchange if the former (the surface area) is large.

To derive energy efficiency in systems approach, radiantly conditioned buildings require, in addition to large TABS thermal mass, a good-performance envelope, a well-known fact but one that has not been systematically studied. A recent paper of ours carries out the systematic, quantitative determination of the functional relationship of building indoor operative temperature in terms of activated thermal mass and envelope thermal resistance. [*1.18*] The finding of the paper is that the effectiveness of TABS radiant cooling in maintaining sufficiently narrow operative temperature range requires the

correct selection of TABS thermal mass at normal value *and* envelope thermal resistance within MERR range (i.e., within minimum envelope resistance range, which is determined based on the building's ambient condition at *neutral* mean ambient temperature [1.18]. A simple set of guidelines is as follows:

- MASS: Both ceiling slab and floor slab of 0.25 m thickness are thermally activated;
- ENVELOPE: Envelope resistance meets the ASHRAE standard in a building's climate zone;
- ENVELOPE-SHADE: Shade blocks 80% of solar insolation.

The effectiveness derives from mass and envelope-resistance (including adequate envelope-shading) synergistically rather than mass itself or envelope-resistance itself. Remarkably, such a building functions robustly albeit with a slightly larger operative temperature variation at mean ambient temperatures higher than neutral mean ambient temperature, i.e., such a building is manageable by the use of off-peak equipment, which can be either mechanical ones or *natural energy gradient* driven lowPE (low power equipment). Without using any equipment we call such a building to have achieved partial homeostasis of the built environment by overcoming the challenge of weather and climate. The equipment and the necessary ambient conditions required for achieving homeostasis is discussed below.

1.2.3 Homeostasis: the opportunity of harnessing diurnal temperature variation irreversibility

Hot daytime weather and cold nighttime weather are challenge that a building has to meet to shelter occupants. To meet the challenge, equipment that consumes power is necessary to maintain the building at the right level of operative temperature. Energy efficiency is often regarded to be achieved by installing new technology such as EnergyStar equipment. In recent years it has been realized that the management of energy

on system level is more important than the individual equipment, "Most energy efficiency achieved through changes in how energy is managed rather than through installation of new technologies." [1.19] Based on the new understanding of the fundamentals of thermodynamics, how irreversibility is managed is the even more fundamental question than how energy is managed: "an external environment that is in constant flux across time and space" is not usually viewed as a form of energy but it is clearly a phenomenon that manifests irreversible gradient both temporally and spatially. Only by thinking in terms of irreversibility management, the phenomenon that is erstwhile viewed as a challenge can be seen as an opportunity.

This dissertation will show the management of this kind of irreversibility in seven locations of North America by using cooling tower as an example of lowPE. The seven locations are: Fullerton, CA; Sacramento, CA; Wilmington, DE; Atlanta, GA; Springfield, IL; Valentine, NE; Albuquerque, NM—which have the "design 1% daily-mean dry-bulb temperature" between 300.2 K and 300.3 K. They have different daily temperature variation (i.e., they have different *hourly* external environment that is in constant flux across time, but with nearly identical *daily-mean* peak external environment). By selecting them with "same" daily-mean peak temperature, we can compare the isolated effect in the range of diurnal temperature variation on building operation in these locations—with Sacramento having the largest diurnal temperature variation.

Result shown in Fig. 1.1 [1.20] is the summer cooling in Sacramento and Atlanta as an example: Each blue cross is one summer day and its position in the plot corresponds to its daily-mean peak temperature vs. temperature amplitude (data are the data of the summer of 2007). Red line separates days that cooling tower (CT) can maintain 25.25 °C from days that CT cannot: days successfully conditioned are shown below the line while ones unsuccessful above the line. Sacramento is the location that is most successful in harnessing its large diurnal temperature variation for cooling with "natural energy" or "natural irreversibility" as evident in all the days below the line. The success of using

natural irreversibility is primarily a function of diurnal temperature variation range and to a small extent a function of how "daily-mean *T*" vs. "amplitude" points are distributed in each location. The larger the irreversibility in diurnal temperature variation of a location, the greater degree of summer homeostasis is possible.

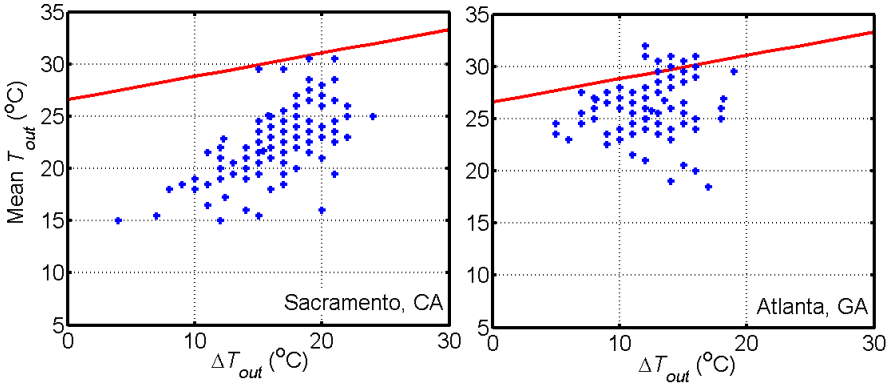

Fig. 1.1. Plot of Sacramento and Atlanta showing summer days (below the red line) that *thermal homeostasis* in buildings can be maintained

1.2.4 Mesoscale climatic process as a new kind of renewable energy

What is the reason for large summer diurnal temperature amplitude prevailing in Sacramento, California? It turns out that this summer weather pattern results from the meso-scale micro-climatic process of *sea breeze*: the summer day time high temperature air at Sacramento rises to pull in the sea breeze through Golden Gate strait, and this breeze travels towards Sacramento and by the night time it reaches Sacramento resulting in cool nighttime air there. It is the combined result of solar heating of air, ocean's moderating temperature effect, and the right distance of the location from ocean that creates this natural energy gradient gift.

The big two of renewable energies are wind and the sun. We prefer to call renewable energies as examples of "natural energy gradient," because the term includes all irreversible processes resources beyond those that can be harnessed into energy stock such as power harnessed from PV panel and wind turbine. Natural energy gradient of the strong micro-climatic process of *sea breeze* may well be the third most consequential kind

of renewable "energies" alongside wind and the sun.

The homeostatic conception makes a homeostatic building into a harnessing system for a new kind of renewable "energy." While traditional green buildings including NZE (net-zero energy) buildings can harness renewable energy with roof-top AST (active solar thermal) system, PV system and wind turbine, homeostatic buildings can harness a new kind of renewable "energy," which can be the most important "energy" source for buildings, alongside the sun and wind. As the architect J. Wines wrote, "If architecture is to become truly green, then a revolution of form and content—including radical changes in the entire look of architecture—is essential." [*1.21*] Homeostasis in buildings and how it is engineered offer an opportunity of creating a new kind of man-made systems with ecological sustainability—a perfect revolutionary form and content for getting the green architecture movement lifting off.

1.3 Main benefits of thermally homeostatic buildings

1.3.1 Energy efficiency of building conditioning

In 2010, the United States, which accounts for 4.6% of the world population, consumed 18.7% of the world primary energy. [*1.22*: 1-7] "Buildings account for 40% (41.1% in 2010) of all energy use in the U.S.. In fact, the construction industry consumes more energy than the industrial or transportation sectors." [*1.23*: 4]

It must be pointed out that more than half of the building energy consumption is electricity, which is one of the most flexible and the highest quality forms of energy. High quality energy is produced at great primary energy cost, as well as high environmental cost. In fact, "buildings accounted for 73.6% (or $301.6 billion) of total U.S. electricity expenditures." [*1.22*: 1-6] "The U.S. is responsible for 20% of the world's carbon dioxide emissions (CO_2e), with U.S. buildings' energy use responsible for 8%." [*1.23*: 4] Additionally, in the United States, 54% of SO_2, 17% of NOx, 5% of CO emissions and

15% of PM-2.5 are produced by the building sector. [*1.22*: 1-26]

"Unlike those two sectors (industrial and transportation), the building sector also has continued to increase its energy use, even during the ongoing economic downturn that began in 2007." [*1.23*: 14] It is predicted that, in 2035, buildings primary energy consumption of the U.S. will be up to 45.52 Quadrillion Btus, which means a 12.9% increase compared with the consumption in 2010. [*1.22*: 1-1]

It is clear that the building industry in the U.S. has a major responsibility in the energy picture of the planet. The responsibility is all the greater because buildings have a lifespan that lasts for 50 to 100 years throughout which they consume energy and produce emissions. The consequences of design decisions now will be with us for a long time.

In a homeostatic building (based on TABS), the fact that water than air is a much more effective heat transfer medium alone brings about typically an immediate 43.4% (36% + 7.4%, see Fig. 1.2 [*1.24,1.25*]) energy saving.

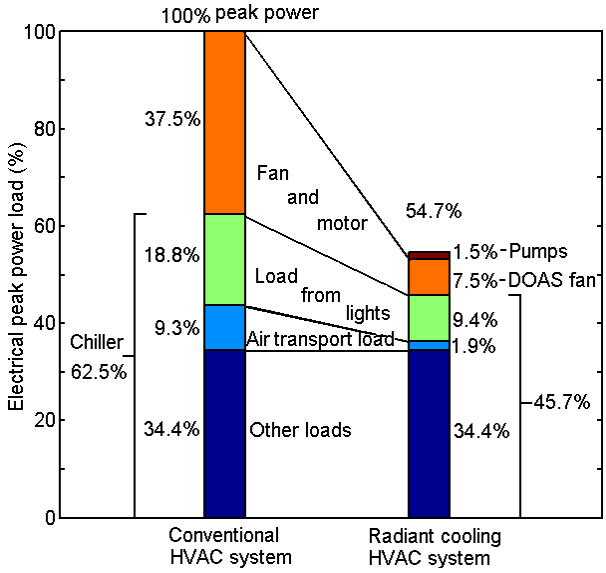

Fig. 1.2. Comparison of electrical peak power load for conventional systems and radiant cooling systems

The radiant cooling system reduces power demand by pumping chilled water to provide radiant cooling, rather than by blowing chilled air. A direct saving of 36% (37.5% – 1.5%) in air fan power requirement is shown. As well as an indirect saving due to lower Air Transport Load (heat gain due to fan operation). Percentages are relative to overall peak power for the conventional system.

1.3.2 Tunneling the cost barrier

Saving energy is important. But, for each decision maker, the cost of saving energy is even more important. We may well address up front the question of the initial cost of energy saving measures that we are going to consider. The conventional wisdom is that the principle of diminishing returns applies to the cost of efficiency improvement. This is clearly shown in a figure (Fig. 1.3) from a report *The Potential Impact of Zero Energy Homes* [ZEH or ZEB], prepared by NAHB Research Center for NREL of DOE. [*1.26*: 15] The conventional wisdom, therefore, says that a ZEH or ZEB, or a high-performance energy efficient building, is a very expensive proposition. And it is, if it is designed on the simple basis of selecting each building components and equipments of highest performance.

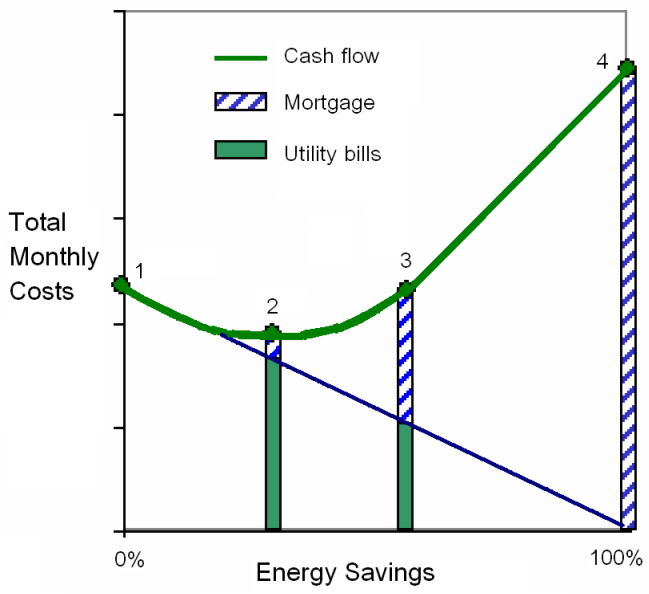

Fig. 1.3. The conventional understanding of increasing initial cost (mortgage) for increasing energy saving

Environmentalist Hawken, physicist A. Lovins, and author L.H. Lovins wrote in *Natural Capitalism: Creating the Next Industrial Revolution* on this topic. [*1.27*: 113] They used Fig. 1.4 to express the same conventional understanding of Fig. 1.3.

If you build a house, you'll be told that thicker insulation, better windows, and more efficient appliance all cost more than the normal, less efficient version…On the cost-versus-savings graph shown on page 113 [i.e., Fig. 1.4], as you save more energy (that is, as you move from lower left end of the curve toward the right), the cost of saving the next unit of energy initially rises more and more steeply. This is called "diminishing returns"…a principle that has taken a death grip on our consciousness [stopping us from action].

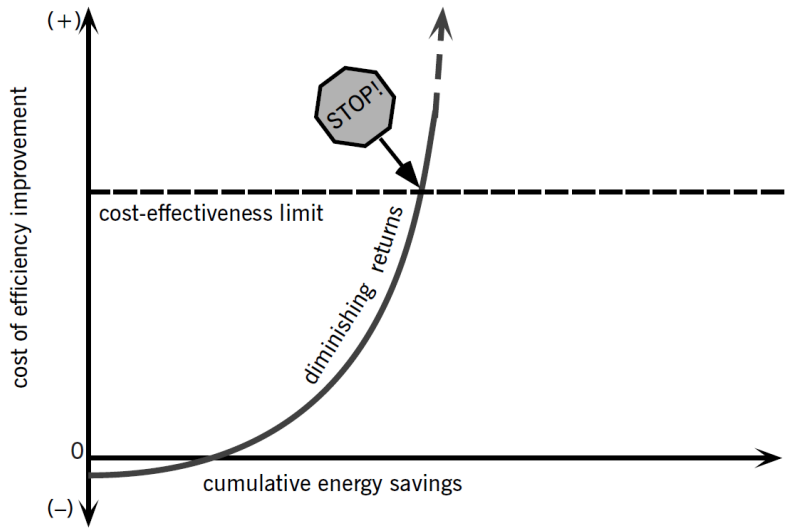

Fig. 1.4. "Economic dogma holds that the more of a resource you save, the more you will have to pay for each increment of saving"

They went on, however, to note the following: [*1.27*: 114]

Actual engineering practice, however, presents a different possibility. Only recently noticed is an additional part of the curve further to the right (see the graph below [Fig. 1.5]): There, saving even more energy can often "tunnel through the cost barrier," making the cost come *down* and the return on investment go up. When intelligent engineering and design are brought into play, big savings often cost even less *up front* than small or zero savings.

This is a visionary insight. The project of thermal homeostasis in buildings as it will be developed in the following will offer the outline of a concrete example that fulfills this insight.

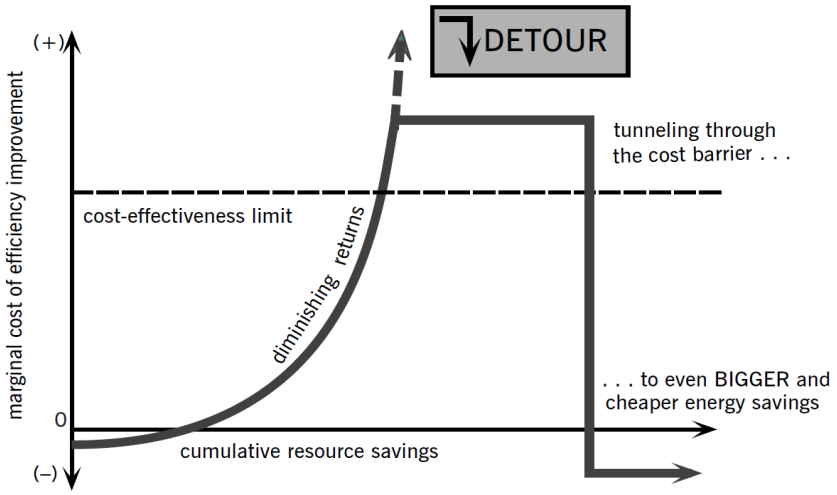

Fig. 1.5. Tunneling through the cost barrier, a wonderful way of describing the possibility when a designer takes a *whole-system engineering* approach

1.3.3 Thermal comfort

The main function of buildings is of course to provide a comfortable internal environment for occupants. In Ref. [*1.28*: 9.12], the comfort zones of buildings specified in *ANSI/ASHRAE Standard 55* are given as shown in Fig. 1.6. The temperature ranges are appropriate for current seasonal clothing habits in the United States and for sedentary and moderately active people.

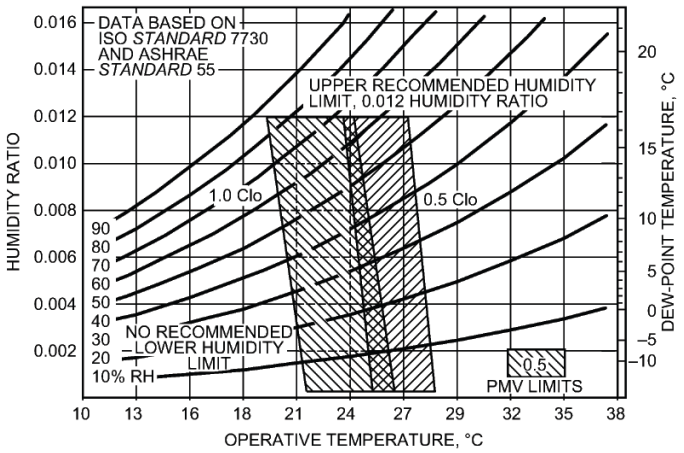

Fig. 1.6. ASHRAE summer and winter comfort zones

Acceptable ranges of operative temperature and humidity with air speed ≤ 0.2 m/s for people wearing 1.0 and 0.5 clo clothing during primarily sedentary activity (≤1.1 met).

In Fig. 1.6, the most important parameter is the operative temperature, which is the "uniform temperature of a radiantly black enclosure in which an occupant exchanges the same amount of heat by radiation plus convection as in the actual nonuniform environment." [*1.29*: 80] The operative temperature T_{op} is defined as the average of the mean radiant and ambient air temperatures, weighted by their respective heat transfer coefficients [*3.28*: 9.3]:

$$T_{op} = \frac{h_r \overline{T}_r + h_c T_{in}}{h_r + h_c} \tag{1.1}$$

where h_r is the linear radiative heat transfer coefficient, h_c is the convective heat transfer coefficient, $\overline{T}_r$ is the mean radiant temperature, and T_{in} is the indoor air temperature.

The radiative heat transfer coefficient h_r is nearly constant for typical indoor temperatures, and for most calculations a value of 4.7 W/m^2-K (0.83 Btu/h-ft^2-^{o}F) suffices. [*1.28*: 9.7] The convective heat transfer coefficient h_c is about 3.1 W/m^2-K (0.55 Btu/h-ft^2-^{o}F) for a seated person in moving air (velocity < 0.2 m/s), and 4.0 W/m^2-K (0.70 Btu/h-ft^2-^{o}F) for a standing person in moving air (velocity < 0.15 m/s). [*1.28*: 9.8]

The mean radiant temperature $\overline{T}_r$ "is a key variable in thermal calculations for the human body. It is the uniform temperature of an imaginary enclosure in which radiant heat transfer from the human body equals the radiant heat transfer in the actual nonuniform enclosure." [*1.28*: 9.10]

In Ref. [*1.28*: 9.10], many methods are given to measure or calculate the mean radiant temperature: it can be estimated by combining measurements of the globe temperature, air temperature, and air velocity; it can be measured by a spherical-shape globe thermometer (which gives a reasonable approximation of a seated person) or an ellipsoid sensor (which gives a better approximation of the shape of a human, both upright and seated); it can be calculated from the measured temperature of surrounding walls and surfaces and their positions with respect to the person; it may also be calculated from the plane radiant temperature t_{pr} [°C] in six directions (up, down, right, left, front,

back) and for the projected area factors of a person in the same six direction. In Ref. [*1.29*: 80], a useful simplification of the mean radiant temperature is given as follows:

$$MRT = \overline{T}_r = \frac{A_1 T_1 + A_2 T_2 + ... + A_N T_N}{A_1 + A_2 + ... + A_N} \tag{1.2}$$

Eq. (1.1) and Eq. (1.2) will be used to calculate the operative temperature in this dissertation.

In Ref. [*1.30*], based on the Fanger comfort equation [*1.31*], the predicted percentage of dissatisfied for sedentary office work and different types of clothing is given as shown in Fig. 1.7. In the figure, the "room temperature" is not the indoor air temperature, but the operative temperature.

> The permissible room temperature (operative temperature) range for the winter/transition period can be derived to be 3.5 K (6% dissatisfied) and 5.5 K (10% dissatisfied). For the summer period, the respective ranges are 5.0 K (6%) and 7.0 K (10%). As these figures suggest, room comfort is not dependent on a constant internal temperature and fluctuations are possible within predetermined limits. Occupants are also free to adjust their attire to the specific temperature conditions. This permissible comfort range forms the basis for the optimization of heating, ventilation and cooling system capacities to achieve maximum energy efficiency. Especially with tabs, the room temperature is floating with a certain amplitude during the day. Thus, the respective permissible temperature ranges are key elements for the design of such systems. [*1.30*]

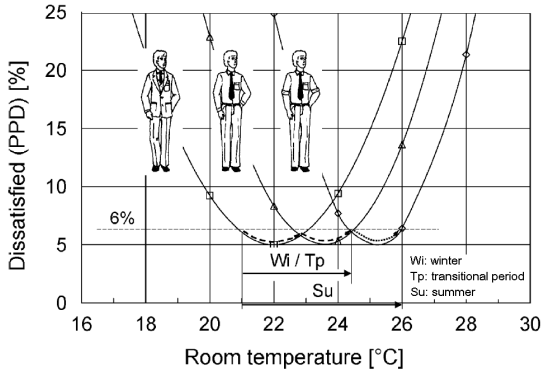

Fig. 1.7. "Predicted percentage of dissatisfied (PPD) for a range of room temperatures (operative temperatures) and different clothing (sedentary activity)"

Ref. [*1.30*] also gave the permissible room temperature ranges for a maximum of 6 and 10% dissatisfied, respectively, as listed in Table 1.1.

Table 1.1. Permissible room temperature ranges for a maximum of 6 and 10% dissatisfied, respectively

Type of clothing	Seasonal applicability of clothing	Comfort range (°C)	
		maximum 6% dissatisfied	maximum 10% dissatisfied
Jacket	Wi/Tp-Su	21.0–23.0	20.0–24.0
Long-sleeve shirt	Wi/Tp-Su	23.0–24.5	21.5–25.5
Short-sleeve shirt	Su	24.5–26.0	23.5–27.0

"A total acceptance (0% of dissatisfied) for a given room climate cannot be reached," [*1.30*] therefore, it is not necessary to keep the room temperature *at a fixed temperature*, as the conventional HVAC equipment did in the previous century and is still doing in the current century. In this dissertation, the room temperature will be allowed to "float" *within an acceptable range at a proper level*. In the partial homeostasis part, the room temperature *range* will be restricted by using adequate thermal mass [*1.32,1.33*] in a building with minimum envelope thermal resistance and maximum window-to-wall ratio (WWR); in the full homeostasis part, the room temperature *level* will be achieved by applying low-power equipment, such as cooling tower and hydronic solar wall (HSW) [*1.34*], or off-peak mechanical equipment.

The new treatment (from a fixed temperature to an acceptable range at a proper level) does not sacrifice thermal comfort of the buildings. Actually, this new kind of thermal environment is more comfortable [*1.35*]: "It turns out that people are more comfortable when they receive radiant heat at a slightly higher temperature of the air around them. The two most primitive examples of this situation are: (1) outdoors, on a spring day when the air is not too hot but the sun is shining. (2) around an open fire, on a cool evening." The homeostatic buildings will provide comfortable and stable internal environments for their occupants in the changing external surroundings.

1.3.4 Unity of architecture and engineering towards simplicity

Building energy consumption is one of the neglected energy problems in the world. One of the main reasons is that the basic conception-and-design of buildings has largely been overlooked by scientists and engineers as a scientific subject. In the architecture field, architects conceive the aesthetic designs of buildings; and after the architectural design completed, its structural and mechanical realizations become the responsibility of engineering: engineers calculate structural requirements and size mechanical equipment for building maintenance. In the process, engineers only play a supporting role.

"Almost everything that distinguishes the modern world from earlier centuries is attributable to science," noted Bertrand Russell [*1.36*: 525]. That is, science and engineering are the enabling factors that have produced almost every necessity in the modern world: from the concrete/steel infrastructure to transports on land, at sea, and in the air; from communication wonder to the information-technology industry and to the modern farming and food industries. Scientific and engineering knowledge is indispensable to the conception and design of every necessity in the modern world.

Yet among all the core human necessities, there is one important exception—in the inside environment of which "we spend 90 percent of our time." [*1.37*: 6] That is human dwellings (buildings). Buildings today are built and serviced by *machine technology*. But the technology has only a supporting role, which is limited to the structural design and construction of building and their heating-cooling and lighting based on mechanical and electrical equipments – not their conception and architectural design. We have heat transfer for heat exchanger design, fluid mechanics for aeronautic engineering, thermodynamics for internal combustion engines; all these discourses correspond to well established disciplines of engineering knowledge. But, we don't have a rigorous discipline of building energy dynamics – which will be the necessary scientific basis for the conception and design of building space achieving ideal lighting/thermal environment.

Thermal homeostasis in buildings is an example of sustainable technologies. The creation of general sustainable technologies represents a paradigm shift in engineering knowledge from the machine technology of the Machine Age to the sustainable technology of the Ecological Age. The creation of this knowledge in the present context requires the partnership of architects and engineers: without architects there can be no science of true relevance; without engineers there can be no satisfactory conception and design. Only when architects join engineers as active participants of generating technology achieving the true unity of art and technology, the new partnership can create revolutionary engineered buildings that are not only ultra-efficient but also of architectural simplicity and beauty, as shown in Fig. 1.8. [*1.38*] In the 21st century, we aim to create such a kind of buildings that using minimal equipment and harnessing natural energy to produce a stable and comfortable internal environment. The project of the thermal homeostasis in buildings is following and achieving this goal.

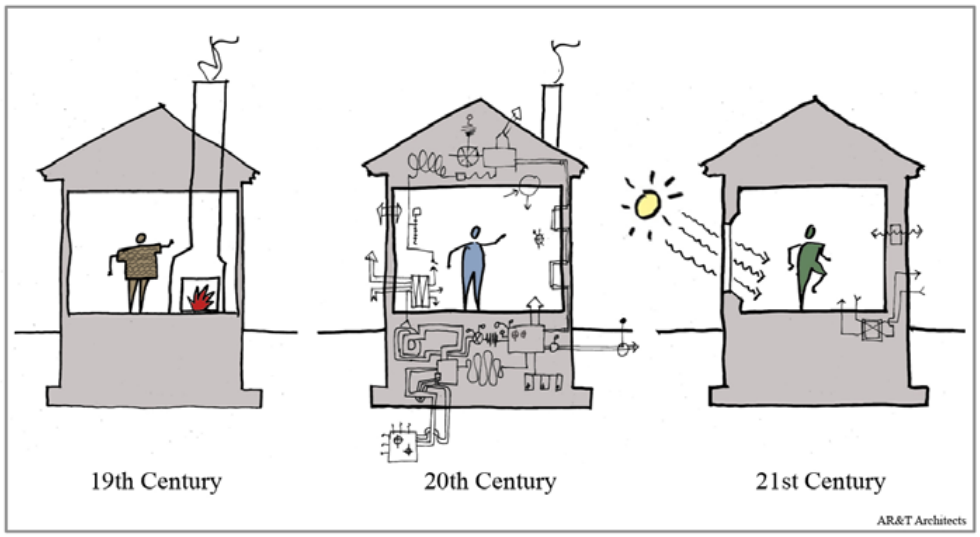

Fig. 1.8. "Moving Towards Simplicity"

A 19th century house offered minimal natural lighting and thermal comfort. With the wide adoption of central heating and the invention of air conditioning, the 20th century dwelling was much more delightful and comfortable; the comfort, however, came with the price of profligate energy consumption. The 20th century architecture failed to integrate mechanical equipment into building system, treating it as an afterthought.

1.4 Goal, tasks and method

1.4.1 Goal

The main goal of this dissertation is to formulate a new concept called Thermal Homeostasis in Buildings (THiB) using numerical simulation-modeling method for studying the thermal performance of buildings and the operation of a TABS-equipped building conditioning. The modeling of homeostatic buildings is informed by the process design approach—which is introduced in a recent paper [*1.39*]—instead of the conventional heat balance design approach.

The THiB project will concentrate on the cooling of commercial and office buildings. Buildings can be classified into two types according to how they use energy [*3.40*]: envelope (externally) load dominated types and internally load dominated types. Residential buildings belong to the first type, which typically require higher heating load. On the other hand, commercial buildings and office buildings are the second type, which use the majority of energy for internal needs (such as lights, computers, equipment and machines, etc.) leading to large internal heat generation. Therefore, it requires much lower heating load except during the coolest days, and cooling of course is the principal concern of internally dominated buildings. According to Refs. [*1.41*,*1.42*], California establishes a 2020 target for all residential new construction to reach Zero Net Energy and a 2030 target for all commercial new construction to reach Zero Net Energy (ZNE). The U.S. Department of Energy (DOE) [*1.43*: 36] has set a goal to achieve marketable ZNE commercial buildings in all climates by 2025. However, Ref. [*1.44*: 61] finds that "The goal of achieving significant levels of construction of cost-effective new zero-energy commercial buildings by 2030 is not obtainable without significant advancement in building technology and without the development and widespread adoption of integrated building design and operation practices." The reference explains the reason later: "Very-low-energy commercial buildings are so rare largely because they are very difficult

to design, construct and operate. The biggest barrier is the complexity of the buildings and their HVAC systems, and the important interactions between the various building systems and components." [*1.44*: 62] The THiB project will dramatically reduce the energy consumption in commercial and office building and will contribute to the ZNE target.

1.4.2 Tasks

Main tasks of this research are listed as follows:

Task 1: Introduction of the Swiss-German building technology—the Thermally Activated Building Systems (TABS);

Task 2: Formulate the new concept Thermal Homeostasis in Buildings (THiB), including partial homeostasis and full homeostasis in buildings;

Task 3: Build an energy model for a TABS-equipped office building in the interactive environment of Matlab and Matlab/Simulink;

Task 4: Investigate the partial homeostasis in the TABS-equipped office building and redefine the thermal envelope of buildings;

Task 5: Investigate the possibility of full homeostasis in the office building under cooling condition by adding a cooling tower in the building model;

Task 6: Design a thermally homeostatic building in Paso Robles, California.

1.4.3 Method

1.4.3.1 The resistor-capacitor model

Numerical simulation method will be used in this dissertation since it is much cheaper and time-saving than empirical method. Based on the principles of heat/mass transfer and thermodynamics, the building will be modeled by the resistor-capacitor (RC) method in Matlab and Matlab/Simulink.

There is a large volume of literature using the RC model on building energy modeling. Ren et al. [*1.45*] developed a simplified RC model for a hollow core concrete

slab thermal storage system and associated room. The model showed good accuracy for normal cyclic operations — the simulated mass and zone temperatures are both in phase with measured data and the root mean square error between the simulated and measured performance is no more than 0.5 °C for the average slab mass temperature and 1.0 °C for the zone air temperature. In Ref. [*1.46*,*1.47*], an RC star-network model was developed and validated by in situ measurement performed at an office building equipped with thermally activated building components, and it concluded that "the validation of the RC star-network against measurement data was successful even for the combined modeling of concrete slab and suspended floor even if the temperature inside the suspended floor could not be calculated exactly." In a building equipped with thermo-active building systems in Ref. [*1.48*], the cooling system, the hydraulic circuit, the slabs and the rooms are all simplified as a RC model based on finite difference method. In Ref. [*1.49,1.50*], based on an RC model of a TABS building, two control methods — UBB (unknown-but-bounded) method and intermittent operation with PWM (pulse width modulation) control — were outlined allowing for automated control of TABS. Bueno et al. [*1.51*] presented an RC model for analysis of interactions between building energy performance and urban climate. The RC model was evaluated against advanced simulation tools that are well accepted and evaluated. The authors pointed out that, due to its simplicity and computational efficiency, the RC model allowed for better understanding the physics of the problem and made it possible to easily evaluate modeling hypotheses and the sensitivity of different parameters. It concluded that the RC model could be used as a research and didactic tool [*1.51*].

Weber et al. [*1.47*] noted that "While these numerical methods [e.g. FEM (finite element method), FDM (finite difference method) or BEM (boundary element method)] provide quite accurate solutions they are time consuming and often causes stability problems … It is therefore of major interest to find simplified models that are limited in their complexity but still sufficiently accurate. One such type of model is the

RC-network." Široky et al. [*1.52*] mentioned that "Both of them [two approaches to building modeling] come from so-called RC modeling. … Largely used computer aided modeling tools (e.g. TRNSYS, EnergyPlus, ESP-r, etc.) are not considered here, as they result in complex models which cannot be readily used for control purposes. … Alternatively to the statistical approach, especially if there is a lack of data or some knowledge of building physics is present, the RC modeling can be used."

In Ref. [*1.53*], the dynamic heat transfer performance of interior Planar Thermal Mass (iPTM) subject to sinusoidal heating and cooling was investigated by analytical method. With the analytical result in hand, the RC model of iPTM is built in Matlab/Simulink and the simulation results are shown in Fig. 1.9: the curve named "Ideal" is the analytical result; the curves with "[*n*] RC" are simulation results of models with *n* resistors and capacitors.

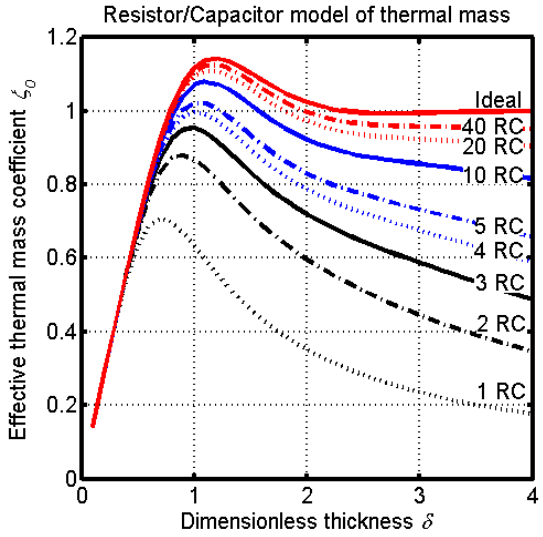

Fig. 1.9. RC model of iPTM

From Fig. 1.9, it is clear: when the iPTM thickness is small, the simulation results coincide with the analytical results; when the iPTM thickness is big, the simulation results of models with more RC have better coincidence with the analytical results. Balancing the accuracy and the calculation complexity, the model with 10 RC is used to evaluate the building performance in this dissertation.

1.4.3.2 Matlab and Matlab/Simulink

Matlab [1.54] is a numeric computation software for engineering and scientific calculations. It was developed by John Little and Cleve Moler of MathWorks, Inc. The name Matlab stands for MATrix LABoratory. Matlab is increasingly being used by students, researchers, engineers and technicians, because of its iterative mode of operation, built-in functions, simple programming, rich set of graphing facilities, possibilities for writing additional functions, extensive toolboxes, and so on.

Simulink is an integral part of Matlab, but it has relatively independent function and usage method. In Matlab main window, Simulink is an extra toolbox. Users may take full advantage of features offered in both environments, since it is easy to switch back and forth during analysis processes.

Simulink is a powerful simulation tool, as introduced in Ref. [*1.55*], "Simulink® is an environment for multidomain simulation and Model-Based Design for dynamic and embedded systems. It provides an interactive graphical environment and a customizable set of block libraries that let you design, simulate, implement, and test a variety of time-varying systems, including communications, controls, signal processing, video processing, and image processing." It is also very convenient since Simulink provides a graphical user interface (GUI) to build models as block diagrams just using click-and-drag mouse operations. It enables rapid construction and simulation of control block diagrams. Simulink has a comprehensive block library of toolboxes for both linear and nonlinear analyses, modeled in continuous time, sampled time, or a hybrid of the two. Using scopes and other display blocks, users can see the simulation results while the simulation is running.

Therefore, it is a good choice to use Simulink to model and simulate the homeostatic buildings in this dissertation.

1.5 Dissertation structure

In Chapter 2, related literature will be reviewed briefly, including hydronic radiant cooling and heating, thermally activated building systems (TABS), thermal mass and cooling tower application in buildings.

The building modeling in Matlab and Matlab/Simulink will be established in Chapter 3, in which building envelope, ventilation and infiltration/exfiltration, solar radiation, internal heat gains, thermal mass and TABS will be considered.

In Chapter 4, the systematic study of the partial homeostasis in buildings will redefine the building thermal envelope.

Full homeostasis in buildings of cooling with a cooling tower will be investigated in Chapter 5.

A partially homeostatic small commercial building in Paso Robles, California, will be designed in Chapter 6. The special geographical and climatic conditions of Paso Robles will also be demonstrated.

Main conclusions and some further research recommendations will be given at end of the dissertation.

Reference

[1.1] See: http://living-future.org (Last access on May 11, 2013)

[1.2] Lisa Heschong (1979) *Thermal Delight in Architecture* (MIT Press)

[1.3] F. Capra (1984) *The Turning Point*: Chapter 8_The systems view of life (Bantam)

[1.4] Luis Fernandez-Galiano (2000) *Fire and Memory*. Translated by Gina Carino (MIT Press)

[1.5] K. Moe (2010) *Thermally Active Surfaces in Architecture* (Princeton Architectural Press)

[1.6] Erwin Schrodinger (1944; 1992) *What is Life?* (Cambridge Univ. Press)

[1.7] Ilya Prigogine (1980) *From Being to Becoming* (New York: W. H. Freedman and Company)

[1.8] Martin Heidegger (1971) *Building Dwelling and Thinking* from *Poetry, Language, Thought* (Harper Colophon Books)

[1.9] ASHRAE, "Overview and Vision," *ASHRAE Research Strategic Plan for 2010-2015*. (P.7)

[1.10] J.M. Fitch (2009) from **Forward** to *Heating, Cooling, and Lighting* by N. Lechner (3rd ed., Wiley, 2009) (p. xiii)

[1.11] L.R. Johnson, *Essential Medical Physiology*, 3rd ed., Academic Press, Oct. 2, 2003

[1.12] F. Feustel, "Instead of a foreword," *Energy and Buildings* **30** (1999) 117

[1.13] L. D. D. Harvey, *Energy savings by treating buildings as systems* in D. Hafemeister, B. Levi, M.D. Levine, & P. Schwartz (Eds.), *Physics of Sustainable Energy, Using energy efficiently and producing it renewably* (AIP Conference Series 1044:67-87)

[1.14] Robert A. Meierhans (1993) "Slab cooling and earth coupling," *ASHRAE Transaction* **99(2)**: 511-518 (DE-93-02-4)

[1.15] D. Sullivan and R. Bean (2011) *Thermally Active Building Design: A path toward carbon neutrality*

[1.16] Beat Lehmann [EMPA, Building Technologies, email: Beat.Lehmann@empa.ch], personal communication, Aug. 4, 2011

[1.17] Energy Design Resources (2012). "Radiant heating and cooling," *EDR e-News #85* (energydesignresources.com)

[1.18] P. Ma, L.-S. Wang, N. Guo, "Modeling of TABS-based thermally manageable buildings in Simulink," *Applied Energy* **104** (2013) 791 – 800

[1.19] Rob Steele: ISO meeting challenges in energy management [17 June 2011]

[1.20] L.-S. Wang, P. Ma (2013) "Thermally autonomous building and the use of the low power equipment of cooling tower," (submitted to *Applied Energy* for publication in October, 2012)

[1.21] J. Wines (2008) "Green architecture: building for the 21st century," *Britannica Book of the Year 2008* (pp.192-95)

[1.22] U.S. Department Of Energy: Energy Efficiency & Renewable Energy, *2011 Buildings Energy Data Book*, Mar. 2012
See: http://buildingsdatabook.eren.doe.gov/ (Last access on May 11, 2013)

[1.23] U.S. Department Of Energy: Energy Efficiency & Renewable Energy, *Energy Efficiency Trends in Residential and Commercial Buildings*, Aug. 2010

[1.24] H. Feustel, *Hydronic radiant cooling systems*, CBS Newsletter, Fall 1994

[1.25] Energy design resources, *Radiant cooling*, Energy design resources: Building envelope design (prepared by Financial Times Energy, Inc., Boulder, CO), 2003

[1.26] NAHB Research Center, Inc., *The potential impact of zero energy homes*, NREL Subcontract Number: ACQ-3-33638-01, Feb. 2006

[1.27] P. Hawken, A. Lovins, L.H. Lovins, *Natural Capitalism: Creating the next Industrial revolution*, 10th anniversary edition, Earthscan Ltd., 2010

[1.28] ASHRAE, Inc., *2009 ASHRAE Handbook - Fundamentals* (I-P & SI Ed.), 2009

[1.29] R.L. Howell, W.J. Coad, H.J. Sauer, Jr., *Principles of heating ventilating and air conditioning* (6th edition), ASHRAE, Inc., 2009

[1.30] B. Lehmann, V. Dorer, M. Koschenz, "Application range of thermally activated building systems tabs," *Energy and Buildings* **39** (2007) 593–598

[1.31] P.O. Fanger, *Thermal Comfort – Analysis and Application in Environmental Engineering*, Technical Press, Kopenhagen, 1970

[1.32] P. Ma, N. Guo, L.-S. Wang, "The role of thermal mass in a US prototypical residential house," (submitted to the ASME 2013 International Mechanical Engineering Congress & Exposition for publication in March 2013)

[1.33] P. Ma, N. Guo, L.-S. Wang, "The role of thermal mass in a small commercial building and the potential improvement by applying thermally activated building systems (TABS)," (submitted to the ASME 2013 International Mechanical Engineering Congress & Exposition for publication in March 2013)

[1.34] L.-S. Wang, *Building thermal activation with Hydronic Solar Wall for passive solar heating*, Stony Brook University Research Foundation *R-8363*, May 2011

[1.35] C. Alexander, S. Ishikawa, M. Silverstein, M. Jacobson, I. Fiksdahl-King, S. Angel, *A Pattern Language: Towns, Buildings, Construction*, New York: Oxford University Press, Aug. 1977

[1.36] Bertrand Russell, *The History of Western Philosophy*, (Simon & Schuster, October 30, 1967)

[1.37] National Science Foundation. Emerging Frontiers in Research and Innovation 2010 *(EFRI-2010), Program Solicitation 09-606*. 2009

[1.38] From "*Form Follows Energy*" Passive House Presentation, Albert, Righter & Tittman Architects, AIA Webinar, June 2012

[1.39] L.-S. Wang, P. Ma, E. Hu, D. Giza-Sisson, G. Mueller, N. Guo, "The passive application of building thermal mass," Applied Energy (submitted in April, 2013)

[1.40] L.-S. Wang, *Thermo-Activic Buildings: Buildings cooled & heated with natural energies*, Stony Brook University research report, 2011

[1.41] California Public Utility Commission, *California Long Term Energy Efficiency Strategic Plan*, September, 2008

[1.42] California Energy Commission, *2011 Integrated Energy Policy Report*, 2011

[1.43] ZNE Stakeholders, *CA Energy Efficiency Strategic Plan, Zero Net Energy-Action Plan: Commercial Building Sector 2010-2012*

[1.44] American Physical Society, *ENERGY FUTURE: Think Efficiency*, September 2008

[1.45] M.J. Ren, J.A. Wright, "A ventilated slab thermal storage system model," *Building and Environment* **33** (1998): 43-52

[1.46] T. Weber, G. Jóhannesson, M. Koschenz, B. Lehmann, T. Baumgartner, "Validation of a FEM-program (frequency-domain) and a simplified RC-model (time-domain) for thermally activated building component systems (TABS) using measurement data," *Energy and Buildings* **37** (2005) 707–724

[1.47] T. Weber, G. Jóhanneson, "An optimized RC-network for thermally activated building components," *Building and Environment* **40** (2005): 1-14

[1.48] B.W. Olesen, M. de Carli, M. Scarpa, M. Koschenz, "Dynamic evaluation of the cooling capacity of thermo-active building systems," *ASHRAE Transactions* **112 (1)** (2006): 350-357

[1.49] M. Gwerder, B. Lehmann, J. Tödtli, V. Dorer, F. Renggli, "Control of thermally-activated building systems (TABS)," *Applied Energy* **85** (2008) 565–581

[1.50] M. Gwerder, J. Tötli, B. Lehmann, V. Dorer, W. Güntensperger, F. Renggli, "Control of thermally activated building systems (TABS) in intermittent operation with pulse width modulation," *Applied Energy* **86** (2009) 1606-1616

[1.51] B. Bueno, L. Norford, G. Pigeon, R. Britter, "A resistance-capacitance network model for the analysis of the interactions between the energy performance of buildings and the urban climate," *Building and Environment* **54** (2012) 116-125

[1.52] J. Široky, F. Oldewurtel, J. Cigler, S. Prívara, "Experimental analysis of model predictive control for an energy efficient building heating system," *Applied Energy* **88** (2011) 3079-3087

[1.53] P. Ma, L.-S. Wang, "Effective heat capacity of interior planar thermal mass (iPTM) subject to periodic heating and cooling," *Energy and Buildings* **47** (2012) 44-52

[1.54] J.O. Attia, *Electronics and circuit Analysis using MATLAB*, Boca Raton: CRC Press LLC, 1999

[1.55] The MathWorks, Inc., *Simulink® Getting Started Guide: R2012a*, 2012

Chapter 2: Literature Review

The concept of the thermally homeostatic buildings is based on the TABS (thermally activated building systems), which is a successful strain of the hydronic radiant conditioning. Review of related technologies will be given in this chapter, including hydronic radiant cooling and heating, thermally activated building systems (TABS), thermal mass, and cooling tower application in buildings.

2.1 Hydronic radiant conditioning

The thermal environment of a building interior space is defined convectively and radiatively. However, since the time of Willis H. Carrier's invention of air-conditioning, a building's thermal environment and its conditioning have become solely based on air and its convective role. The forced-air HVAC paradigm is primarily the direct conditioning of the interior air of the building; the distribution of heat energy is also through either the direct air convection of heat energy through air ducts, or the hot-water pipes which then indirectly condition air convectively around hot-water baseboard. In this air-based paradigm heating (or cooling) of the interior space and air ventilation are combined into one single HVAC operation.

In the hydronic radiant cooling and heating systems, the air-based paradigm is replaced with the water-based paradigm. Water is 832 times denser than air; a 1" water pipe delivers the same amount of heat as an 18" air duct – and is much easier to install in small spaces. Compared with air, water is a more space-efficient method of transferring heat and coolness around a building, as well as a more energy-efficient method: heat loss from air ducts is eliminated; air infiltration energy loss is reduced; the effective use of

building elements as thermal mass; and so on.

Hydronic radiant cooling and heating has a very long history. It can be dated back to more than 7,000 B.C. [2.1] when human beings started to use hydronic radiant cooling. Scientist Hauptmann [2.2] from the University of Heidelberg found the remains of the Kurdish settlement Nevali Çori in eastern Turkey. Houses in this settlement were actively cooled. The cooling systems consist of an intermediate space below the stone floor, which in summer could be flooded with water from the nearby Kantara Creek.

According to Ref. [*2.1*], the earliest technical papers [2.3,2.4] on the utilization of hydronic radiant cooling and heating in modern buildings were published in German in 1938. The first paper was about radiant cooling and forced ventilation in a large warehouse, and the second one was about the indoor climate issues caused by ceiling radiant heating. In Ref. [*2.5*] published in 1951, the construction and operation of radiant heating and cooling was investigated, and the advantages of hydronic radiant heating and cooling were demonstrated in projects. Several buildings with hydronic radiant cooling systems were mentioned in the paper, including an office building in Paris, a department store in Zürich, the Museum for Modern Art in Paris, the Hotel Excelsior in Rome, the Banque de Rome in Milan and the Palais des Journaux in Milan.

In the 1930s, architect Frank Lloyd Wright introduced floor heating to the United States in his Usonian houses [2.6], as described in Ref. [*2.7*] as follows.

> Frank Lloyd Wright was very against air conditioning; … He wasn't against heating, but in an effort to free space in the plan to allow more living, he strove to remove the large radiators that were typically found in North American homes. He did this by using an in-floor heating system. This system used steam or hot water piping within the floor slab, which sat upon a gravel bed. What this system did was keep the feet warm and head cool. … Since most of the nerve endings of the body terminate in the feet, keeping them warm is far more effective. … This combination of under-floor heating and lack of air-conditioning, which Frank Lloyd Wright employed, was most effective in the temperate zone of the

United States where the Usonian house was first used. As houses were built in other zones, they became either slightly too warm or slightly too cold.

The physiological effects of hydronic radiant cooling were investigated by Ronge and Lofstedt [2.8] in 1957. This research on the draft sensation of cold ceilings leaded to a comfort chart, which showed the interrelation between the indoor air temperature and the ceiling surface temperature.

In 1960, based on the heat exchange of the human body with the environment, Baker [2.9] described the advantages of hydronic heating and cooling: a comfortable, healthful and more invigorating environment, more uniform air temperatures, cleaner surfaces, neater appearance, and improved efficiency. Baker remarked that the radiation heat transfer had not been given adequate consideration.

In 1973, Obrecht et al. [2.10] reported that radiant panel ceilings were increasingly being applied as building heating and cooling devices. The report also pointed out that, for hygienic reasons, part of the sensible cooling might still be provided by the ventilation system when applying radiant cooling panels.

Until the near end of last century, hydronic radiant cooling and heating had still not been commonly used in buildings. As noticed by Feustel in 1993 [2.1], "Although, many authors have reported significant advantages of hydronic radiant cooling over *All-Air Systems*, even the two energy crises did not seem to have an effect on the development and the use of hydronic radiant cooling systems. Increasing energy prices did not change the market share of hydronic radiant cooling systems."

However, during the last two decades, hydronic radiant cooling and heating are becoming common in residential, commercial and industrial buildings. The pivotal development is the 1993 proposal of the so called thermally activated building systems (TABS), one form of hydronic radiat conditioning, and its successful adoption in Europe, especially in Switzerland and Germany.

2.2 Thermally activated building systems

The Thermally Activated Building Systems (TABS, or Thermo-Active Building Systems) was originally established by a Swiss engineer — Robert Meierhans in 1990s. Meierhans published two important research papers entitled *Slab cooling and earth coupling* in 1993 [2.11] and *Room air conditioning by means of overnight cooling of the concrete ceiling* in 1996 [2.12].

In the first paper, an office building with ceiling slab cooling system in Horgen, Switzerland, was introduced. With the system, in daytime, heat was stored in concrete mass of building structure and the indoor air temperature was kept in comfort range; in nighttime, the structure was cooled by cold water, which went through a water/air heat exchanger where heat was dissipated into cool outdoor air. Numerical calculations and experimental measurements were done for the building. Results showed that cooling load could be successfully shifted into night hours. Slab cooling was also proposed for an Austria museum: the cooling medium was a water circuit that could be cooled without difficulty by embedding 24 posts 18 m deep into ground with large layers of groundwater. Two models were built for the behavior of the temperature and humidity conditions, but no detailed conclusions were given. The author pointed out that "the slab cooling system … combines the advantages of radiant cooling with the thermal storage of massive concrete ceilings."

In the second paper, the office building introduced in the first paper was reported to show that its ceiling slab cooling system had proven successful over a period of three summers. Comfort measurements in actual and under load-simulated operating conditions confirmed the suitability of the system for small and medium loads. However, the paper reported that the proportion of cooling water generated in the free-cooling mode was below expectation, which was attributable to the low inner thermal loads and the outdated facade insulation. It concluded that the system was suitable for both heating and cooling of well-insulated buildings with small and medium cooling loads.

With architect Peter Zumthor, Meierhans developed two hugely successful projects [2.13,2.14] on the *Thermal Bath at Vals* in Switzerland (1996) and the *Kunsthaus Bregenz* in Bregenz, Austria (1997). The TABS movement has since gathered great momentum in Europe, especially in Switzerland and Germany.

TABS is primarily a water-based (hydronic) regulating circulatory system – both as the primary heat transfer medium and the means of creating and controlling thermal environment. A typical example of TABS section is shown in Fig. 2.1.

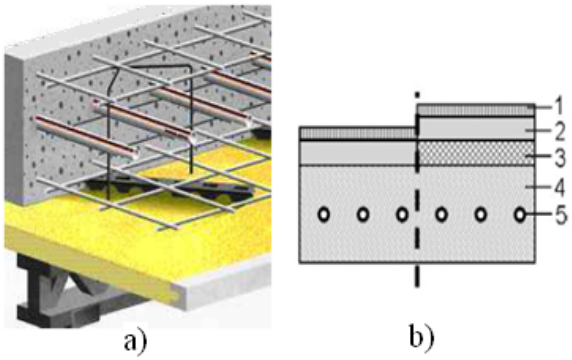

Fig. 2.1. A typical TABS section

a) Cross-section of the on-site constructed TABS core section, PEX pipes are shown between the reinforcements; b) TABS with and without acoustic insulation: 1=floor surface covering, 2=screed, 3=acoustic insulation, 4=building structure, and 5=plastic (PEX) pipes. (Diameter of the pipes varies between 17 and 20 mm. The distance between pipes is in the range of 150 to 200 mm.)

Unlike the periodic heating and cooling by air of a concrete slab where only a slab's surface layer is thermally activated [2.15], with water pipe placed in the middle of the slab the whole slab (with its large thermal mass) is activated. As a result, a building's operative temperature T_{op} remains within thermal comfort zone in the daytime, even with the water pump off, as shown in Fig. 2.2 [2.16].

In an air conditioned room, a room's temperature is controlled in terms of air temperature T_{in} with no explicit reference to the room's surface temperature. In a thermally activated room its thermal environment is defined in terms of both thermally activated surfaces and air contained in space enclosed by the surfaces. For cooling in Fig. 2.2, the thermal environment of a TABS building is a function of the surface temperature

(mean radiant temperature, or *MRT*) in the range around 70 °F and the air temperature T_{in} in the range up to 80 °F. The two temperatures together define the operative temperature T_{op}. The high level surface temperature makes it possible to be conditioned by various means efficiently. The even higher air temperature mitigates the infiltration loss in enthalpy or the enthalpy loss associated with DOAS (dedicated outdoor air system) operation.

Fig. 2.2 shows comparison of two cases [2.16]: (b) thermal activation of slab core with 24 hours cooling; (c) thermal activation of slab core with cooling only outside of the building occupancy period (after hour 18, i.e., 6:00PM). It is seen from the figures that the results of the latter case are almost the same as the 24 hours cooling.

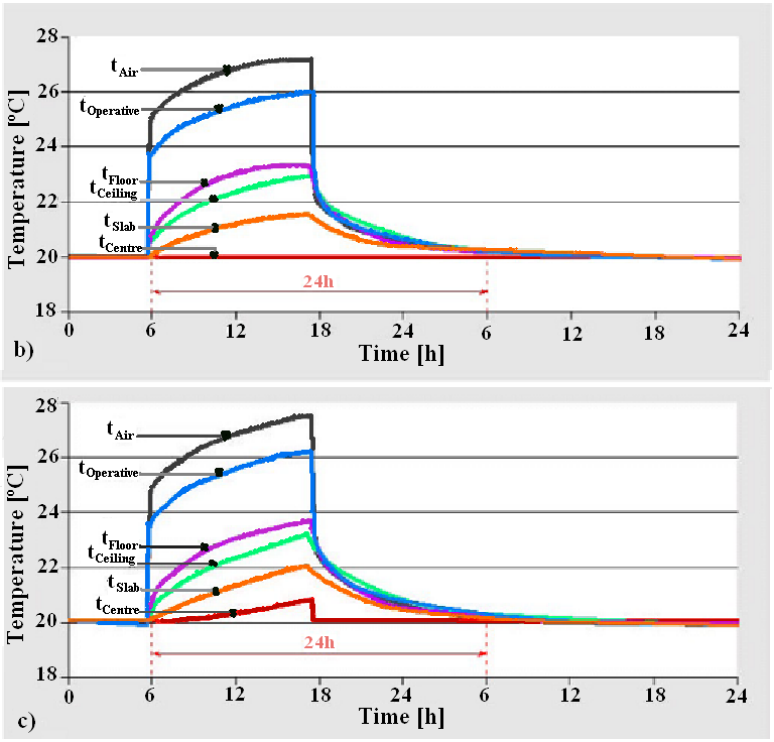

Fig. 2.2. Core thermal mass activation-cooling

Calculated 24 hours temperature variations for a space with a constant internal heat gain of 90 W/m^2 of air T_{in}, operative T_o, floor $T_{s2,0}$, ceiling $T_{s1,0}$, average slab T_{s1} or T_{s2}, and slab core T_c. (b) shows a 24 hour cooling of the slab center temperature. (c) shows slab cooling only after the building occupancy period.

In the recent two decades, many researches on TABS were published. Some

important TABS projects were done by a research and services institution, EMPA (Swiss Federal Laboratories for Materials Testing and Research) in Switzerland. Some publications from EMPA and its partners are as follows.

In 2000, M. Koschenz and B. Lehmann from EMPA published a book *Thermoaktive Bauteilsysteme tabs* [2.17], which introduced and modeled TABS in detail in German. A key work in the book is that the complicated three-dimensional, unsteady heat transfer problem of TABS was approximated to a simplified one-dimensional version under minor restrictions. Another important point is that the influences of the inserted pipes were converted into equivalent thermal resistances, so that a relationship between the flow temperature in the pipes and the average temperature of the concrete core were created.

A thermally activated ceiling panel with PCM (phase change material) was developed for application in lightweight and retrofitted buildings in Ref. [*2.18*]. The high thermal storage capacity of the PCM paraffin during phase change enabled the overall panel thickness to be limited to a mere 5 cm. The system allowed use of renewable energy sources for the heating and cooling of office and industrial buildings. The paper also developed a numerical model for computation of the thermal behavior of wall and ceiling systems incorporating PCMs. Simulations were performed to determine the necessary thermal properties of the ceiling panels and specify requirements for the materials to be used. Laboratory tests were performed to verify the system's performance.

In Ref. [*2.19*], detailed in situ measurements were performed in an office building equipped with TABS for heating and cooling in Germany. The measurements included temperature measurements at different heights of the concrete slabs, as well as in the suspended floor, and in both adjacent rooms. The supply and return water temperature, the volume flow for the TABS coil, as well as the heat flow at the surface of the concrete slab were also measured. A two-dimensional FEM-program working in the frequency-domain and a time-domain RC star-network model were built and validated by the measurement.

Ref. [*2.20*] developed RC-networks for the description of heat transfer in thermally activated building constructions, including a simplified star-network and a triangular network. It showed that the star-network could only be used for a restricted type of construction such as activated concrete slabs, while the triangular network could be used both for surface radiant systems such as floor heating and ceiling cooling as well as for concrete core conditioning.

Application range and functionality of TABS were presented in Ref. [*2.21*]. Thermal comfort, maximum permissible internal heat gains and building mass re-cooling were analyzed, based on a simulation study for a typical office building. It was shown that typical heat gain profiles with peak loads up to around 50 W/m^2 of floor area could be managed, but the transitional (mid-season) periods with high solar gains and restricted comfort range, was critical for determining TABS dimension, and thus lowered the maximum loads. The results also showed that processes on the room side were almost unaffected from the processes on the supply side. This work might serve as orientation guide whether TABS applicable in a specific building, and provide relevant parameters for the dimensioning of TABS.

In Ref. [*2.22*], an integral method, which was termed the Unknown-But-Bounded (UBB) method, was outlined allowing both for dimensioning and for automated control of TABS, with automatic switching between cooling/heating modes for variable comfort criteria. Applying the method guaranteed that comfort could be maintained if the actual heat gains stayed within the predefined range. The method could also handle non-predictable day-to-day variations and room-to-room variations of the heat gains. The paper outlined the underlying thermal models and assumptions, and gave the procedure and an example for the application of the method.

In Ref. [*2.23*], a method was outlined allowing for automated control of TABS in intermittent operation with pulse width modulation (PWM). This method represented one part of a TABS control solution with automatic switching between cooling and heating

modes for variable comfort criteria. Based on a simple 1st order model of TABS, a first PWM control solution was derived. Then a second simpler solution was given to reduce the tuning effort. At last, it outlined a PWM control procedure and gave two application examples of the PWM control carried out in a laboratory test room.

The impact of different aspects of TABS regarding the energetic performance of such systems was analyzed in Ref. [*2.24*]. Based on a simulation case study for a typical Central European office building, it showed that the energy efficiency of TABS was significantly influenced by hydronic circuit topology and control strategy; by using PWM control, the electricity demand for the water circulation pumps could be reduced by more than 50% compared to continuous operation; concerning cold generation for TABS, free cooling with a wet cooling tower was most efficient, if the cold source is the outside air. It concluded that significant energy savings could be achieved using adapted system topologies and applying appropriate control solutions for TABS.

Besides articles from EMPA, there exists a large volume of literature on TABS as briefly listed in the following.

Ref. [*2.25*] discussed the possibility of using hydronic systems with pipes embedded in the building structure for heating and cooling of buildings. It showed that for well designed buildings, those types of systems provide an interesting and viable alternative to full air-conditioning. The paper pointed out that "surface heating and cooling systems use water at a temperature close to the room temperature. This increases the possibility of using renewable energy sources and increasing the efficiency of boilers, heat pumps and refrigeration machines."

Schmidt and Jóhannesson [*2.26*] presented an effective modeling method called the macro element modeling (MEM) method for the thermal simulations of thermally activated building constructions or hybrid systems, such as hydronic floor and wall heating or hollow core slabs. It showed that the advantage of the MEM method is that only a limited number of nodes were required to obtain reliable results for the simulation.

Olesen et al. [2.27] offered a guide for the design of water-based embedded heating/cooling systems to promote the use of renewable energy sources and provide a method for actively integrating the building mass to reduce peak loads, transfer heating/cooling loads to off-peak times, and decrease system size. The paper showed that peak loads could be reduced by activating the building mass using TABS. It also presented a simplified method that was being implemented as a European standard.

Ref. [*2.28*] made measurements in a room equipped with TABS combined with an acoustic ceiling covering part of the ceiling so that both acoustic and thermal requirements could be met. The results showed that even with a covering of 83% of the ceiling surface area, the cooling capacity was still around 70% of the uncovered ceiling for the same temperature difference between mean fluid temperature and room operative temperature, while at the same time the reverberation time in the room was clearly acceptable. It concluded that acoustic ceilings and TABS could be combined.

In Ref. [*2.29*], it presented a simulation study comparing the primary energy and comfort performance of ventilation assisted TABS relative to a conventional all-air system in a compact office building for the continental climate of Omaha, Nebraska. TABS heating and cooling were accomplished using a geothermal heat pump and a geothermal heat exchanger, respectively. It observed clear advantages of the TABS approach respect to thermal comfort. It concluded that ventilation assisted TABS appeared to be a very promising alternative to conventional all-air systems offering both significant primary energy and thermal comfort advantages.

Ref. [*2.30*] focused on the thermal comfort of schools, in three of which, TABS was examined and measurements were undertaken to determine the comfort generated by the indoor climate concepts. The paper concluded that the application of TABS could lead to a small improvement of perceived thermal comfort for the occupants of school buildings in the winter.

In Ref. [*2.31*], measurements in a TABS building with room temperature feedback

showed that the HVAC system switching between heating and cooling in a very short time frame. The paper also described a simplified room model, representing the dominant time constants of the building zone and zone loads. The model proved adequate to gain insight into the effect of the control strategy on heating and cooling system behavior. Simulations revealed that only 45% of the cold and 15% of the heat produced were actively used to control room temperatures. The remainder was exchanged between the heating and cooling system.

Ref. [*2.32*] introduced and evaluated a heating and cooling concept employing TABS and environmental energy, harnessed from two 11-m^3 rainwater cisterns for a 285-m^2 residential building in passive house standard in Germany. A comprehensive long-term monitoring was carried out for the building for two years with an accompanying commissioning of the building performance. It showed that the building strived for a significantly reduced primary energy use with carefully coordinated measures.

Ref. [*2.33*] presented general guidelines for the required cooling capacity of an entire office building using TABS. On-site measurements were performed to obtain the required cooling power of an entire building as well as individual zones. The internal climate conditions of rooms and surface temperatures of the TABS were measured, and then the measured data were used to analyze the predictive performance of a simulation model. It was found that reductions up to 50% of the cooling capacity for a chiller could be achieved using TABS.

Saelens et al. [*2.34*] analyzed the influence of occupant behavior on the energy performance and thermal comfort of a typical office floor equipped with TABS. A multi-zone TRNSYS model with 10 adjacent zones per orientation for a typical moderate Belgian climate was set up. The paper showed that occupant behavior might have an important influence on the cooling demand and thermal comfort. However, as long as good solar protection was foreseen and operated in a correct way, TABS were able to

cope with different user behavior. In this case, normal daily stochastic processes did not considerably affect the cooling demand and thermal comfort during summer.

Sourbron and Helsen [2.35] evaluated the effects of thermal comfort models and a real warm year on the energy use of a typical TABS-equipped office building zone under moderate climate by a model built in TRNSYS. Simulation revealed that the energy use for cooling is higher when the indoor operative temperature limits were set by the ASHRAE55 and ISSO74 adaptive models compared to the non-adaptive ISO7730 model.

In Ref. [*2.36*], annual primary energy use in a central module of an office building consisting of two offices separated with a corridor was estimated by simulations. The simulations were conducted for conventional all-air VAV ventilation system and TABS supplemented with CAV ventilation. Results showed that with the moderate climate, the TABS decreased the primary energy use by about 16% as compared with the VAV; with hot-humid climate, the energy saving by TABS was ca. 50% even with the supply air dehumidification taken into account.

Ref. [*2.37*] presented a detailed analysis of the heating and cooling performance of environmental heat sources and sinks for 12 low-energy buildings in Germany, in which TABS served as the main delivery system for heating and cooling in all buildings, except two are additionally equipped with radiators. Comprehensive long-term monitoring in fine time-resolution occurred over a period from two to five years. The paper showed that the choice of suitable plant components, the accurate design of the hydraulic system and the correct dimension of the environmental heat source/sink played a central role in achieving higher efficiencies.

De Wit and Wisse [2.38] presented results from measurements of two buildings with advanced hydronic circuit topology. The measurements show that with an appropriate control strategy the issue of energy squandering within TABS can be eliminated. The article concluded that, in order to meet thermal comfort requirements, TABS should be divided into several zones; for zone division, differences in both external and internal

heat loads should be taken into account.

"Integrating the building structure to act as an energy-storage, thermally-activated building system (TABS) has proved to be energy efficient and economically viable for cooling and heating of buildings." [2.23] The high effective thermal mass of TABS makes such buildings very low energy-consuming in their operation: energy use is typically 60% to 75% less than a conventionally constructed [old system] "low energy building" that uses forced-air HVAC system. At this point, TABS buildings have been widely adopted and become the new standard of commercial buildings in Switzerland and Germany. The rest of Europe is not far behind. "Already by the year 2003 [in Germany], the proportion of new commercial buildings in which concrete core temperature control systems [the most common type of TABS] were planned or realized, was estimated to be as much as one third." [2.39: 8] "In Switzerland, the installed area of TABS [in 2003] was estimated to be around 100,000 m^2. The installed area of thermo-active building systems in 2007 is estimated to amount to 490,000 m^2 (76% office building and 5% residential buildings)." [2.40] The innovation that transformed passive cooling into thermally activated building elements with natural overnight cooled water is applied in Europe principally to commercial and office buildings.

However, in other parts of the world, including the North America, the practice is not well known. There is little public awareness. For instance, one can find on the DOE website only the information for radiant heating, not thermal activation. In the recently published exhaustive list of building sustainability practices, *AIA 50 to 50*, by AIA, one does find one mention of radiant cooling, "Although in use for a decade or more in Europe, radiant cooling systems [of which TABS is one version] are relatively new in the United States." [2.41: 150]

2.3 Thermal mass

A thermal mass [2.42,2.43,2.44], "which can be in the form of water, earth, rock, wood,

brick, concrete, or metal, has the ability to absorb and store heat energy during a warm period of heating and to release heat energy during a cool period later." [2.45]

There exists a large volume of architectural literature on the use of thermal mass in building applications.

In Ref. [*2.46*], a simple office building model with air-conditioning at daytime and free cooling at nighttime was analyzed in detail to quantify the hourly and overall variation of cooling load of air-conditioning. Zhou et al. [2.47] developed a simple model coupling thermal mass and natural ventilation, and analyzed the impact of thermal mass on the indoor air temperature for six external walls. Yam et al. [2.48] proposed an ideal naturally ventilated building model, which allowed a theoretical study of the effect of thermal mass associating with non-linear coupling between airflow rate and indoor air temperature. In Ref. [*2.49*], a simplified lumped thermal network model was used to describe all heat storage materials inside a building and a genetic algorithm estimator was developed to estimate the lumped internal thermal parameters using operation data collected from site monitoring.

In these papers, the temperature distribution of thermal mass was assumed to be uniform (i.e., thermal mass heating and cooling was treated as "quasi-static" processes) in response to changing air temperature. This means that the thermal diffusion process within thermal mass is much faster than the convective heat transfer at thermal mass surface. Lumped method can be used only if the Biot number, *Bi*, is smaller than 0.1. According to Ref. [*2.50*], the heat transfer coefficient of indoor air film is typically 1.08~1.63 Btu/h-ft^2-°F (6.13~9.26 W/m^2-K). The thermal conductivity of fir, pine or similar soft wood [2.51] is about 0.12 W/m-K. Then we can calculate that the thickness of a wood planar thermal mass (most building thermal mass can be considered as planar in shape) should be less than 2 mm, if the Biot number is smaller than 0.1. It is obvious that most wood furniture and internal wood walls are thicker than 2 mm, and the lumped method of course cannot be used.

In EnergyPlus [2.52], which is a whole building energy simulation program supported by the U.S. Department of Energy (DOE) and first released in 2001, an "equivalent surface" method [2.53] is used to deal with building "surface." In this method, there are two types of "surfaces": heat transfer surfaces and heat storage surfaces. For "internal mass," two heat storage surfaces were defined. "All heat storage surfaces of the same construction within a zone may be defined as a single rectangular surface" and "the size of this equivalent surface will equal the sum of all the areas of all the heat storage surfaces in the zone." The problem is that two thermal masses with same surface area but different thickness will store different amount of heat, even if they are made of the same material and under the same thermal environment.

There are many papers using softwares, such as TRNSYS, ENERGY, AccuRate energy rating tool, and so on, as shown in Ref. [*2.54*], [*2.55*] and [*2.56*]. However, in these papers, the specifics of the assumptions made in the analysis of thermal mass in these softwares were not presented.

A few papers did report research on dynamic heat transfer problem of thermal mass. In Ref. [*2.51*], there was a brief discussion on the dynamic heat storage of a homogeneous single-layer wall, whose back surface was insulated and front surface underwent a sinusoidally varying temperature change with period. It was found that "with further increases in thickness, the energy stored goes through a maximum value and then actually decreases slightly" and it pointed out that "the physical explanation for this is that heat stored in this wall from previous days is trying to flow out of the wall and interferes with current heat flow into the wall." In Ref. [*2.57*], the superposition principle was used for the construction of the temperature and heat current density inside the wall with sinusoidal surface thermal wave and insulated at the other surface. In Ref. [*2.58*], the effect of varying in convention coefficients on the energy storage performance of interior massive wall was studied under both sinusoidal and "realistic" interior air temperature profiles and it concluded that variations in interior convection coefficients within the

range commonly occurring in buildings can have a significant effect on the thermal performance of massive interior walls.

It is generally held that the design-application of thermal mass is a powerful tool for controlling temperature and "appropriate use of thermal mass throughout your home can make a big difference to comfort and heating and cooling bills." [2.42] However, the improper of ineffective use of thermal mass may cause overheating or overcooling. Therefore, recently, research on the effective heat capacity of interior Planar Thermal Mass (iPTM) and exterior Planar Thermal Mass (ePTM) was conducted and this research was published in two papers.

In the first paper [2.45], the dynamic heat transfer performance of iPTM subject to sinusoidal heating and cooling was investigated by analytical method. It found that the effective heat storage capacity of iPTM reached maxima at an optimal thermal mass thickness. Thus it concluded that there was no rationale of using thickness greater than optimal thickness from the consideration of building material as thermal mass rather than as structural material. Because of the convective effect and the nonlinearity of the heat storage of iPTM, it pointed out that "the lumped method, which is used to do interior thermal mass calculations in most papers and softwares, is incorrect under most circumstances." Another conclusion of the paper is that concrete is a better thermal mass than wood because of its higher heat capacity and lower thermal conductivity.

In the second paper [2.59], the dynamic heat transfer performance of ePTM subject to sinusoidal heating and cooling was investigated. When the mean value of outdoor air temperature was equal to indoor air temperature, analytical solutions of temperature distribution and heat flux in ePTM were deduced. When the two temperatures were not equal, an approximated solution of temperature distribution was developed based on the principle of superposition. The time-lag effect and the decrement factor were investigated later in the paper. It showed that wood was better as exterior walls than same-thickness concrete in terms the time-lag effect and the decrement factor. It also found that, no

matter as iPTM or ePTM, the effective heat storage capacity was identical for the same thermal mass.

Although the developed solutions gave more accurate methods in interior and exterior thermal mass calculations, research in these two papers does not represent the complete investigation of a building as a whole thermal system since the indoor air temperature was assumed to act as an input function rather than an output result. It is worthwhile to note that the ASHRAE heat balance design approach has the same kind of shortcoming by assuming a constant indoor air temperature. [2.60] It is therefore hard to predict the effect of thermal mass on the indoor air temperature, which is an important parameter in building thermal comfort conditions. If the sizing of thermal mass (especially interior thermal mass) is improper, over-heating or over-cooling will occur. This will cause uncomfortable thermal condition and high energy consumption. For this reason, in this dissertation, a resistor-capacitor (RC) model will be developed to link building thermal mass and its thermal environments to investigate the thermal performance of homeostatic buildings.

2.4 Cooling tower application in buildings

"A Cooling Tower is a heat rejection device that extracts waste heat to the atmosphere by cooling a stream of hot water in the tower." [2.61] There are two basic types of commonly used cooling tower: wet and dry cooling towers. In a dry cooling tower the water and air are separated, and in a wet cooling tower, the hot process water is in direct contact with the cooler air. A large volume of literature of the cooling tower application in buildings exists.

When combining the advantages of radiant cooling with the thermal storage of massive concrete ceilings, Meierhans [2.11] suggested that "The concrete core is cooled by cold water during the night. The water circuit includes a water/air heat exchanger, which cools down the ceiling to 20° to 22°C by means of heat exchange with the cool night air.

During the day, the ceiling absorbs the room loads and keeps the air temperature in the comfort range. The heat exchange in the building occurs at a relatively high temperature level (20° to 26°C), which allows the use of alternative cooling sources, e.g., earth coupling." A dry cooling tower is similar to an outdoor water/air heat exchanger. In the reference, it showed the measured variation in temperature of an especially warm week (Fig. 2.3, which is reproduced according to Figure 11 in Ref. [*2.11*]). We will see that the temperature trends are similar to that in our model shown at the end of Chapter 3. In Fig. 2.3, the difference between the supply water temperature and the minimum ambient air temperature is about 6 °C; in the cases in Chapter 3, the temperature difference is 12 °C. Therefore, there is no problem to apply the cooling tower in our cases.

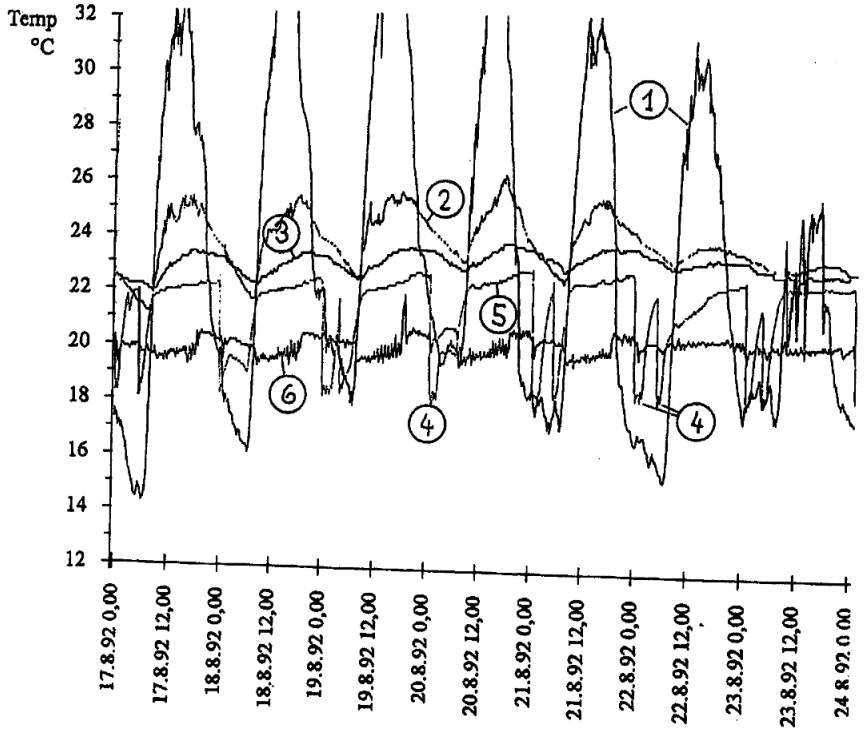

Fig. 2.3. Monitored temperature data for week 34

Ambient air temperature (1), room air temperature (2), ceiling surface temperature (3), water supply temperature (4), water temperature when pump is off (5), supply air temperature (6). Please note the short cooling period (4) during night hours.

Maiya [2.62] claimed that "evaporative air cooling for human comfort and other applications, whenever possible and feasible, is less expensive than conventional air

conditioning." In the reference, a cooling tower was used in the centralized evaporative air cooling system. Two modified cooling towers were modeled and their thermal performances are compared with a conventional counter-flow cooling tower. It found that the modified cooling towers were better than the conventional one in lowering the tower approaches below about 2 °C. It concluded that these cooling towers were quite useful in evaporative air cooling applications.

According to a research of Gan and Riffat [2.63], the use of chilled ceilings in commercial office buildings made it possible for cooling by evaporative cooling of water in closed wet cooling towers. The reference optimized the design of wet cooling towers to generate cooling for chilled ceilings. The technique was based on computational flow dynamics (CFD) for the two-phase flow of gas and water droplets. Numerical simulation indicated that CFD could be used to predict the performance of a closed wet cooling tower, given the appropriate rate of heat generation from the heat exchanger.

Facão and Oliveira [2.64,2.65] also investigated the cooling tower application in buildings with chilled ceilings by experimental and numerical methods. The tested tower had a dimension of 0.6 m × 1.2 m × 1.55 m and its designed cooling capacity was 10 kW. Different models were used and their results compared to experimental ones. It was found that, for such a small tower, the models gave better results when using the new correlations. It was also found that simpler models, with a global approach, could give as good, or even better, results as models based on finite difference techniques.

Ref. [*2.66*] presented the theoretical analysis and computational modeling of closed wet cooling towers. The tower transfer coefficients are defined using experimental measurements for performance of a prototype tower. Tower flow rates and number of tubes and rows were optimized for the required cooling load and to achieve a high coefficient of performance (COP). The performance of a cooling system used to cool office buildings was simulated in TRNSYS. The cooling system consisted of a closed wet cooling tower, chilled ceilings, pumps and a fan. A control strategy, including night

cooling, was introduced in the simulation. The results indicated efficient performance and high COP values for the system.

For indirect cooling towers behavior, Ref. [*2.67*] developed a simplified model devoted to building simulation tools. The model introduced only two parameters, air-side and water-side heat-transfer coefficients which could be identified from only two rating points, data easily available in manufacturers' catalogues. The error in heat-transfer rate was less than 10% and the results were in good agreement with manufacturers' catalogue data. The model allowed one to estimate energy and water consumptions under different operating conditions, such as variable wet-bulb temperatures or variable airflow rates.

Ref. [*2.68*] presented a case study on the application and utility of solar collectors heating system to control the visible plume from wet cooling towers of a huge commercial building. The study was on the control of plume from wet cooling towers of a huge commercial building, particularly, in Hong Kong and could be used as a base for other places in general. The analysis was done based on the hourly weather data available from the metrological department for a particular year.

Vangtook and Chirarattananon [*2.69*] found that air-conditioning is highly energy intensive in hot and humid Southeast Asian Region. While in the interest of energy saving, they explored the possibility of use of cooling tower to provide cooling water to ceiling radiant cooling panels, or the use of direct or indirect evaporative cooling. A cooling tower rated at 10 kW_{th} was used to cool the return cooling water from the active wall or the radiant panel. Chilled water at 10 °C was supplied to cooling coil to precool ventilation air while water cooled by cooling tower was used for radiant cooling in daytime application. For night-time, cooling water from cooling tower was found to be sufficient to achieve thermal comfort.

Ref. [*2.70*] proposed a new, simple, yet accurate mechanical cooling tower model for the purpose of energy conservation and management. The proposed model had simple characteristic parameters to be determined and without requiring iterative computation

when the operating point changes compared with the existing models. The model was validated by real operating data from the cooling towers of a HVAC system of a commercial hotel. The testing results showed that the performance of the cooling tower varied from time to time due to different operating conditions and the proposed model was able to reflect these changes by tuning its parameters. It concluded that the proposed model could be used to predict the performance of the real-time operating cooling tower.

Ref. [*2.71*] investigated the energy performance of chiller and cooling tower systems and developed models of the chiller and cooling tower to assess how different control methods influence the trade-off between the chiller power, pump power, fan power and water consumption. With regard to an example chiller system serving an office building, a proposed optimal control could reduce the annual system electricity use by 5.3% and operating cost by 4.9% comparing to the equivalent system using constant speed fans and pumps with a fixed set point for cooling water temperature control.

Sarker et al. [*2.72*] noticed that "the use of cooling towers to reject heat, cool buildings and reduce the temperature of water circulated through various heat rejection equipments have increased considerably." They did experimental study on a hybrid closed circuit cooling tower having a rated capacity of 136 kW. Bare-type copper coil was used in the 1.14 m × 2.36 m × 3.2 m dimensional tower. Performance characteristics from the experimental study were found to conform well to the rated ones. It concluded that the result obtained from the study was supposed to provide basic relevant data that could be referred for the optimum design of the hybrid closed circuit cooling towers.

Ref. [*2.73*] presented a case study based on the economic considerations and comparisons between the heat pump and solar collector heating systems for the application and utility to control the visible plume from wet cooling towers of a huge commercial building in Hong Kong. There was a central air conditioning system, containing 6 water-cooled chillers and 10 wet cooling towers. It found that all the costs were much lesser for a solar collector system while it was reverse in the case of an

air-cooled geothermal heat pump system.

Ref. [*2.74*] carried out extensive field experimental work on the heat and mass transfer characteristics of a reversibly used cooling tower in an office building located in Changsha, Hunan province, a hot summer and cold winter region in China. The tested cooling tower was an induced draft cross flow type with the cross sectional area of 9.9 m^2, filled with 144 pieces of packing with each surface area of 6 m^2. Simulation results revealed that artificial neural network model can be used effectively for predicting the performance characteristics of the cooling tower under cross flow conditions.

In Ref. [*2.75*], a Greek hot dominated climate was examined which accounts for a cooling dominated system. A hybrid ground source heat pump system, which included a cooling tower and consisted of a rectangular field of 15 borehole heat exchangers, was utilized to cover the energy demands of a five-floor office building with total cooled area of 1000 m^2. The energy demands were computed by TRNSYS 16.1. Assuming different cooling tower capacity, the desired flow rate was estimated for a cooling range of 5.7 °C.

Ref. [*2.76*] developed a thermodynamic model to assess the sensitivity of thermal performance characteristics of a closed wet cooling tower to inlet air conditions. The reliability of simulations was tested against experimental data from literature. When combined with liquid desiccant air-condition systems, the beneficial effect of the serpentine water temperature fall of the examined closed wet cooling tower was observed, providing heating-cooling and dehumidification for buildings without using energy consuming equipment and common environmentally harmful refrigerants.

Ref. [*2.77*] proposed three operation modes with different heat rejection methods for building cooling in tropical areas, in which Mode 1 was an open-loop groundwater cooling system combined with cooling towers. Located in the western part of Singapore, the investigated building is mainly used for research offices and laboratories. The total floor area was 3430 m^2 while the air condition area was 2253 m^2. The air conditioning system was provided by three water cooled chillers, with a total capacity of 560 kW.

These chillers were cooled using a cooling tower with a capacity of 1050 kW. Detailed comparison showed that Mode 1 was a better option for application in Singapore.

With all the literature above, there is no doubt that cooling tower can be applied for building cooling. In this dissertation, a parametric cooling tower is employed for cooling of thermally homeostatic buildings.

2.5 Chapter summary

Since the time of Willis H. Carrier's invention of air-conditioning, a building's thermal environment and its conditioning have become solely based on air and its convective role. In the hydronic radiant conditioning systems, the air-based paradigm is replaced with the water-based paradigm. A successful strain TABS (thermally activated building systems), which uses water to activate the heavy thermal mass in buildings, has proved to be energy efficient and economically viable for building conditioning. TABS buildings have been widely adopted and become the new standard of commercial buildings in Switzerland and Germany. The related technologies—hydronic radiant conditioning, TABS, thermal mass, and cooling tower application in buildings—are reviewed in this chapter.

Reference

[2.1] H. E. Feustel, *Hydronic Radiant Cooling: Overview and preliminary performance assessment*, Lawrence Berkeley Laboratory Report No.: LNL-33194 UC 350, 1993

[2.2] J. Hoelzgen, *Die Schwelle zur Zivilisation*, Der Spiegel, (45), No. 33, p160-165, Spiegel Verlag, Hamburg, Aug. 1991

[2.3] M. Hottinger, Strahlungsheizung, "Lueftung und Kuehlung in eines grossen Warenhaus," *Gesundheits-Ingenieur* **61** (1938) 129-134

[2.4] F. Bradtke, "Raumklimatische Fragen zur Deckenheizung," *Gesundheits-Ingenieur* **61** (1938) 510-511

[2.5] H. Bilden, *Bau und Betrieb der Strahlungsheizung und der Strahlungskühlung*, Heizung, Lueftung, Haustechnik **2** (1951), p5-9

[2.6] B.W. Olesen, "Radiant floor heating in theory and practice," *ASHRAE Journal* **44(7)** (2002) 19-24

[2.7] M. Wildman, *An historical view of Frank Lloyd Wright's Usonian concept*, Housing Seminar 1 ARC 301-630A, Fall 2000

[2.8] H.E. Ronge, B.E. Lofstedt, "Radiant draft from cold ceilings," *Heating, Piping & Air Conditioning* **9** (1957) 167-174

[2.9] M. Baker, "Improved comfort through radiant heating and cooling," *ASHRAE Journal* **2** (1960) 54-57

[2.10] M.F. Obrecht, R.J. Salinger, A. LaVanture, *Radiant panel ceilings*, Heating, Piping, Air Conditioning (1973), No. 9, p55-62

[2.11] Robert A. Meierhans (1993) "Slab cooling and earth coupling," *ASHRAE Transaction* **99(2)**: 511-518 (DE-93-02-4)

[2.12] R. A. Meierhans, "Room air conditioning by means of overnight cooling of the concrete ceiling," *ASHRAE Transactions* V. **102 (1)**: 693-697, (AT-96-08-2), 1996

[2.13] P. Zumthor, Exhibition brochure KUB 07.03: *Peter Zumthor Buildings and Projects 1986 – 2007*, September 2007

[2.14] P. Zumthor, H. Binet, *Peter Zumthor Works: Buildings and Projects 1979-1997*, November 1999

[2.15] P. Ma, *Dynamic Heat Transfer: Effective heat capacity of planar thermal mass subject to periodic heating and cooling,* M.S. Thesis, Stony Brook University, May 2010

[2.16] R. Meierhans, B.W. Olesen, *Betonkernaktivierung* (Velta Norderstedt, Germany), 1999

[2.17] M. Koschenz, B. Lehmann, *Thermoaktive Bauteilsysteme tabs*, EMPA, Duebendorf Switzerland, ISBN 3-905594-19-6, 2000 (German only)

[2.18] M. Koschenz, B. Lehmann, "Development of a thermally activated ceiling panel with PCM for application in lightweight and retrofitted buildings," *Energy and Buildings* **36** (2004) 567–578

[2.19] T. Weber, G. Jóhannesson, M. Koschenz, B. Lehmann, T. Baumgartner, "Validation of a FEM-program (frequency-domain) and a simplified RC-model (time-domain) for thermally activated building component systems (TABS) using measurement data," *Energy and Buildings* **37** (2005) 707–724

[2.20] T. Weber, G. Jóhannesson, "An optimized RC-network for thermally activated building components," *Building and Environment* **40** (2005) 1 – 14

[2.21] Beat Lehmann, Viktor Dorer, Markus Koschenz, "Application range of thermally activated building systems tabs," *Energy and Buildings* **39** (2007) 593–598

[2.22] M. Gwerder, B. Lehmann, J. Tödtli, V. Dorer, F. Renggli, "Control of thermally-activated building systems (TABS)," *Applied Energy* **85** (2008) 565–581

[2.23] M. Gwerder, J. Tötli, B. Lehmann, V. Dorer, W. Güntensperger, F. Renggli, "Control of thermally activated building systems (TABS) in intermittent operation with pulse width modulation," *Applied Energy* **86** (2009) 1606–1616

[2.24] B. Lehmann, V. Dorer, M. Gwerder, F. Renggli, J. Tötli, "Thermally activated building systems (TABS): Energy efficiency as a function of control strategy, hydronic circuit topology and (cold) generation system," *Applied Energy* **88** (2011) 180–191

[2.25] B.W. Oleson, D. F. Liedelt, "Cooling and Heating of Buildings by Activating their Thermal Mass with Embedded Hydronic Pipe Systems," *CIBSE Conference*, 2000

[2.26] D. Schmidt, G. Jóhannesson, "Optimised RC Networks Incorporated within Macro-Elements for Modelling Thermally Activated Building Constructions," *Nordic Journal of Building Physics* **3** (2004)

[2.27] B.W. Olesen, M. de Carli, M. Scarpa, M. Koschenz, "Dynamic evaluation of the cooling capacity of thermo-active building systems," *ASHRAE transactions* (2006) 350-357

[2.28] P. Weitzmann, E. Pittarello, B.W. Olesen, "The cooling capacity of the Thermo Active Building System combined with acoustic ceiling," *Nordic Symposium on Building Physics*, DTU, 2008

[2.29] G.P. Henze, C. Felsmann, D.E. Kalz, S. Herkel, "Primary energy and comfort performance of ventilation assisted thermo-active building systems in continental climates," *Energy and Buildings* **40** (2008) 99-111

[2.30] W. Zeiler, G. Boxem, " Effects of thermal activated building systems in schools on thermal comfort in winter," *Building and Environment* **44** (2009) 2308 – 2317

[2.31] M. Sourbron, R. De Herdt, T. Van Reet, W. Van Passel, M. Baelmans, L. Helsen, "Efficiently produced heat and cold is squandered by inappropriate control strategies: A case study," *Energy and buildings* **41** (2009) 1091-1098

[2.32] D.E. Kalz, J. Wienold, M. Fischer, D. Cali, "Novel heating and cooling concept employing rainwater cisterns and thermo-active building systems for a residential building," *Applied Energy* **87** (2010) 650-660

[2.33] D.O. Rijksen, C.J. Wisse, A.W.M. van Schijndel, "Reducing peak requirements for cooling by using thermally activated building systems," *Energy and buildings* **42** (2010) 298-304

[2.34] D. Saelens, W. Parys, R. Baetens, "Energy and comfort performance of thermally activated building systems including occupant behavior," *Building and Environment* **46** (2011) 835-848

[2.35] M. Sourbron, L. Helsen, "Evaluation of adaptive thermal comfort models in moderate climates and their impact on energy use in office buildings," *Energy and Buildings* **43** (2011) 423 – 432

[2.36] J. Kolarik, J. Toftum, B.W. Olesen, K.L. Jensen, "Simulation of energy use, human thermal comfort and office work performance in buildings with moderately drifting operative temperatures," *Energy and Buildings* **43** (2011) 2988-2997

[2.37] D.E. Kalz, J. Pfafferott, S. Herkel, A. Wagner, "Energy and efficiency analysis of environmental heat sources and sinks: In-use performance," *Renewable Energy* **36** (2011) 916-929

[2.38] A.K. de Wit, C.J. Wisse, "Hydronic circuit topologies for thermally activated building systems–design questions and case study," *Energy and Buildings* **52** (2012) 56–67

[2.39] J. Pfafferott, D. Kalz, *Thermo-active building systems: High-comfort, energy-efficient heating and cooling of non-residential buildings*, BINE Themeninfo 1. 2007

[2.40] D.E. Kalz, *Heating and cooling concepts employing environmental energy and thermo-active building systems for low-energy buildings: system analysis and optimization*, Fraunhofer Verlag, Jan. 2011

[2.41] The American Institute of Architects, *AIA 50 to 50*, version 1, 2007

[2.42] C. Reardon, *Your home: design for lifestyle and the future. technical manual* 4th edition, 2008

[2.43] G. Z. Brown, Mark DeKay, *Sun, Wind & Light: Architectural Design Strategies* 2nd Edition, John Wiley & Sons, Oct. 2000

[2.44] N. Lechner, *Heating, Cooling, Lighting: Sustainable Design Methods for Architects* 3rd edition, John Wiley & Sons, 2008

[2.45] P. Ma, L.-S. Wang, "Effective heat capacity of interior planar thermal mass (iPTM) subject to periodic heating and cooling," *Energy and Buildings* **47** (2012) 44 – 52

[2.46] L. Yang, Y. Li, "Cooling load reduction by using thermal mass and night ventilation," *Energy and Buildings* **40** (2008) 2052–2058

[2.47] J. Zhou, G. Zhang, Y. Lin, Y. Li, "Coupling of thermal mass and natural ventilation in buildings," *Energy and Buildings* **40** (2008) 979–986

[2.48] J. Yam, Y. Li, Z. Zheng, "Nonlinear coupling between thermal mass and natural ventilation in buildings," *International Journal of Heat and Mass Transfer* **46** (2003) 1251–1264

[2.49] S. Wang, X. Xu, "Parameter estimation of internal thermal mass of building dynamic models using genetic algorithm," *Energy Conversion and Management* **47** (2006) 1927–1941

[2.50] ASHRAE, Inc, *2009 ASHRAE Handbook - Fundamentals (I-P Edition & SI Edition)*, Chapter 26, 2009

[2.51] K. W. Childs, G. E. Courville, E. L. Bales, *Thermal Mass Assessment—An Explanation of the Mechanisms by Which Building Mass Influences Heating and Cooling Energy Requirement*, Sep. 1983

[2.52] See http://www.energyplus.gov (Last access on May 11, 2013)

[2.53] University of Illinois, University of California, Ernest Orlando Lawrence Berkeley National Laboratory, US Department of Energy, *EnergyPlus Documentation: Getting Started with EnergyPlus*, Oct. 2010

[2.54] S. A. Kalogirou, G. Florides, S. Tassou, "Energy analysis of buildings employing thermal mass in Cyprus," *Renewable Energy* **27** (2002) 353–368

[2.55] E. Shaviv, A. Yezioro, I. G. Capeluto, "Thermal mass and night ventilation as passive cooling design strategy," *Renewable Energy* **24** (2001) 445–452

[2.56] K. Gregory, B. Moghtaderi, H. Sugo, A. Page, "Effect of thermal mass on the thermal performance of various Australian residential constructions systems," *Energy and Buildings* **40** (2008) 459–465

[2.57] P. Gruber, J. Toedtli, "On the optimal thermal storage capacity of a homogeneous

wall under sinusoidal excitation," *Energy and Buildings* **13** (1989) 177–186

[2.58] H. Akbari, D. Samano, A. Mertol, F. Baumann and R. Kammerud, "The effect of variations in convection coefficients on thermal energy storage in buildings Part I – interior partition walls," *Energy and Building* **9** (1986) 195–211

[2.59] P. Ma, L.-S. Wang, "Effective heat capacity of exterior Planar Thermal Mass (ePTM) subject to periodic heating and cooling," *Energy and Buildings* **47** (2012) 394–401

[2.60] L.-S. Wang, P. Ma, E. Hu, D. Giza-Sisson, G. Mueller, N. Guo, "The passive application of building thermal mass," Applied Energy (submitted in April, 2013)

[2.61] A. Bhatia, *Cooling Towers*, CED engineering course material, Course No: M07-001

[2.62] M.P. Maiya, "Analysis of modified counter-flow cooling towers," *Heat Recovery Systems & CHP* **15 (3)** (1995) 293–303

[2.63] G. Gan, S.B. Riffat, " Numerical simulation of closed wet cooling towers for chilled ceiling systems," *Applied Thermal Engineering* **19** (1999) 1279–1296

[2.64] J. Facão, A.C. Oliveira, "Thermal behaviour of closed wet cooling towers for use with chilled ceilings," *Applied Thermal Engineering* **20** (2000) 1225–1236

[2.65] J. Facão, A.C. Oliveira, " Heat and mass transfer correlations for the design of small indirect contact cooling towers," *Applied Thermal Engineering* **24** (2004) 1969–1978

[2.66] A. Hasan, K. Sirén, "Theoretical and computational analysis of closed wet cooling towers and its applications in cooling of buildings," *Energy and Buildings* **34(5)** (2002) 477–486

[2.67] P. Stabat, D. Marchio, "Simplified model for indirect-contact evaporative cooling-tower behaviour," *Applied Energy* **78** (2004) 433–451

[2.68] S.W. Wang, S.K. Tyagi, A. Sharma, S.C. Kaushik, "Application of solar collectors to control the visible plume from wet cooling towers of a commercial building in Hong Kong: A case study," *Applied Thermal Engineering* **27** (2007) 1394–1404

[2.69] P. Vangtook, S. Chirarattananon, " Application of radiant cooling as a passive cooling option in hot humid climate," *Building and Environment* **42** (2007) 543–556

[2.70] G.-Y. Jin, W.-J. Cai, L. Lu, E.L. Lee, A. Chiang, "A simplified modeling of mechanical cooling tower for control and optimization of HVAC systems," *Energy Conversion and Management* **48** (2007) 355–365

[2.71] F.W. Yu, K.T. Chan, "Optimization of water-cooled chiller system with load-based speed control," *Applied Energy* **85** (2008) 931–950

[2.72] M.M.A. Sarker, E. Kim, C.G. Moon, J.I. Yoon, "Performance characteristics of the hybrid closed circuit cooling tower," *Energy and Buildings* **40** (2008) 1529–1535

[2.73] S.K. Tyagi, S. Wang, S.R. Park, A. Sharma, "Economic considerations and cost comparisons between the heat pumps and solar collectors for the application of plume control from wet cooling towers of commercial buildings," *Renewable and Sustainable Energy Reviews* **12** (2008) 2194–2210

[2.74] J. Wu, G. Zhang, Q. Zhang, J. Zhou, Y. Wang, "Artificial neural network analysis of the performance characteristics of a reversibly used cooling tower under cross flow conditions for heat pump heating system in winter," *Energy and Buildings* **43** (2011) 1685–1693

[2.75] Z. Sagia, C. Rakopoulos, E. Kakaras, "Cooling dominated Hybrid Ground Source Heat Pump System application," *Applied Energy* **94** (2012) 41–47

[2.76] V.D. Papaefthimiou, E.D. Rogdakis, I.P. Koronaki, T.C. Zannis, "Thermodynamic study of the effects of ambient air conditions on the thermal performance characteristics of a closed wet cooling tower," *Applied Thermal Engineering* **33-34** (2012) 199–207

[2.77] Y. Liu, X.S. Qin, Y.M. Chiew, "Investigation on potential applicability of subsurface cooling in Singapore," *Applied Energy* **103** (2013) 197–206

Chapter 3: Modeling of TABS-Equipped Building in Simulink

In this chapter, an RC (resistor-capacitor) model of a south-west corner room in a TABS-equipped office building is built in detail in Matlab and Matlab/Simulink. The main characteristics of buildings are considered, including building envelope and its thermal resistance, ventilation and infiltration/exfiltration, solar radiation, internal heat gains, thermal mass and TABS.

3.1 The TABS-equipped building and its modeling

The TABS-equipped office building is first introduced in Refs. [*3.1*,*3.2*]. The building is located in Zürich, Switzerland. Its configuration is chosen according to the widespread characteristics of office buildings using TABS as shown in Fig. 3.1: two main orientations (south and north) with normal offices along the main façades and corner offices with glazing on two sides at the front faces. It has five stories and each story has 12 normal offices and 4 corner offices. The total floor area is 2,880 m^2 with dimensions of 6m×6m×3m of each room. The main parameters and indicators of rooms in the reference building are summarized in Table 3.1. In this dissertation, a south-west corner room will be modeled as a benchmark and then parameters of the benchmark room will be varied to do the investigation. The values of the benchmark room in the model may be different from the corresponding values in Table 3.1.

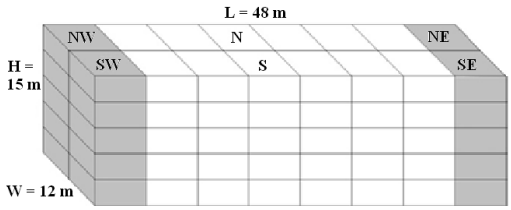

Fig. 3.1. Configuration and orientations of the reference building

Table 3.1. Main parameters and indicators of rooms in the reference building

Room dimensions $L \times W \times H$	6m×6m×3m	Internal wall construction[c]	Light-weight concrete
Mean U-value of the façades	0.65 W/m^2-K	Internal wall area[c]	36 m^2
Air change infiltration[c]	0.1 h^{-1}	**TABS configuration**	
Glazing fraction[a]		Thickness concrete slab	0.25 m
Normal office	21%	Pipe spacing	0.20 m
Corner office	42%	External/internal pipe diameter[c]	20/15 mm
Solar heat gain coefficient for		Specific mass flow rate[b]	15 kg/(h m^2)
Glazing alone	0.41	TABS coverage fraction	80% of floor area
Glazing with sun-shading	0.08	Floor/ceiling covering[c]	Carpet (0.125m^{2}K/W)

[a] Ratio between glazing area and net floor area.

[b] With reference to TABS pipe register area.

[c] These values are from Table 1 of Ref. [*3.2*].

In Refs. [*3.1*,*3.2*], the room of the building was modeled by a resistor-capacitor electric circuit as shown in Fig. 3.2—with various "thermal resistor" *resistance* values, "heat capacity" *capacitance* values, input and output "temperature" *potential* values, and "heat energy gain" *current* values. Notice that, in the references, the symbol ϑ was used for temperatures; we use T as the symbol of temperature here.

Notations:

T_{sw} temperature of the supply water of TABS

T_c core temperature (temperature of the concrete slab at the plane of PEX pipes)

T_{s1} mean temperature of the ceiling slab's interior layer below the core

T_{s2} mean temperature of the floor slab's interior layer above the core

T_{in} indoor air temperature

T_{op} operative temperature of the room

T_{out} outdoor air temperature

q_i'' internal heat gains (including occupants, lighting and appliances)

q_s'' solar heat inputs from windows

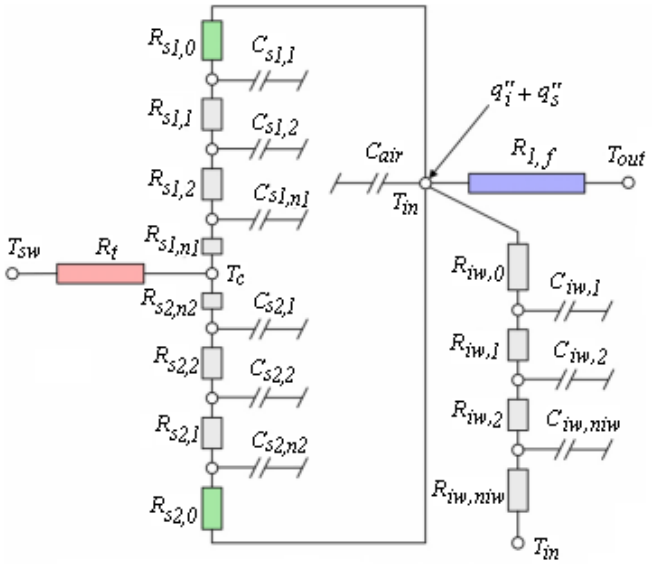

Fig. 3.2. Resistor-capacitor model of a room in the TABS-equipped office building

This model is described in Ref. [*3.1*] as follows:

The slab's core temperature node ϑ_c (T_c) is linked to the supply-water temperature ϑ_{sw} (T_{sw}) by the TABS-resistance R_t and to the (operative) room temperature ϑ_r (T_{in}) by a resistance/capacitor element per slab layer (for modeling purposes the slab is subdivided into several layers). The heat gains (internal, solar) affect the room node, which is linked to the outside air temperature ϑ_{oa} (T_{out}) by a façade-resistance $R_{1,f}$. Investigations have shown that it is essential to incorporate, besides the slabs, additional thermal mass and surface area in the room model to account for heat exchange from/to inside walls and furniture. This is realized by an internal wall link, which consists again of a resistance/capacitor element per wall layer.

The RC model is further developed and investigated in the interactive environment of Matlab and Matlab/Simulink as shown in Fig. 3.3. [*3.3*] Each rectangle is a subsystem and more details are inside. The modules of the internal heat gains, the internal walls and the other interior thermal mass are in the "Building inside" subsystem.

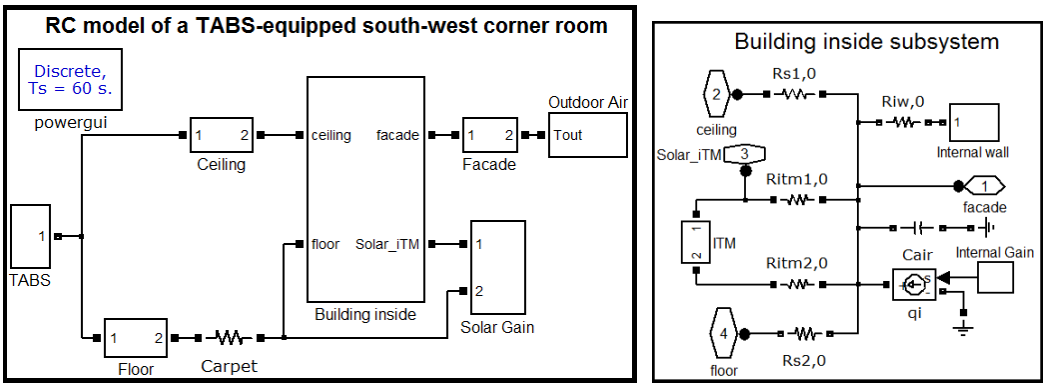

Fig. 3.3. RC model of the south-west corner room in Matlab/Simulink

The model in Fig. 3.3 is slightly modified comparing the model in Refs. [*3.1*,*3.2*]:

(1) A south-west corner room, but not in the bottom or top story, is modeled under cooling condition;

(2) The façade thermal resistance is separated into three parts: resistance of the exterior walls, resistance of the windows, and resistance of infiltration/exfiltration and ventilation;

(3) The operative temperature is calculated by equations given in the *ASHRAE Handbook* [*3.4*: 9.3] and the book *Principles of Heating, Ventilating and Air Conditioning* [*3.5*: 80];

(4) Interior thermal mass (iTM) will be separately considered as TABS, internal walls and other interior thermal mass (including internal furniture, equipment and so on);

(5) The heat gain q_g'' will be divided into internal heat gain q_i'' (from persons, lighting, and equipment) and solar energy input q_s'';

(6) The solar energy input is calculated from the solar geometry and is put onto surfaces of the floor and the thermal mass in the room.

The units of the symbols in the thermal network of the room are compared with that in the electric circuit network. Take one equation from Appendix 2 in Ref. [*3.1*]:

$$C_r \frac{dT_r}{dt} = \frac{1}{R_{1,f}}\left(T_{out} - T_{in}\right) + \frac{1}{R_{iW,0}}\left(T_{iW,1} - T_{in}\right) + \frac{1}{R_{s1,0}}\left(T_{s1,1} - T_{in}\right) + \frac{1}{R_{s2,0}}\left(T_{s2,n2} - T_{in}\right) + q_g'' \qquad (3.1)$$

The units of the symbols in the equation above should be:

C: J/K; T: K; R: K/W; q_g'': W=J/s.

Notice that for electric circuit, the corresponding units of the symbols are:

C: F=C/V; U: V; R: Ω=V/A; I: A=C/s.

The operations of the TABS-equipped room in the daytime and the nighttime are shown in Fig. 3.4 and Fig. 3.5, respectively. In an air conditioned room, a room's temperature is controlled in terms of air temperature T_{in} with no explicit reference to the room's surface temperature. In a thermally activated room, its thermal environment is defined in terms of both thermally activated surfaces and air in space enclosed by the surfaces.

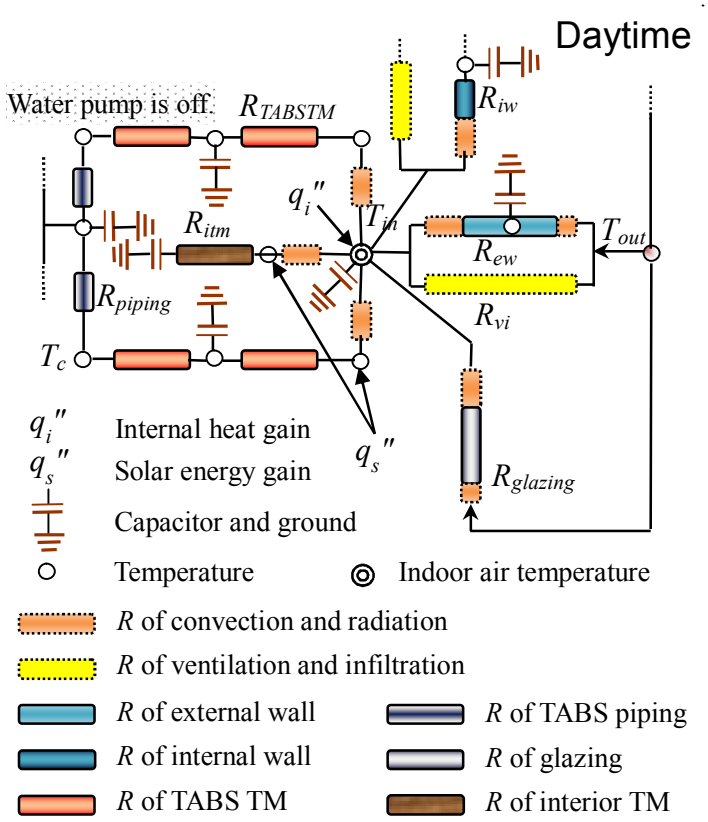

Fig. 3.4. Daytime operation of the TABS-equipped office room
Water pump is off and both rooms' operative temperatures are permitted to float.

Unlike the periodic heating and cooling by air of a concrete slab where only a slab's surface layer is thermally activated [3.6], with water pipe placed in the middle of the slab the whole slab (with its large thermal mass) is activated. As a result, a building's operative temperature T_{op} remains within thermal comfort zone in the daytime, even with

the water pump off [3.7].

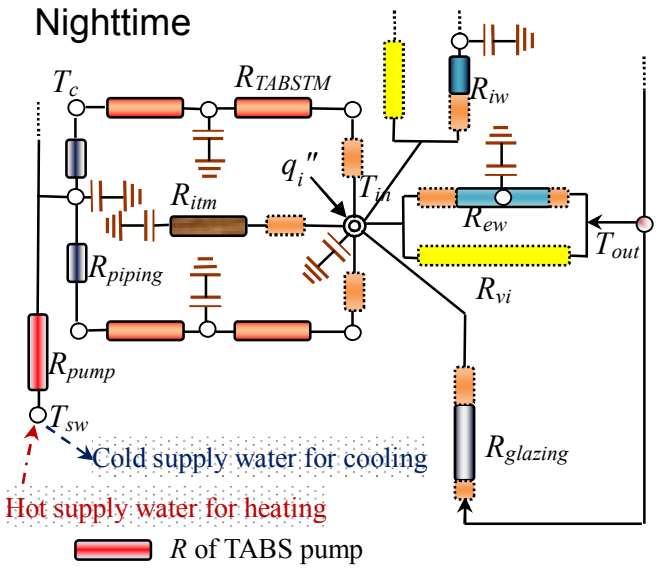

Fig. 3.5. Nighttime operation of the TABS-equipped office room

For cooling, cold water is supplied to remove heat stored in the daytime; for heating, hot water is supplied to add heat into the building and to balance the heat loss in the nighttime and/or daytime.

3.2 Building envelope and its thermal resistance

Main materials in the building are: wood (Fir, pine or similar soft wood), normal-weight (NW) concrete, structural light-weight (LW) concrete, insulating light-weight (LW) concrete and insulation. Their properties are listed in Table 3.2. The properties of the insulation are simplified in the simulations.

Table 3.2. Specifications of building materials

	Conductivity k (W/m K)	Density ρ (kg/m^3)	Heat capacity c_p (kJ/kg K)	c_v (kJ/m^3 K)	Description
Wood	0.12	510	1.382	704.8	low k and small c_v
NW concrete	1.90	2320	0.795	1844.4	high k and large c_v
Structural LW concrete	0.61	1600	0.921	1473.6	moderate k and c_v
Insulating LW concrete	0.14	480	1.000	480.0	low k and very small c_v
Insulation	0.04	0	0	0	very low k and no c_v

The overall thermal resistance of the building envelope contains two parts: the thermal resistances of building materials and the surface air film resistances (interior R_i

and exterior R_o).

Shown in Fig. 3.6 is the *IECC climate zone map* [3.8]. These zones may be further combined into five climate categories: Hot-humid, hot-dry/mixed dry, mixed humid, marine, and cold/very cold. Thus the IECC map allows for up to 24 potential climate designations.

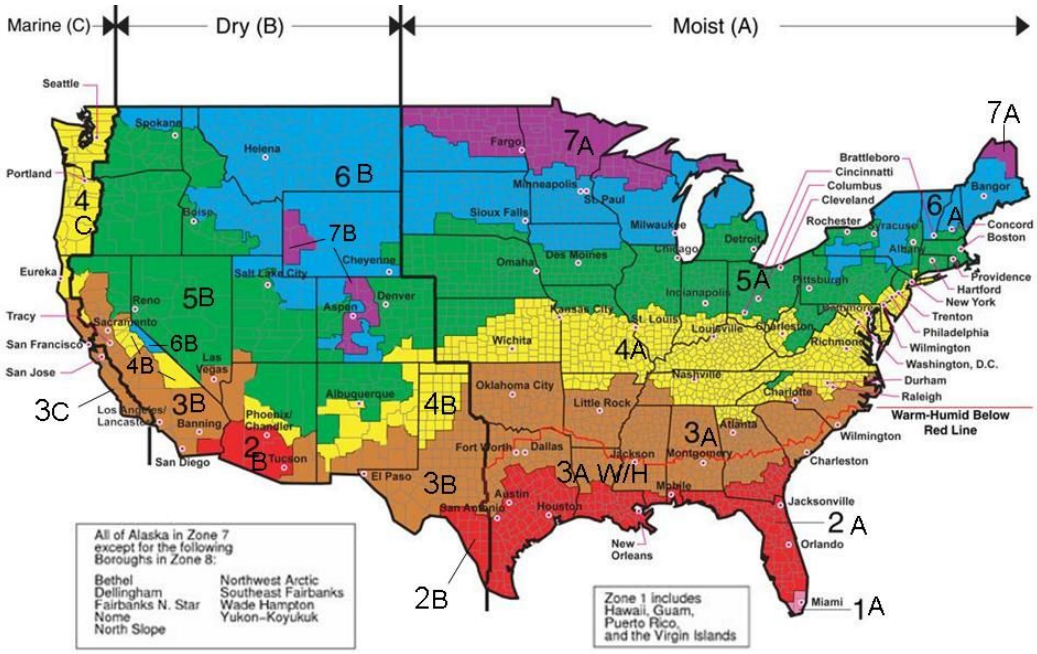

Fig. 3.6. IECC climate zone map

The factors influencing the macro-climate are *latitude*, pattern of *westerlies*, proximity to *ocean*, and *elevation.* For instance: The direction of westerlies benefits west coast states with the temperature moderation of Pacific Ocean making them to be classified Marine climate (but not the eastern coast states, which are influenced by Atlantic but not to the same degree of western coast zone). Some areas of the very cold zone in Rocky Mountain region are clearly the result of high elevation. States of hot-humid climate are near the Gulf of Mexico with warm water and humid air stream.

The IECC map was developed to provide a simplified, consistent approach to defining climate for implementation of various codes. It was based on widely accepted classifications of world climates that have been applied in a variety of different

disciplines. The IECC map was developed by the PNNL (Pacific Northwest National Lab.) and was adopted by the IECC in 2004. The map was adopted by ASHRAE as well; it first appeared in the *ASHRAE Standard 90.1-2004*. The same map is used in the ASHRAE's *AEDG* [3.9].

Both ICC (International Code Council) Code and ASHRAE Standard prescribe their requirements on the basis of the map. Typically the requirement is specified as the thermal resistance of the thermal envelope including wall, ceiling, floor (opaque elements) and fenestration (window element and curtain-wall). ICC uses *2006 IECC* standard as the reference point and ASHRAE uses *ASHRAE Standard 90.1-2004* as the reference point. Both organizations issue revised higher standard every few years and at this time both published standards that are 50% higher than their references. ASHRAE's standard is given in Ref. [*3.9*] and its associated publications as well as the *ASHRAE Standard 90.1-2010* [3.10]. ICC's standard is given in *2012 IECC* [3.8].

Note that both the typical Codes and ASHRAE Standards take into consideration only of macro-climate in terms of climate zone and design temperatures of both summer and winter. No explicit consideration is given to the diurnal temperature variation and the corresponding meso-scale micro-climate as well as numerous other factors in addition to diurnal temperature variation. Clearly these other factors are important in the design of every individual building. In the following chapters, this dissertation will show that diurnal temperature variation must be taken into consideration in the design of all buildings and by doing so we can harness the process of meso-scale micro-climate.

For Zürich, although it is not in the United States, its weather conditions are similar to that of climate zone 5 in the map [3.10: 143]. Therefore, the thermal resistance requirements in Zürich can be found in the IECC and ASHRAE Standard based on zone 5's requirements. The requirements of buildings in zone 5 are listed in Table 3.3, which is part of Table 5.5-5 in the *ASHRAE Standard 90.1-2010* [3.10: 30]. In the table, units of the U-values are W/m^2-K and units of the R-values are m^2-K/W.

Table 3.3. Building Envelope Requirements for Climate Zone 5 (A, B, C)

Opaque Elements	Nonresidential		Residential	
	Assembly Maximum	**Insulation Min. R-Value**	**Assembly Maximum**	**Insulation Min. R-Value**
Roofs				
Insulation Entirely above Deck	U-0.273	R-3.5 c.i.	U-0.273	R-3.5 c.i.
Metal Building	U-0.312	R-2.3+R-2.3	U-0.312	R-2.3+R-2.3
Attic and Other	U-0.153	R-6.7	U-0.153	R-6.7
Walls, Above-Grade				
Mass	U-0.513	R-2.0 c.i.	U-0.453	R-2.3 c.i.
Metal Building	U-0.391	R-2.3+R-1.0 c.i.	U-0.391	R-2.3+R-1.0 c.i.
Steel-Framed	U-0.365	R-2.3+R-1.3 c.i.	U-0.365	R-2.3+R-1.3 c.i.
Wood-Framed and Other	U-0.365	R-2.3+R-0.7 c.i.	U-0.291	R-2.3+R-1.3 c.i.
Walls, Below-Grade				
Below-Grade Wall	C-0.678	R-1.3 c.i.	C-0.678	R-1.3 c.i.
Floors				
Mass	U-0.420	R-1.8 c.i.	U-0.363	R-2.2 c.i.
Steel-Joist	U-0.214	R-5.3	U-0.214	R-5.3
Wood-Framed and Other	U-0.188	R-5.3	U-0.188	R-5.3
Slab-On-Grade Floors				
Unheated	F-1.264	NR	F-0.935	R-1.8 for 600 mm
Heated	F-1.489	R-2.6 for 600 mm	F-1.489	R-2.6 for 600 mm
Opaque Doors				
Swinging	U-3.975		U-2.839	
Nonswinging	U-2.839		U-2.839	
Fenestration	**Assembly Max. U**	**Assembly Max. SHGC**	**Assembly Max. U**	**Assembly Max. SHGC**
Vertical Glazing, 0%–40% of Wall				
Nonmetal framing (all)	U-1.99	SHGC-0.40 all	U-1.99	SHGC-0.40 all
Metal framing (curtainwall/storefront)	U-2.56		U-2.56	
Metal framing (entrance door)	U-4.54		U-4.54	
Metal framing (all other)	U-3.12		U-3.12	

For window systems, the thermal resistances are listed in Table 3.4 [*3.11*: 452].

Table 3.4. Thermal resistance of window system

Window Type	Thermal Resistance	
	ft^2-°F-hr/Btu (m^2-K/W)	
Single Glazing	1	(0.176)
Glass Block	2	(0.353)
Double Glazing Or Storm Window	2.3	(0.406)
Double Glazing With Low-E Coating	3	(0.529)
Triple Glazing	3	(0.529)
Triple Glazing With One Low-E Coating	4	(0.705)
Quadruple Glazing	4	(0.705)
Quadruple Glazing With Low-E	6	(1.058)
Translucent Insulated Composite Panel, 10% Light Transmittance	7	(1.234)
Super Window	8	(1.410)

For wall, roof, floor and door surfaces, standardized surface conductances and resistances are given in Table 3.5 [3.4: 26.1]. Therefore, for non-reflective surfaces with emittance ε = 0.90, standardized inside surface resistances due to air films vary from R-0.61 hr-ft^2-°F/Btu (0.11 m^2-K/W) to R-0.92 (0.16). In this dissertation for simplicity, the value R-0.7 (0.12) will be chosen. For outside surfaces, the resistance is R-0.25 (0.044) in summer or R-0.17 (0.030) in winter.

Table 3.5. Surface conductances and resistances for air

	Position of surface	Direction of heat flow	Surface emittance, ε					
			Non-reflective		Reflective			
			ε = 0.90		ε = 0.20		ε = 0.05	
			h_i	R	h_i	R	h_i	R
Still Air	Horizontal	Upward	1.63 (9.26)	0.61 (0.11)	0.91 (5.17)	1.10 (0.19)	0.76 (4.32)	1.32 (0.23)
	Sloping at 45°	Upward	1.60 (9.09)	0.62 (0.11)	0.88 (5.00)	1.14 (0.20)	0.73 (4.15)	1.37 (0.24)
	Vertical	Horizontal	1.46 (8.29)	0.68 (0.12)	0.74 (4.20)	1.35 (0.24)	0.59 (3.35)	1.70 (0.30)
	Sloping at 45°	Downward	1.32 (7.50)	0.76 (0.13)	0.60 (3.41)	1.67 (0.29)	0.45 (2.56)	2.22 (0.39)
	Horizontal	Downward	1.08 (6.13)	0.92 (0.16)	0.37 (2.10)	2.70 (0.48)	0.22 (1.25)	4.55 (0.80)
Moving Air (any position)			h_o	R				
	15 mph wind (for winter)	Any	6.00 (34.0)	0.17 (0.030)	—	—	—	—
	7.5 mph wind (for summer)	Any	4.00 (22.7)	0.25 (0.044)	—	—	—	—

Notes: 1. Surface conductance h_i and h_o measured in Btu/h-ft^2-°F (W/m^2-K); resistance R in h-ft^2-°F/Btu (m^2-K/W);

2. No surface has both an air space resistance value and a surface resistance value;

3. Conductances are for surfaces of the stated emittance facing virtual black-body surroundings at same temperature as ambient air. Values based on surface/air temperature difference of 10°F (5.5K) and surface temperatures of 70°F (21°C);

4. Condensate can have significant effect on surface emittance.

Indoor surface thermal resistance of the windows is a little different from that of walls, roofs, floors and doors. Indoor surface heat transfer coefficients of vertical glazing are listed in Table 3.6 [3.4: 15.6]. With this table, the indoor surface resistance of the windows can be calculated. Again for simplicity, R-0.7 (0.12) will be chosen.

Table 3.6. Indoor vertical surface heat transfer coefficients (still air conditions)

Glazing type	Glazing height, ft (m)	Winter Conditions[a]			Summer Conditions[b]		
		Glass temp., °F (°C)	Temp. diff., °F (°C)	h_i, Btu/hr-ft^2-°F (W/m^2-K)	Glass temp., °F (°C)	Temp. diff., °F (°C)	h_i, Btu/hr-ft^2-°F (W/m^2-K)
Single glazing	2 (0.6)	17 (-9)	53 (30)	1.41 (8.04)	89 (33)	14 (9)	1.41 (8.10)
	4 (1.2)	17 (-9)	53 (30)	1.31 (7.42)	89 (33)	14 (9)	1.33 (7.64)
	6 (1.8)	17 (-9)	53 (30)	1.25 (7.10)	89 (33)	14 (9)	1.29 (7.41)
Double glazing with 1/2" air space	2 (0.6)	45 (7)	25 (14)	1.36 (7.72)	89 (35)	14 (11)	1.41 (8.30)
	4 (1.2)	45 (7)	25 (14)	1.27 (7.21)	89 (35)	14 (11)	1.33 (7.82)
	6 (1.8)	45 (7)	25 (14)	1.22 (6.95)	89 (35)	14 (11)	1.29 (7.58)
Double glazing with ε=0.1 on surface 2 and 1/2" argon space	2 (0.6)	56 (13)	14 (8)	1.31 (7.44)	87 (34)	12 (10)	1.38 (8.20)
	4 (1.2)	56 (13)	14 (8)	1.23 (7.00)	87 (34)	12 (10)	1.31 (7.73)
	6 (1.8)	56 (13)	14 (8)	1.19 (6.77)	87 (34)	12 (10)	1.27 (7.50)
Triple glazing with ε=0.1 on surfaces 2 and 5 and 1/2" argon spaces	2 (0.6)	63 (17)	7 (4)	1.25 (7.09)	93 (40)	18 (16)	1.45 (8.73)
	4 (1.2)	63 (17)	7 (4)	1.18 (6.72)	93 (40)	18 (16)	1.36 (8.20)
	6 (1.8)	63 (17)	7 (4)	1.15 (6.53)	93 (40)	18 (16)	1.32 (7.94)

Notes: a. Winter conditions: room air temperature t_i = 70°F (21°C), outdoor air temperature t_o = 0°F (-18°C), no solar radiation;

b. Summer conditions: room air temperature t_i = 75°F (24°C), outdoor air temperature t_o = 89°F (32°C), direct solar irradiance E_D = 248 Btu/hr-ft^2 (748 W/m^2).

The thermal resistance network of a common building envelope is shown in Fig. 3.7.

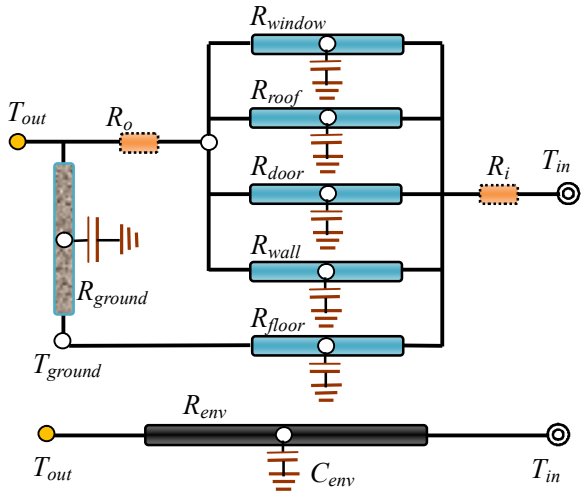

Fig. 3.7. Thermal network of the building envelope

In the benchmark room, only the south- and west-facing walls are exposed to the outdoor air. The roof, floor and the other two walls are all considered as interior thermal mass (iTM). There is no external door and internal doors are neglected. Therefore, only

the required *R*-value or *U*-value of the exterior walls is needed. In this chapter, the *U*-0.365 W/m^2-K is chosen for the benchmark room according to the *ASHRAE Standard 90.1-2010*. The room has a very large Window-to-Wall area Ratio (WWR): 42%, which corresponds a window area of 15.12 m^2.

The external walls consists 20cm-thick normal-weight concrete and insulation outside of the concrete. Due to the insulation, the thermal resistance of the external walls meets the Zone 5's requirements of nonresidential buildings in Table 3.3. The TABS concrete in the roof and floor is 25cm-thick normal-weight concrete and half of it is counted into the room. The floor is covered by carpet with thermal resistance of 0.125 m^2-K/W. The internal walls are made of structural light-weight concrete with thickness of 20 cm. Other interior thermal mass, such as furniture, are considered as wood with dimensions of 6m×6m×0.1m. All the windows are modeled as "double glazing with low-e coating (e=0.05 on surface 2 or 3)" fixed windows. Thermal resistance of the windows is R-3 hr-ft^2-°F/Btu (0.53 m^2-K/W). [*3.11*: 452]

3.3 Ventilation and infiltration/exfiltration

Air exchange of outdoor air and indoor air comes in two classifications [*3.5*: 145~158]: ventilation, which is "the intentional introduction of air from the outside into a building," and infiltration/exfiltration, which is "the uncontrolled flow of outdoor air into a building through cracks and other unintentional openings and through the normal use of exterior doors for entrance and egress." "In passively heated or cooled buildings that are well insulated and maintain a substantial difference in temperature between inside and outside and in buildings with a high occupancy level, the heating and cooling of outside air can become a significant percentage of the thermal load." [*3.12*: 51]

Table 3.7 lists the heat gain/loss of building floor area from ventilation and infiltration/exfiltration in residential buildings. [*3.12*: 52] The thermal resistance due to ventilation and infiltration/exfiltration is the reciprocal of the heat gain/loss values and is

parallel to the building envelope thermal resistance.

Table 3.7. Heat gain/loss from residential ventilation and infiltration/exfiltration

Residential Construction Type	Infiltration heat gain Btu/hr-F-ft^2		Infiltration heat gain W/K-m^2	
	Average (7.5 mph)	Maximum (15 mph)	Average (3.4 m/s)	Maximum (6.7 m/s)
Older building with leaky doors and windows	0.18	0.36	1.02	2.04
Conventional insulated frame construction	0.14	0.27	0.77	1.53
+ plastic vapor barrier	0.09	0.18	0.51	1.02
+ sealed joints & foamed cracks	0.05	0.09	0.26	0.51
+ advanced sealing & heat recovery unit/system	0.02	0.05	0.13	0.26

Notes: 1. The table presents the heat loss/gain of building floor area;
2. For heat gain that imposes a cooling load on the building, the values in the table are for sensible heat only and do not include the energy that would be necessary for dehumidification.

For commercial buildings, a common term used for scaling the ventilation and infiltration/exfiltration is air change per hour (ACH). The infiltration rate of the building is 0.1 ACH (see Table 3.1), which is very air-tight. According to Refs. [*3.4*,*3.5*], the required minimum air change to provide acceptable indoor air quality for office buildings is 5 cfm/person plus 0.06 cfm/ft^2. Therefore, for the room the requirement is about 43 cfm (cubic feet per minute). Therefore, extra ventilation is needed to meet the requirement for indoor air quality. The total air change rate of infiltration and ventilation is 0.7 ACH, which is about 44.5 cfm.

Given in Chapter 18 of Ref. [*3.4*], the total heat gain/loss q_t corresponding to the air change of a given standard flow rate Q_s through an enthalpy difference Δh is

$$q_t = 4.5\, Q_s \Delta h \tag{3.2}$$

in I-P unit (q_t: Btu/h; Q_s: cfm; Δh: Btu/lb), or

$$q_t = 1.2\, Q_s \Delta h \tag{3.3}$$

in S-I unit (q_t: W; Q_s: m^3/s; Δh: J/kg).

Where the enthalpy difference, when the temperature and pressure differences are not very big, can calculated by the following equation:

$$\Delta h = c_p \Delta T \tag{3.4}$$

where c_p is the specific heat at constant pressure in Btu/lb-°F or J/kg-K.

According to the equations above and after some unit conversions, the thermal resistance of ventilation and infiltration/exfiltration is 8.01 hr-ft^2-°F/Btu (1.41 m^2-K/W). Consequently, the heat gain/loss of building floor area is 0.71 W/m^2-K.

3.4 Solar radiation

Radiation solar energy input through glazing is one important part of building energy inputs, especially if the Window-to-Wall area Ratio (WWR) is large. In this section, the total solar energy input through the windows of the building will be calculated by using the method given in Ref. [*3.13*: 18~53].

3.4.1 Solar geometry

The angle of declination, D [degree or °], represents the amount by which the earth's north polar axis is tilted toward the sun. An approximation for D is:

$$D = 23.44 \sin\left(360d/365\right) \tag{3.5}$$

where d is the number of days following the vernal equinox which usually falls near March 21 (or day 80).

The hour angle, H [°], represents one 24-hour day as 360° of angle:

$$H = 15t \tag{3.6}$$

where t is the time in hours (decimally) from solar noon.

The angle of elevation of the sun, A [°] (positive above the horizon and negative below the horizon) and the azimuth angle of the sun, Z [°] (positive to the east and negative to the west if measured from the south), can approximately determine the position of the sun:

$$\sin A = \cos D \cos H \cos L + \sin D \sin L \tag{3.7}$$

$$\sin Z = -\cos D \sin H / \cos A \tag{3.8}$$

or
$$\tan \frac{Z}{2} = \frac{\cos D \sin H}{\cos L \sin D - \sin L \cos D \cos H - \cos A} \tag{3.9}$$

where L [°] is the latitude of the site. Notice that if A is negative, there is no sunshine.

The incident angle, θ [°], represents the angle between the sun's rays and the normal to a plane surface:

$$\cos\theta = \sin A \cos\Sigma + \cos A \sin\Sigma \cos(Z - \phi) \tag{3.10}$$

where Σ [°] is the tilt angle of the plane as measured up from a horizontal surface, and the angle, Φ [°], is the direction in which the plane is tilted measured from Φ=0 at due south and increasing positive as it faces a more easterly direction, and negative to the west.

The solar geometry [3.13: 26] is shown in Fig. 3.8.

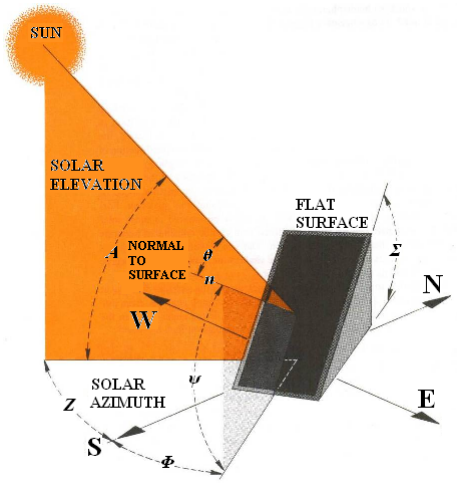

Fig. 3.8. Solar geometry

3.4.2 Solar irradiance

Solar irradiance is the solar intensity that is incident perpendicular (normal) to one unit area of the plane surface.

The direct beam solar irradiance on the tilted plane surface, I_b [Btu/hr-ft^2]:

$$I_b = I_n \cos\theta \tag{3.11}$$

where I_n [Btu/hr-ft^2] is the solar irradiance or direct normal intensity of the sun's radiation.

On a clear day,

$$I_n = I_r e^{-mB} \tag{3.12}$$

where I_r [Btu/hr-ft^2] is the apparent solar irradiation at air mass=1,

B is the atmosphere extinction coefficient,

and m is the air mass given by:

$$m = 1/\sin A \tag{3.13}$$

An approximate formula for I_r is given by:

$$I_r = 0.862\left[I_0 + 27\cos\left(y - 8°\right)\right] \tag{3.14}$$

and for B: $$B = 0.172 - 0.033\cos\left(y - 11°\right) \tag{3.15}$$

where I_0 [Btu/hr-ft^2] is the solar constant:

$$I_0 = 429\,\text{Btu/hr-ft}^2 = 1354\,\text{W/m}^2 \tag{3.16}$$

and y [°] is the year angle:

$$y = \frac{360}{365}\left(d + 80\right) \tag{3.17}$$

If considering the effect of altitude on solar irradiance, m should be replaced by m':

$$m' = me^{-E/E_0} \tag{3.18}$$

where m' is the air mass at elevation E,

E [feet] is the elevation above sea level of the site,

and E_0=30000 feet is the approximate elevation where the atmospheric density is 1/e=37 percent of the standard atmospheric density at sea level.

3.4.3 Total solar energy input through glazing

The total solar irradiance incident upon a flat surface, I_T [Btu/hr-ft^2], is given by:

$$I_T = I_b + I_d + I_f \tag{3.19}$$

where I_b [Btu/hr-ft^2] is the direct beam component of solar irradiance given previously,

I_d [Btu/hr-ft^2] is the diffuse component of solar irradiance,

and I_f [Btu/hr-ft^2] is the reflected component of solar irradiance.

On clear days (i.e., cloudless and sunny), I_d and I_f are approximated by:

$$I_d = C_d I_n F_s \tag{3.20}$$

$$I_f = C_f I_n F_g \tag{3.21}$$

where $F_s = (1+\cos\Sigma)/2$ and $F_g = (1-\cos\Sigma)/2$ are weighted view factors for the sky and ground, respectively.

C_d can be approximately represented by:

$$C_d = 0.094 - 0.031\cos y - 0.013\sin(3y/2) \tag{3.22}$$

C_f is given in Table 3.8 and choose $C_f = 0.2$ in this dissertation.

Table 3.8. Coefficients for reflected solar irradiance on a clear day

Surface	C_f	Surface	C_f
Snow	0.7-0.87	Concrete	0.21-0.33
Bituminous and gravel roofs	0.12-0.15	Grass	0.20-0.30
Bituminous paving	0.10		

A program is written in Matlab to calculate the hour-by-hour solar irradiance. The program is verified by a small software—*RadOnCol*[①]. On July 15 around PSU (Pennsylvania State University, whose latitude is 40.796 °N and elevation is 1154 ft = 351.74 m), when the sky is clear, the solar energy input through one square foot of south-, east-, west- and north-facing window are shown in Fig. 3.9. Notice that in the figure the points of the direct beam and diffuse components of solar irradiance are obtained from

[①] The *Radiation On Collector* program is used to estimate the solar radiation energy incident on a collector based on: the direction the collector is aimed, time of year, position on the earth, altitude of the collector, and the area of the collector.

the *RadOnCol* software. [*3.14*]

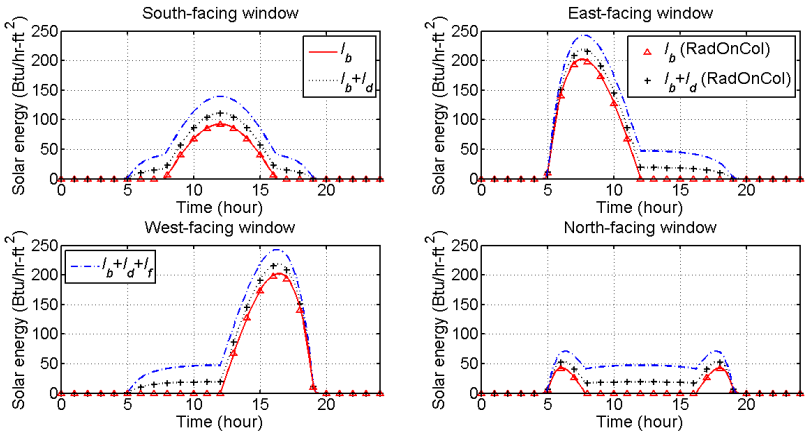

Fig. 3.9. Solar energy input through 1 ft^2 window (PSU, July 15)

Obviously, the program works well and it can be used to calculate the solar energy input through windows. Using the program, the whole-year radiation solar energy gains upon flat surfaces in Zürich can be calculated, as shown in Fig. 3.10.

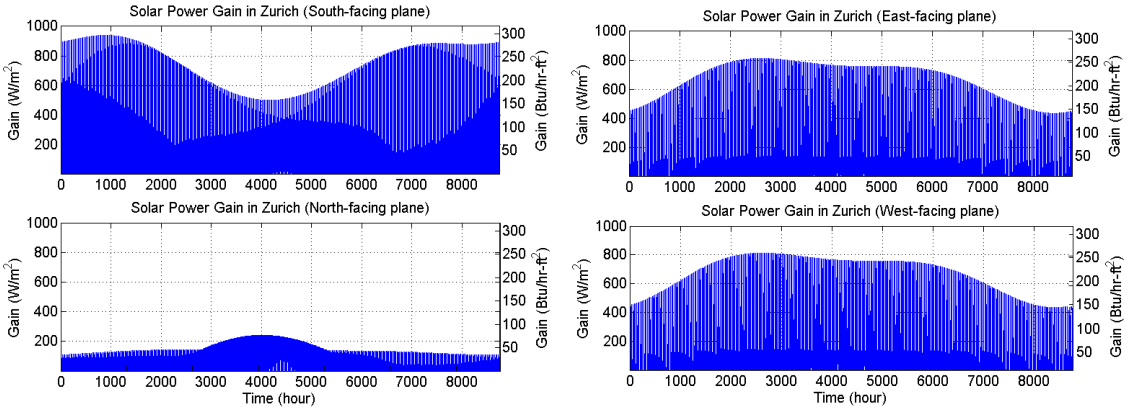

Fig. 3.10. Solar energy gains on vertical planes in Zürich

The average percentage of possible sunshine (a symbol C_{ss} is given) can be found in Ref. [*3.13*: 38]. The percentage of the solar energy through the glazing is defined by the solar heat gain coefficient (*SHGC*, dimensionless). Here we use the value *SHGC* = 0.4. In most buildings, shading strategies are important to control solar heat gain to minimize cooling requirements. In Chapter 15 of Ref. [*3.4*], many details about shading are given. It mentions that outdoor shading devices reduce solar heat gain more effectively than indoor devices, but indoor devices are easier to operate and adjust. It also points out that

"fenestration products fully shaded from the outside reduce solar heat gain by as much as 80%." So assume that only 20% solar energy can go into the building and give a coefficient C_{sd} = 0.20. Therefore, on clear days (i.e., cloudless and sunny), the heat flux of solar energy gain, q_s'' [W/m^2], can be obtained as

$$q_s'' = 3.152 C_{sd} SHGC\left(C_{ss} I_b + I_d + I_f\right) \tag{3.23}$$

Notice that the unit of I_T in the equation is Btu/hr-ft^2, and 1 Btu/hr-ft^2 = 3.152 W/m^2.

3.5 Internal heat gains

The internal heat gains, which are the heat energy generated by occupants, lighting, and appliances, contribute a significant amount of heat to the total sensible and latent heat gains with a building.

According to Table 1 in Ref. [*3.4*: 18.4], the sensible heat and the latent heat from occupants are about 75 W and 55 W, respectively.

The heat gains of the room include internal heat gains q_i'' and solar energy input q_s''. The internal heat gains are put into the indoor air directly. The solar energy input can be calculated from the solar geometry of Zürich, and only 8% goes through the windows because of the good shading by external blinds. The internal heat gains and solar energy input of the south-west corner room are shown in Fig. 3.11.

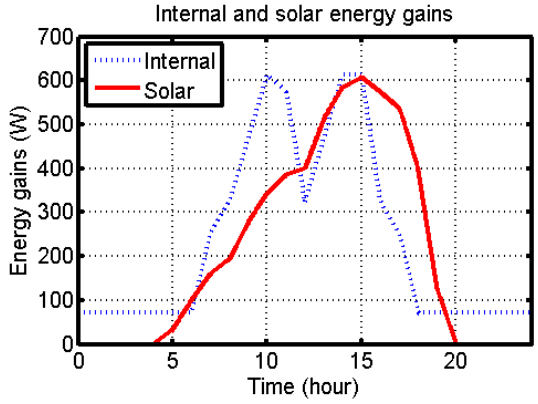

Fig. 3.11. Internal heat gains and solar energy inputs of the south-west corner room

3.6 Thermal mass

"A thermal mass, which can be in the form of water, earth, rock, wood, brick, concrete, or metal, has the ability to absorb and store thermal energy during a warm period of heating (acting as a heat sink, as shown in Fig. 3.12.a) and to release thermal energy during a cool period later (acting as a heat source, as shown in Fig. 3.12.b)." [3.15]

Based on its location and function, building thermal mass can be classified as interior thermal mass (iTM for short, such as furniture, appliances and interior walls, ceilings and floors) and exterior envelope mass (eEM for short, such as exterior walls, roofs/ceilings, floors and windows).

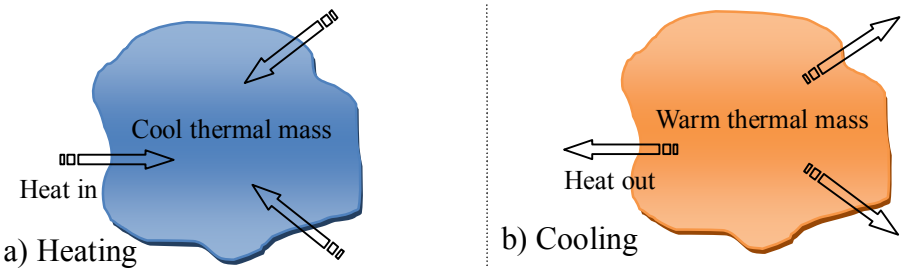

Fig. 3.12. Heating/Cooling of a thermal mass

3.6.1 Problem of using lumped method in thermal mass calculations

Two common measures of the performance of a thermal mass are heat capacity per unit mass (i.e., mass specific heat c_p [kJ/kg-K]), and heat capacity per unit volume (i.e., volumetric specific heat c_{vol} [kJ/m^3-K], which is the product of the density ρ [kg/m^3] and the mass specific heat c_p). If a thermal mass system is subject to a *quasi-static* heating or cooling, the energy balance equation of the system is:

$$Q = mc_p\Delta T = \rho Vc_p\Delta T = Vc_{vol}\Delta T = ALc_{vol}\Delta T \tag{3.24}$$

where Q [kJ] is the amount of heat energy put into or flowed out of a thermal mass, m [kg] is the mass, V [m^3] is the volume, A [m^2] is the heat transfer area, L [m] is the thickness, and ΔT [K or °C] is the change in temperature.

In most literature, heating and cooling of thermal mass was treated as quasi-static processes, that is, the temperature distribution of thermal mass was assumed to be uniform in response to changing air temperature. This means that the thermal diffusion process within thermal mass is much faster than the convective heat transfer at thermal mass surface. This is called lumped method. However, as shown in Ref. [*3.16*], the lumped method can be used only if the Biot number, *Bi*, is very small, that is,

$$Bi = \frac{h}{k}\frac{V}{A} < 0.1 \tag{3.25}$$

where h [W/m^2-K] is the heat transfer coefficient, and k [W/m-K] is the thermal conductivity. For planar thermal mass (most building thermal mass can be considered as planar in shape), it can be simplified as

$$Bi = \frac{hL}{k} < 0.1 \tag{3.26}$$

But, is this condition for the applicability of the lumped method true? A consideration whether this condition applies in building application is in order.

Let's first consider iTM, which usually act as heat storage media. According to Ref. [*3.4*: 26.1], the heat transfer coefficient of indoor air film is typically h_i=1.08~1.63 Btu/h-ft^2-°F, which is 6.13~9.26 W/m^2-K. The thermal conductivity [*3.17*] of fir, pine or similar soft wood is about 0.12 W/m-K. Then we can figure out that the thickness of a wood planar thermal mass should be less than 2 mm, if the Biot number is smaller than 0.1. For normal-weight concrete, the thermal conductivity is 1.90 W/m-K, and the corresponding thickness is about 31 mm. For building brick, the two values are 0.73 W/m-K and 12 mm. It is obvious that, for most furniture, interior walls and especially heavy thermal mass used for controlling indoor temperatures (for example, Trombe wall), the thicknesses are much bigger than the corresponding critical thicknesses, and of course the lumped method cannot be used.

The heat transfer coefficient of outdoor air film [*3.4*: 26.1] is typically h_o=4.00~6.00 Btu/h-ft^2-°F, which is much larger than that of indoor air film. Therefore, for eTM, the critical thicknesses are much smaller and thus lumped method cannot be used, either.

The sizing of thermal mass based on the improper method (lumped method in calculation) will lead to over-heating and over-cooling. These problems will cause uncomfortable thermal condition and high energy consumption. Therefore, in order to saving energy and money by using thermal mass and keeping indoor thermal comfort, it is crucial to developed a more accurate method, rather than the simple lumped method, in thermal mass calculations to determine the proper amount of thermal mass.

3.6.2 Effective heat capacity of interior planar thermal mass

It is difficult to get the heat capacity of a thermal mass if the variation of the environment temperature is irregular. When the indoor air temperature is allowed to float, the temperature variation can be considered approximately as a sine wave; the temperature at the iTM surface can be regarded approximately as a sinusoidal function with a period of 24 hours. In Ref. [*3.16*], this is referred to as *quasi-steady* condition, which "is meant that the unsteady temperature changes repeat themselves steadily." A typical building thermal mass is a planar layer of a given thickness L, which is called Planar Thermal Mass (PTM) in Ref. [*3.15*]. The effective heat capacity of interior PTM (iPTM) subject to sinusoidal heating and cooling was investigated in Ref. [*3.15*].

As shown in Fig. 3.13, the surface temperature T_s [K or °C] of the iPTM is a sinusoidal function with a mean value T_m [K or °C]; the peak amplitude and the period of T_s are $(\Delta T)_s$ and P [s], respectively. The Governing Differential Equation (G.D.E) and the Boundary Conditions (B.C.s) of the iPTM problem are

G.D.E.: $$\frac{\partial^2 T}{\partial x^2} = \frac{1}{\alpha}\frac{\partial T}{\partial t} \tag{3.27}$$

B.C.s: $$-k\left(\frac{\partial T}{\partial x}\right)_L = 0 \tag{3.28}$$

$$T(0,t) = T_s = (\Delta T)_s \sin\left(\frac{2\pi}{P}t\right) + T_m \tag{3.29}$$

where α [m^2/s] is the thermal diffusivity and t [s] is the time.

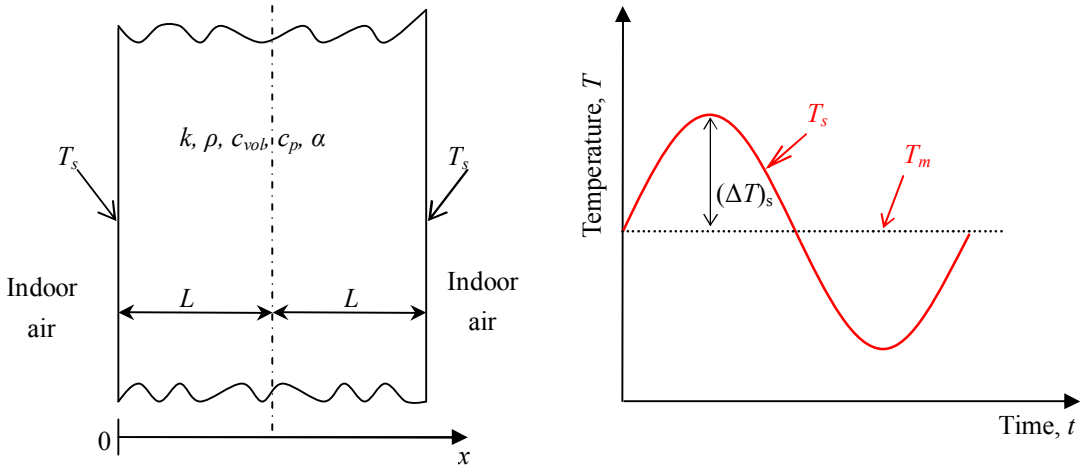

Fig. 3.13. IPTM and its surface temperature T_s

Assumptions and limitations of the problem are summarized as follows:

(1) It is for interior Planar Thermal Mass (iPTM);

(2) The iPTM is single-layer and homogeneous;

(3) All the thermo-physical properties of the iPTM are constant;

(4) The surface temperature of the iPTM is a sinusoidal function with a 24-hour period;

(5) There is no energy sources/sinks in the iPTM.

By defining a temperature variable as

$$\theta(x,t) = T(x,t) - T_m \tag{3.30}$$

the G.D.E. and B.C.s can be rewritten as

G.D.E.: $$\frac{\partial^2 \theta}{\partial x^2} = \frac{1}{\alpha}\frac{\partial \theta}{\partial t} \tag{3.31}$$

B.C.s: $$\left(\frac{\partial \theta}{\partial x}\right)_L = 0 \tag{3.32}$$

$$\theta(0,t) = T_s - T_m = (\Delta T)_s \sin\left(\frac{2\pi}{P}t\right) \tag{3.33}$$

Analytical solution of the problem above was given by Ref. [*3.15*]:

$$\theta(x,t)=(\Delta T)_s \frac{\left\{\begin{array}{l} e^{\frac{\delta x}{L}}\sin\left(\frac{2\pi t}{P}+\frac{\delta x}{L}\right)+e^{2\delta-\frac{\delta x}{L}}\sin\left(\frac{2\pi t}{P}-\frac{\delta x}{L}+2\delta\right) \\ +e^{2\delta+\frac{\delta x}{L}}\sin\left(\frac{2\pi t}{P}+\frac{\delta x}{L}-2\delta\right)+e^{4\delta-\frac{\delta x}{L}}\sin\left(\frac{2\pi t}{P}-\frac{\delta x}{L}\right) \end{array}\right\}}{1+2e^{2\delta}\cos(2\delta)+e^{4\delta}} \tag{3.34}$$

where $$\delta \equiv L\sqrt{\frac{\pi}{\alpha P}} \tag{3.35}$$

which is called dimensionless thickness.

From the Fourier's Law of heat conduction for a one-dimensional system

$$q'' = -k\frac{\partial T}{\partial x} = -k\frac{\partial \theta}{\partial x} \tag{3.36}$$

the heat flux q'' [W/m^2] at any distance x from the surface can be obtained

$$q''=-k(\Delta T)_s \frac{\sqrt{2}\delta}{L}\frac{\left\{\begin{array}{l} e^{\frac{\delta x}{L}}\sin\left(\frac{2\pi t}{P}+\frac{\delta x}{L}+\frac{\pi}{4}\right)-e^{2\delta-\frac{\delta x}{L}}\sin\left(\frac{2\pi t}{P}-\frac{\delta x}{L}+2\delta+\frac{\pi}{4}\right) \\ +e^{2\delta+\frac{\delta x}{L}}\sin\left(\frac{2\pi t}{P}+\frac{\delta x}{L}-2\delta+\frac{\pi}{4}\right)-e^{4\delta-\frac{\delta x}{L}}\sin\left(\frac{2\pi t}{P}-\frac{\delta x}{L}+\frac{\pi}{4}\right) \end{array}\right\}}{1+2e^{2\delta}\cos(2\delta)+e^{4\delta}} \tag{3.37}$$

Let $x = 0$, and the heat flux at the surface is given by

$$q_0'' = -\frac{\sqrt{2}k\delta(\Delta T)_s}{L}\sqrt{\frac{1+e^{4\delta}-2e^{2\delta}\cos(2\delta)}{1+e^{4\delta}+2e^{2\delta}\cos(2\delta)}}\sin\left(\frac{2\pi t}{P}-\varphi_0\right) \tag{3.38}$$

where $$\tan\varphi_0 = \frac{2e^{2\delta}\sin(2\delta)+e^{4\delta}-1}{2e^{2\delta}\sin(2\delta)-e^{4\delta}+1} \tag{3.39}$$

By integrating the surface heat flux in a half period, the amount of net-in or net-out heat per unit area of the iPTM in one period can be obtained as

$$\frac{Q_{0\,max}}{A} = \zeta_0 c_{area}^{eff}(\Delta T)_s \tag{3.40}$$

where $$\zeta_0 = \sqrt{\frac{1+e^{4\delta}-2e^{2\delta}\cos(2\delta)}{1+e^{4\delta}+2e^{2\delta}\cos(2\delta)}} \tag{3.41}$$

$$L^{eff} = \sqrt{2\alpha P/\pi} \tag{3.42}$$

and $$c_{area}^{eff} = \rho c_p L^{eff} \tag{3.43}$$

ζ_0, c_{area}^{eff} [kJ/m^2-K] and L^{eff} [m] are called effective thermal mass coefficient, effective area specific heat and effective thickness, respectively.

The curve of ζ_0 against δ is shown in Fig. 3.14.

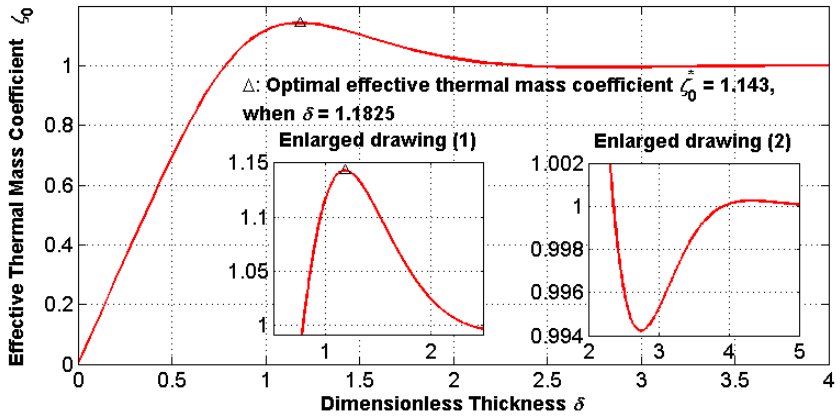

Fig. 3.14. Effective thermal mass coefficient ζ_0

From Fig. 3.14, we find the optimal effective thermal mass coefficient ζ_0^* =1.143 at the optimal dimensionless thickness δ^* = 1.1825. Thus the maximum amount of heat stored by an iPTM is

$$Q_{0max}\left(2L^*\right) = 2\zeta_0^* A c_{area}^{eff} \left(\Delta T\right)_s \tag{3.44}$$

where $$L^* = \delta^* L^{eff} / \sqrt{2} \tag{3.45}$$

which is called optimal thermal mass thickness.

Therefore, from the consideration of building material as thermal mass rather than as structural material, there is no rationale of using thickness greater than the optimal thermal mass thickness.

If the surface temperature T_s is replaced by an indoor air temperature T_{in}

$$T_{in} = \left(\Delta T\right)_{in} \sin\left(\frac{2\pi t}{P}\right) + T_m \tag{3.46}$$

a convective effect coefficient ς should be multiplied:

$$Q_{0max} = \varsigma\zeta_0 A c_{area}^{eff} \left(\Delta T\right)_{in} \tag{3.47}$$

where $$\varsigma = \frac{\left(\Delta T\right)_s}{\left(\Delta T\right)_{in}} = \frac{R_{eff}}{1/h + R_{eff}} \tag{3.48}$$

and $$R_{eff} = \frac{P/2}{\zeta_0 c_{area}^{eff}} \tag{3.49}$$

which is called effective thermal resistance [m^2-K/W].

The variation of the convective effect coefficient is very large, depending on material and thickness of iPTM and the heat transfer coefficient of indoor air film.

If the thickness of iPTM is small (less than 10 cm), the amount of heat storage is almost linear with thickness for most iPTMs. In Ref. [*3.15*], a new definition— effective volumetric specific heat c_{vol}^{eff} is suggested to replace the volumetric specific heat c_{vol} in lumped method for heating and cooling calculations of thin iPTMs. For wood, normal-weight concrete and steel, the values of c_{vol}^{eff} are 594.5, 1326.5 and 2162.5 kJ/m^3-K, respectively, while the values of c_{vol} are 704.8, 1844.4 and 3930.7 kJ/m^3-K, respectively.

However, there are also many iPTMs whose thickness exceeds the linear part. For example, interior walls, ceilings, floors, and especially Trombe walls which are used to control the indoor air temperature. In these cases, the analytical solutions should be used to get more acute results.

3.6.3 Effective heat capacity of exterior planar thermal mass

In Ref. [*3.18*], the dynamic heat transfer problem of exterior PTM (ePTM) under external sinusoidal heating and cooling and internal constant thermal environment was investigated. The G.D.E and the B.C.s of the ePTM problem are

G.D.E.: $$\frac{\partial^2 T}{\partial x^2} = \frac{1}{\alpha}\frac{\partial T}{\partial t} \tag{3.50}$$

B.C.s: $$T(0,t) = T_s = (\Delta T)_s \sin\left(\frac{2\pi}{P}t\right) + T_m \tag{3.51}$$

$$-k\left(\frac{\partial T}{\partial x}\right)_L = h\left[T(L,t) - T_{in}\right] = h\left[T_{sL} - T_{in}\right] \tag{3.52}$$

Again, let

$$\theta(x,t) = T(x,t) - T_m \tag{3.53}$$

the G.D.E. and B.C.s can be rewritten as

G.D.E.: $$\frac{\partial^2 \theta}{\partial x^2} = \frac{1}{\alpha}\frac{\partial \theta}{\partial t} \tag{3.54}$$

B.C.s: $$\theta(0,t) = T_s - T_m = (\Delta T)_s \sin\left(\frac{2\pi}{P}t\right) \tag{3.55}$$

$$\left(\frac{\partial \theta}{\partial x}\right)_L = -\frac{h}{k}\theta(L,t) \tag{3.56}$$

When the indoor air temperature is equal to the mean value of the ePTM outer surface temperature, analytical solution of the problem above is:

$$\theta(x,t) = (\Delta T)_s \frac{A_2 B_1 - A_1 B_2}{B_1^2 + B_2^2} \tag{3.57}$$

where $$A_1 = \left\{ \begin{array}{l} \varepsilon\left[e^{\left(2\delta - \frac{\sqrt{2}x}{L^{eff}}\right)} \cos\left(2\delta - \frac{\sqrt{2}x}{L^{eff}} + \frac{2\pi t}{P}\right) - e^{\frac{\sqrt{2}x}{L^{eff}}} \cos\left(\frac{\sqrt{2}x}{L^{eff}} + \frac{2\pi t}{P}\right)\right] \\ +\sqrt{2}\left[e^{\left(2\delta - \frac{\sqrt{2}x}{L^{eff}}\right)} \cos\left(2\delta - \frac{\sqrt{2}x}{L^{eff}} + \frac{2\pi t}{P} + \frac{\pi}{4}\right) + e^{\frac{\sqrt{2}x}{L^{eff}}} \cos\left(\frac{\sqrt{2}x}{L^{eff}} + \frac{2\pi t}{P} + \frac{\pi}{4}\right)\right] \end{array} \right\} \tag{3.58}$$

$$A_2 = \left\{ \begin{array}{l} \varepsilon \left[e^{\left(2\delta - \frac{\sqrt{2}x}{L^{eff}}\right)} \sin\left(2\delta - \frac{\sqrt{2}x}{L^{eff}} + \frac{2\pi t}{P}\right) - e^{\frac{\sqrt{2}x}{L^{eff}}} \sin\left(\frac{\sqrt{2}x}{L^{eff}} + \frac{2\pi t}{P}\right) \right] \\ +\sqrt{2}\left[e^{\left(2\delta - \frac{\sqrt{2}x}{L^{eff}}\right)} \sin\left(2\delta - \frac{\sqrt{2}x}{L^{eff}} + \frac{2\pi t}{P} + \frac{\pi}{4}\right) + e^{\frac{\sqrt{2}x}{L^{eff}}} \sin\left(\frac{\sqrt{2}x}{L^{eff}} + \frac{2\pi t}{P} + \frac{\pi}{4}\right) \right] \end{array} \right\} \tag{3.59}$$

$$B_1 = \varepsilon\left[e^{2\delta}\cos(2\delta) - 1\right] + \left[e^{2\delta}\cos(2\delta) - e^{2\delta}\sin(2\delta) + 1\right] \tag{3.60}$$

$$B_2 = \varepsilon\left[e^{2\delta}\sin(2\delta)\right] + \left[e^{2\delta}\cos(2\delta) + e^{2\delta}\sin(2\delta) + 1\right] \tag{3.61}$$

and $$\varepsilon \equiv \frac{hL^{eff}}{\sqrt{2}k} \tag{3.62}$$

which is called dynamic Biot number.

Since A_1 and A_2 are functions of x and B_1 and B_2 are not,

$$q'' = -k\frac{\partial T}{\partial x} = -k\frac{\partial \theta}{\partial x} = -k\frac{(\Delta T)_0}{B_1^2 + B_2^2}\left(B_1\frac{\partial A_2}{\partial x} - B_2\frac{\partial A_1}{\partial x}\right) \tag{3.63}$$

Let $x = 0$, and the heat flux at the outer surface can be gotten as

$$q_0'' = -\frac{\sqrt{2}k(\Delta T)_0}{L^{eff}}\sqrt{\frac{D_1^2 + D_2^2}{B_1^2 + B_2^2}}\sin\left(\frac{2\pi t}{P} - \varphi_0\right) \tag{3.64}$$

where $$D_1 = \varepsilon\left(e^{2\delta}\sin 2\delta + e^{2\delta}\cos 2\delta + 1\right) + 2\left(e^{2\delta}\cos 2\delta - 1\right) \tag{3.65}$$

$$D_2 = \varepsilon\left(e^{2\delta}\sin 2\delta - e^{2\delta}\cos 2\delta - 1\right) + 2e^{2\delta}\sin(2\delta) \tag{3.66}$$

and $$\tan\varphi_0 = \frac{B_1D_1 + B_2D_2}{B_1D_2 - B_2D_1} \tag{3.67}$$

Let $x = L$, and the heat flux at the inner surface can be gotten as

$$q_L'' = -\frac{\sqrt{2}k(\Delta T)_0}{L^{eff}}\sqrt{\frac{F_1^2 + F_2^2}{B_1^2 + B_2^2}}\sin\left(\frac{2\pi t}{P} - \varphi_L\right) \tag{3.68}$$

where $$F_1 = 2\varepsilon e^{\delta}\left(\sin\delta + \cos\delta\right) \tag{3.69}$$

$$F_2 = 2\varepsilon e^{\delta}\left(\sin\delta - \cos\delta\right) \tag{3.70}$$

and $$\tan\varphi_L = \frac{B_1F_1 + B_2F_2}{B_1F_2 - B_2F_1} \tag{3.71}$$

At the inner surface, the amount of heat exchanged in the duration from t_1 to t_2 can be gotten as

$$\frac{Q_L}{A} = \int_{t_1}^{t_2} q_L^{"} dt = \frac{1}{2}\zeta_{\varepsilon,\delta}^{L} c_{area}^{eff} (\Delta T)_0 \cos\left(\frac{2\pi t}{P} - \varphi_L\right)\Bigg|_{t_1}^{t_2} \tag{3.72}$$

where $$\zeta_{\varepsilon,\delta}^{L} = \frac{\sqrt{2}}{2}\sqrt{\frac{F_1^2 + F_2^2}{B_1^2 + B_2^2}} \tag{3.73}$$

which is called inner effective heat exchange coefficient for certain ε and δ.

The amount of heat stored in the ePTM in a period from t_1 to t_2 can be gotten as

$$\frac{Q_{stor}}{A} = \int_{t_1}^{t_2} \left(q_0^{"} - q_L^{"}\right) dt = \frac{1}{2}\zeta_{\varepsilon,\delta}^{stor} c_{area}^{eff} (\Delta T)_0 \cos\left(\frac{2\pi t}{P} - \varphi_{stor}\right)\Bigg|_{t_1}^{t_2} \tag{3.74}$$

where $$\tan\varphi_{stor} = \frac{B_1D_1 + B_2D_2 - B_1F_1 - B_2F_2}{B_1D_2 - B_2D_1 - B_1F_2 + B_2F_1} \tag{3.75}$$

and $$\zeta_{\varepsilon,\delta}^{stor} = \frac{\sqrt{2}}{2}\sqrt{\frac{(D_1 - F_1)^2 + (D_2 - F_2)^2}{B_1^{\,2} + B_2^{\,2}}} \tag{3.76}$$

which is called effective thermal storage coefficient for certain ε and δ, as shown in Fig. 3.15. The curve when $\varepsilon \to 0$ in Fig. 3.15 is exactly the same as the curve in Fig. 3.14.

When the indoor air temperature is not equal to the mean value of the ePTM outer surface temperature, an approximated solution of temperature distribution was developed [*3.18*] based on the principle of superposition and validated by numerical method. It found that the effective thermal storage capacity is identical for the same thermal mass.

Although the two papers [*3.15,3.18*] focused on iPTM and ePTM are the first literature in English that systematically investigated the dynamic heat transfer and storage problem of thermal mass in buildings, they are not complete. Especially in the second paper [*3.18*], the indoor air temperature is treated as a constant, that is, it assumed a fixed indoor air temperature, which is exactly the same treatment in the ASHRAE's air heat balance

design approach. [3.4] This shortcoming limits its wide application in building thermal mass design. In this dissertation, the RC model built in Matlab is a dynamic (time-dependent) model, which will overcome the shortcoming and give a better method for thermal mass design in buildings.

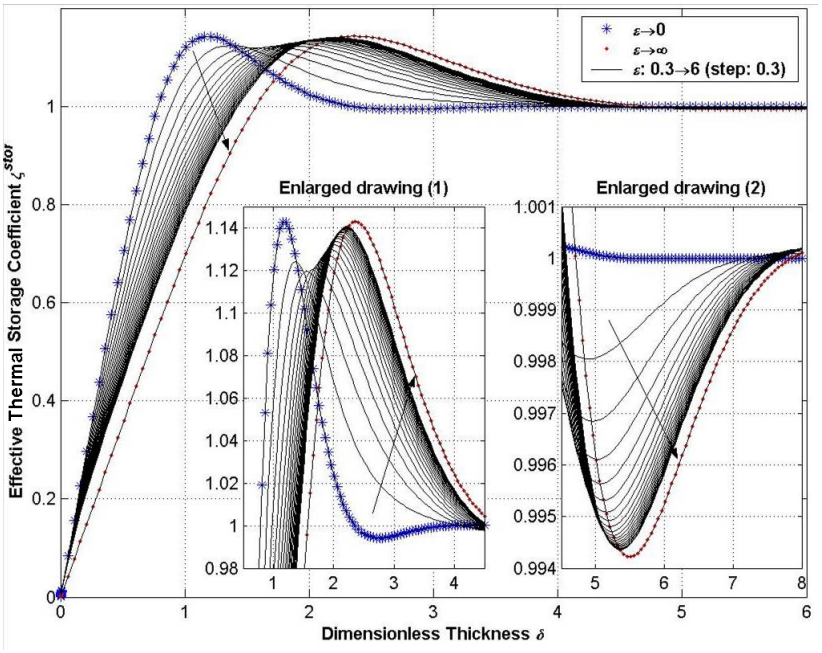

Fig. 3.15. Effective thermal storage coefficient

3.6.4 Thermal mass in the room

In the benchmark room, the external walls consists 20cm-thick NW concrete and insulation outside of the concrete. So the total heat capacity of the exterior envelope mass (eEM) is 7.70×10^6 J/K. The TABS concrete in the roof and floor is 25cm-thick NW concrete and half of it is counted into the room. Thus the total heat capacity of the TABS mass is 16.60×10^6 J/K. The water in the TABS pipes is about 51.5 kg and its heat capacity is 0.22×10^6 J/K, which is ignorable. The internal walls are made of structural LW concrete with thickness of 20 cm. As half of them are counted into the room, the total heat capacity of the interior walls is 5.30×10^6 J/K. Other interior thermal mass, such as furniture, is considered as wood with dimensions of 6m×6m×0.1m. The total heat

capacity of the thermal mass is 2.54×10^6 J/K. The heat capacity of the windows is neglected. The indoor air also has a very small heat capacity 0.14×10^6 J/K.

3.7 TABS total thermal resistance

The floor and ceiling (with TABS in them) can be considered as a piping system embedded in a slab, as shown in Fig. 3.16. [3.1]

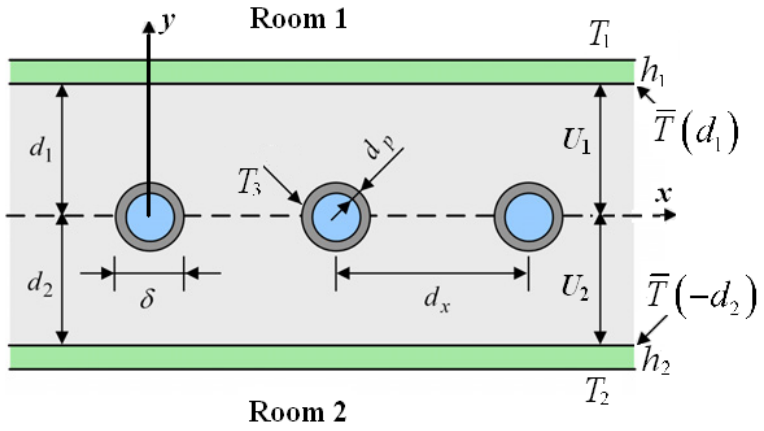

Fig. 3.16. Piping system embedded in a slab

In Ref. [*3.19*], the 2-dimensional stationary temperature distribution in a cross section with inserted pipes and adjacent rooms (as shown in Fig. 3.16) was given by the following equation:

$$T(x,y)=T_1+\frac{\frac{1}{h_1}+\frac{d_1-y}{k_b}}{\frac{1}{U_1}+\frac{1}{U_2}}(T_2-T_1)-\Gamma\left(T_3-T_1-\frac{U_2}{U_1+U_2}(T_2-T_1)\right)\cdot \left\{\frac{\pi}{d_x}\left(\frac{U_1-U_2}{U_1+U_2}y-\frac{2k_b}{U_1+U_2}+|y|\right)-\sum_{s=1}^{\infty}\frac{1}{s}\left[e^{-\frac{2\pi s}{d_x}|y|}+g_1(s)e^{-\frac{2\pi s}{d_x}y}+g_2(s)e^{\frac{2\pi s}{d_x}y}\right]\cdot\cos\left(2\pi s\frac{x}{d_x}\right)\right\} \tag{3.77}$$

where

$$\Gamma=\left[\ln\left(\frac{d_x}{\pi\cdot\delta}\right)+\frac{2\pi k_b}{d_x(U_1+U_2)}+\sum_{s=1}^{\infty}\frac{g_1(s)+g_2(s)}{s}\right]^{-1} \tag{3.78}$$

$$U_i=\left[\frac{1}{h_i}+\frac{d_i}{k_b}\right]^{-1}\qquad i\in\{1,2\} \tag{3.79}$$

and
$$g_i(s) = \frac{\frac{\frac{h_i}{k_b}d_x + 2\pi s}{\frac{h_i}{k_b}d_x - 2\pi s} \cdot e^{-\frac{4\pi s}{d_x}d_{3-i}} - e^{-\frac{4\pi s}{d_x}(d_1+d_2)}}{e^{-\frac{4\pi s}{d_x}(d_1+d_2)} - \frac{\frac{h_1}{k_b}d_x + 2\pi s}{\frac{h_1}{k_b}d_x - 2\pi s} \cdot \frac{\frac{h_2}{k_b}d_x + 2\pi s}{\frac{h_2}{k_b}d_x - 2\pi s}} \tag{3.80}$$

In the equations above, T_i [K or °C] are the average temperatures of the TABS on surface i; h_i [W/m^2-K] are the heat transfer coefficients on surface i; d_i [m] are the distances from the TABS core surface to surface i; U_i [W/m^2-K] are the thermal conductances between the TABS core surface and surface i; d_x [m] is the space between two adjacent water pipes; δ [m] is the outer diameter of the TABS pipes; and k_b [W/m-K] is the thermal conductivity of the TABS concrete.

In Chapter 4 of Ref. [*3.20*], based on the analysis of Equation (3.77), the 3-dimensional, unsteady heat transfer problem of TABS was approximated to a 1-dimensional version under the assumption of $d_{in}/d_x > 0.3$ and $\delta/d_x < 0.2$, where d_{in} [m] is the inner diameter of the water pipes. Fig. 3.16 was simplified in Fig. 3.17.

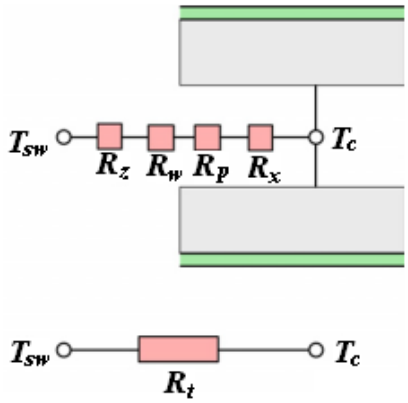

Fig. 3.17. Total resistance between the supply-water temperature and the mean core temperature in TABS

The total thermal resistance of TABS R_t [m^2-K/W] between the supply-water temperature T_{sw} [K or °C] and the TABS mean core temperature T_c [K or °C] was

obtained by the series connection of individual thermal resistances:

$$R_t = R_z + R_w + R_p + R_x \tag{3.81}$$

where R_z [m^2-K/W] is the equivalent resistance in the z-direction (along the pipe):

$$R_z = \frac{1}{2\dot{m}_{sp} c_w} \tag{3.82}$$

R_w [m^2-K/W] is the resistance caused by convection with the reference surface $d_x \cdot l$:

$$R_w = \frac{d_x}{\pi h_w d_{in}} \tag{3.83}$$

R_p [m^2-K/W] is the resistance due to the cylindrical pipe wall with the reference surface $d_x \cdot l$:

$$R_p = \frac{d_x \ln\left(\frac{\delta}{d_{in}}\right)}{2\pi k_p} \tag{3.84}$$

and R_x [m^2-K/W] is the resistance due to the inserted pipe:

$$R_x = \frac{d_x \ln\left(\frac{d_x}{\pi\delta}\right)}{2\pi k_b} \tag{3.85}$$

In this case, turbulent flow ($\mathrm{Re} \geq 2300$) was used for the convective heat transfer coefficient h_w [W/m^2-K] from the water to the pipe wall:

$$h_w = 2040\left(1 + 0.015 T_w\right) \frac{v_w^{0.87}}{d_{in}^{0.13}} \tag{3.86}$$

where v_w [m/s] is the fluid velocity in the pipe, which can be determined as follows:

$$v_w = \frac{\dot{m}}{\rho_w \frac{\pi}{4} d_{in}^2} \tag{3.87}$$

$\dot{m}$ [kg/s] is the mass flow rate of the water:

$$\dot{m} = \dot{m}_{sp} d_x l \tag{3.88}$$

In the equations above, $\dot{m}_{sp}$ [kg/s-m^2] is the specific mass flow rate of the water; c_w [J/kg-K] is the specific heat capacity of the water; T_w [K or °C] is the mean temperature of the water; ρ_w [kg/m^3] is the density of the water; l [m] is the length of the pipe; k_p [W/m-K] is the thermal conductivity of the pipe wall.

In Section 4.5 of Ref. [*3.20*], this simplified model was compared with time-dependent FEM (Finite Element Method) calculation, as shown in Fig. 3.18. It was concluded that there is a good agreement between the simplified model and the FEM calculation.

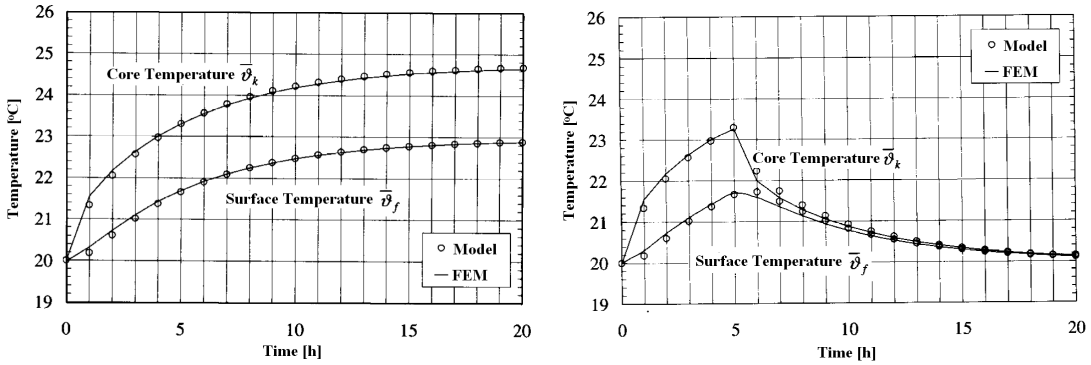

Fig. 3.18. Comparison between the simplified model and the FEM calculation

When the ratio of the pipe spacing to the pipe diameter is small, that is, $\delta/d_x > 0.2$, a different calculation method was developed in Chapter 5 of Ref. [*3.20*]. For the convective heat transfer coefficient h_w in Eq. (3.86), laminar flow in capillary pipes ($\mathrm{Re} < 2300$) should be chosen:

$$h_w = \frac{k_w}{d_{in}}\left(49.03 + 4.17 \frac{4}{\pi} \frac{\dot{m}_{sp} c_w d_x}{k_w} \right)^{\frac{1}{3}} \tag{3.89}$$

Furthermore, Eq. (3.85) should be changed into:

$$R_x = \frac{d_x \frac{1}{3}\left(\frac{d_x}{\pi\delta} \right)}{2\pi k_{ts}} \tag{3.90}$$

where k_{ts} [W/m-K] is the thermal conductivity of the rectangular pipe layer, in which the capillary pipes are inserted.

The TABS-resistance in the benchmark room is R_t = 0.102 m^{2}K/W according to Table 2 in Ref. [*3.1*] or Table 3.1 in this chapter.

3.8 The time-dependent temperatures of the room

Using the RC model, the time-dependent temperatures of the benchmark room are calculated. Let us consider two basic cases. Basic case 1: supply constant temperature water for the whole day; Basic case 2: supply constant temperature water from 6:00PM to 6:00AM. Temperatures in the two basic cases are shown in Fig. 3.19. In July in Zürich, the monthly average-low, mean and average-high temperatures [*3.21*] are 8 °C, 19 °C and 29 °C, respectively. So the daily outdoor air temperature is assumed as a sinusoidal function with mean value of 19 °C and amplitude of 10 °C. According to the heating and cooling curves in Ref. [*3.1*], the supply water temperature is 21.0 °C.

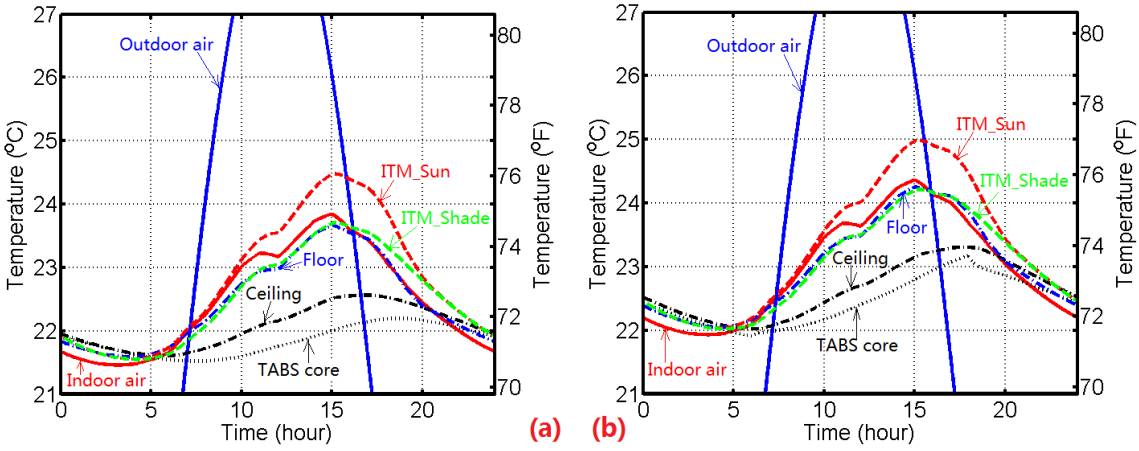

Fig. 3.19. Time-dependent temperatures of the benchmark room

(a) Basic case 1: constant supply water temperature; (b) Basic case 2: constant supply water temperature from 6:00PM to 6:00AM. The floor temperature is at the carpet surface, so it is higher than the ceiling surface temperature.

In part (a) of Fig. 3.19 (Basic case 1), it is clear that the variations of indoor temperatures are much smaller than outdoor air temperature variation. Since solar energy is partially put onto the iTM surface, the Sun-facing surface temperature can increase up to 24.5 °C near 3:00PM; the shaded iTM surface temperature is more stable. The indoor air temperature range is 21.4 °C ~ 23.8 °C, which is cozy in hot summer. Due to the

activation by the cold water circuits, the floor and ceiling surface temperatures are lower than the indoor air temperature in the daytime; in the nighttime, because of the heat loss through the room envelope, the indoor air temperature is even lower than the floor and ceiling surface temperatures. The floor is hotter due to the carpet cover and the solar energy gain; around peak load time, the temperature difference between the floor and ceiling is about 1.0 °C. The TABS core temperature varies in about 0.7 °C, which is very small.

In part (b) of Fig. 3.19 (Basic case 2), all temperatures increase about 0.5~1.0 °C comparing with the corresponding temperatures in Basic case 1. The trends of the temperatures, except the TABS core temperature, are the same as that in Basic case 1. In Basic case 2, the TABS core temperature increases about 1.3 °C in the daytime because of the heat energy absorption and storage.

Combining all the temperatures in the room, include temperatures of the windows and the external and internal walls that are not shown in Fig. 3.19, the operative temperatures of the two basic cases are shown in Fig. 3.20. In the figures, the variation trends and the ranges of the two operative temperatures are almost the same; the operative temperature level increases about 0.5 °C in the second case; the total variation of the operative temperatures is about 2.0 °C, which is good for thermal comfort.

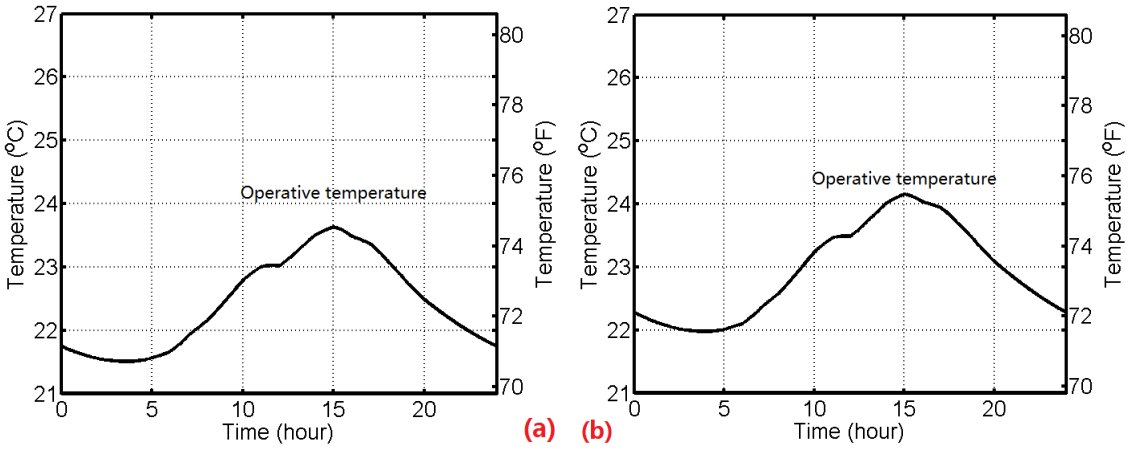

Fig. 3.20. Time-dependent operative temperatures of the benchmark room

3.9 Chapter summary

In this chapter, an RC (resistor-capacitor) model of a south-west corner room in a TABS-equipped office building is built in Matlab and Matlab/Simulink. In the RC model of the room, it considers: the thermal resistances of the building envelope, the surface air films, and the ventilation and infiltration/exfiltration; the heat capacity of the envelope; the solar energy input from the windows; the internal heat gains; the interior thermal mass; and the total thermal resistance of the TABS between the supply-water temperature and the TABS mean core temperature. With the model, the time-dependent temperatures of the indoor air and the surfaces of each element in the room can be calculated. The temperatures can then be combined into the operative temperature, which is one of the most important parameters in a building.

Reference

[3.1] M. Gwerder, B. Lehmann, J. Tötli, V. Dorer, F. Renggli, "Control of thermally activated building systems TABS," *Applied Energy* **85** (2008): 565-581

[3.2] B. Lehmann, V. Dorer, M. Gwerder, F. Renggli, J. Tötli, "Thermally activated building systems (TABS): Energy efficiency as a function of control strategy, hydronic circuit topology and (cold) generation system," *Applied Energy* **88** (2011): 180-191

[3.3] P. Ma, L.-S. Wang, N. Guo, "Modeling of TABS-based thermally manageable buildings in Simulink," *Applied Energy* **104** (2013) 791–800

[3.4] ASHRAE, Inc., *2009 ASHRAE Handbook - Fundamentals (I-P Edition & SI Edition)*, 2009

[3.5] R.L. Howell, W.J. Coad, H.J. Sauer, Jr., *Principles of heating ventilating and air conditioning* (6th edition), ASHRAE, Inc., 2009

[3.6] P. Ma, "Dynamic Heat Transfer: Effective heat capacity of planar thermal mass subject to periodic heating and cooling," M.S. Thesis, Stony Brook University, May 2010

[3.7] R. Meierhans, B.W. Olesen, *Betonkernaktivierung* (Velta Norderstedt, Germany), 1999

[3.8] International Code Council, Inc., *IECC 2012 International Energy Conservation Code*, July 11, 2011

[3.9] ASHRAE Inc., *Advanced Energy Design Guide for Small to Medium Office Buildings (AEDG): Achieving 50% Energy Savings Toward a Net Zero Energy (NZE) Building*, 2011

[3.10] ASHRAE Inc., *ANSI/ASHRAE/IES Standard 90.1-2010: Energy Standard for Buildings Except Low-Rise Residential Buildings*, S-I ed., 2010

[3.11] Norbert Lechner, *Heating, Cooling & Lighting—Design methods for architects* (2nd edition), John Wiley & Sons, Inc., 2000

[3.12] G. Z. Brown, Mark Dekay, *Sun, Wind & Light—Architectural design strategies* (2nd edition), John Wiley & Sons, Inc., 2000

[3.13] AMETEK, Inc., *Solar energy handbook: theory and applications* (2nd edition), Chilton book company, 1983

[3.14] Gary Reysa, *Manual of radiation on collector program*, January 2009
See: http://www.builditsolar.com/Tools/RadOnCol/radoncol.htm (Last access on

May 11, 2013)

[3.15] P. Ma, L.-S. Wang, "Effective heat capacity of interior planar thermal mass (iPTM) subject to periodic heating and cooling," *Energy and Buildings* **47** (2012) 44-52

[3.16] S. Kakaç, Y. Yener, *Heat Conduction*, 3rd edition, Taylor & Francis, 1993

[3.17] K. W. Childs, G. E. Courville, E. L. Bales, *Thermal mass assessment: an explanation of the mechanisms by which building mass influences heating and cooling energy requirement,* Oak Ridge National Laboratory, Report No. ORNL/CON-97, US Department of Energy, Oak Ridge, Tennessee, 1983

[3.18] P. Ma, L.-S. Wang, "Effective heat capacity of exterior Planar Thermal Mass (ePTM) subject to periodic heating and cooling," *Energy and Buildings* **47** (2012) 394-401

[3.19] B. Glück, *Strahlungsheizung - Theorie und Praxis*, Verlag C. F. Müller, Karlsruhe 1982

[3.20] M. Koschenz, B. Lehmann, *Thermoaktive Bauteilsysteme*, EMPA, 2000

[3.21] http://www.weather.com/weather/climatology/monthly/SZXX0033 (Last access on May 11, 2013)

Chapter 4: Partial Homeostasis in Buildings —

The passive application of building thermal mass

Everyone intuitively knows that building envelopes should be constructed with high thermal resistance and sufficient mass, both in the envelopes and in their interior, to utilize mass' heat storage capacity. However, common building codes mandate only minimum thermal resistance values in a building's envelope, making no provision for its structural mass. This inconsistency or enigma in building science results from the conventional *heat balance* design philosophy to control *indoor air at a fixed seasonal temperature* — i.e., the indoor air is considered as a static object subject to heat interaction with indoor heat source and indoor-outdoor heat flow, with resulting heat in-balance accounted for by HVAC equipment. It is reasoned that an ultra energy-efficient building must be conceived as a dynamic (i.e., a process) system. However, by itself, a given volume of air defined by a building's indoor space cannot be treated dynamically: the astrophysicist and meteorologist Jacob Robert Emden long ago exposed the logical inconsistency in the thermodynamic understanding of heating a building's air as a process without the explicit inclusion of temperature variation in its structural mass. That is, the explicit consideration of thermal mass is necessary in the dynamic conception of a building in accordance with the new *process* design philosophy of *archi.engineering building's interior air + structural-mass to be partially homeostatic within a temperature range*. This new design philosophy manifests in two overlapped archi.engineering design steps. The first is the "architectural" step of designing the envelope resistance and the architectural/structural mass requirement, which will be introduced in this chapter.

4.1 Introduction

A building's thermal resistance and its mass are the most important passive elements of its thermal-control (or thermal-management) system. This chapter addresses the effective use of a building's mass, as a cost-effective means for controlling building temperatures via its "ability to absorb [convectively and radiatively] and store heat energy during a warm period and to release heat energy during a cool period later." [4.1] Building mass can be classified as either exterior envelope mass (eEM), which functions as both a storage medium and a heat transfer medium, or interior thermal mass (iTM), which predominately functions as a storage medium.

"Many of us have experienced that moment during a warmer summer day, upon entering an old church. One step into the space and the climate changes totally…allows us to feel a temperature even below the air temperature, precipitated by the radiation exchange of our body with the colder room surface," noted the green building engineer M. Schuler [4.2]. Most of us have the same intuitive appreciation of thermal mass (e.g., that of the building envelope of an old church) in making a building thermally comfortable, and a large number of research papers on thermal mass have been published.

In the 1990s Robert Meierhans, a Swiss engineer, proposed an attractive solution that has become known as the thermally activated building systems (TABS) [4.3,4.4], which combines hydronically-based radiant conditioning with a building's mass (typically interior concrete slabs). The 2012 publication of ISO 11855 [4.5], which standardized the world-wide design and construction of TABS, proves that it is possible to use thermal mass by hydronically activating iTM.

Here in the United States, the *ASHRAE Standard 90.1-2010* [4.6] and the *2012 IECC* [4.7] contain the most up-to-date and innovative energy-efficiency requirements for both commercial and residential buildings, including requirements for envelope (ceilings, walls, windows, doors), lighting (skylights, lighting equipment), and mechanical equipment (HVAC systems). However, in contrast with the codified minimum

requirement in envelope thermal resistance, no requirements for thermal mass—despite the ISO standardization of TABS—are codified by ANSI/ASHRAE and ICC. This discrepancy may well be resulting from the fact that TABS is a relatively new, unfamiliar and complicated technology, causing ASHRAE to view it as an emerging technology rather than a standard practice [4.8]. We shall nonetheless show that the theoretical fact that ASHRAE views the built environment in terms of a *static* model based on a *heat balance* design approach contributes to its slow embracing of TABS technology. Furthermore, a critical examination of this theoretical-philosophical background can teach a worthwhile lesson for the scientific study of thermal mass.

We propose that a practical path towards the adoption of a new building technology begins with presenting familiar changes. One way of achieving this incremental change is to introduce the passive application of the technology before its active and elaborate mechanical control applications. There is amble evidence for the attractiveness of passive approach to building owners by their enthusiastic acceptance of passive solar buildings and the passivhaus movement.

This path will be supported by a fundamental examination of the question: should a building be modeled as a static object or as a dynamic system? This study of two competing design philosophies reveals the reason why ASHRAE is content to neglect codifying the thermal mass requirement: Thermal mass, if not explicitly and quantitatively investigated, is already an integral part in the static building model, but only a dynamic model can prescribe a quantitative requirement of mass. Furthermore, only a dynamic study can explain the passive use of mass without hydronic activation. That is, thermal mass can be used in buildings for good effect in a passive first step without its active hydronic-system control as in TABS. This “architectural” design of a building’s structural mass in order to enhance its thermal performance, is the pre-condition for achieving homeostasis in buildings through the second, “mechanical engineering,” step of the process design philosophy. This chapter focuses on

archi.engineering to achieve a required indoor temperature range without considering indoor temperature level, which will be the focus of the second design step.

This chapter first presents a brief review of the heat balance design approach of ASHRAE in Section 4.2. Section 4.3 recounts the Emden exemplum, which shows the difference between the static model and the dynamic model and explains why a dynamic model necessitates the explicit consideration of a building's mass. Sections 4.4 and 4.5 demonstrate that only a *dynamic* model of the indoor built environment can identify the advantages of passively using thermal mass without its activation. The major findings of this chapter are an optimal slab mass thickness for iTM and a proposed re-definition of thermal envelope, which are given in Sections 4.4 and 4.5, respectively. Section 4.6 gives a recapitulation of the two design philosophies, the *process* design philosophy and the *heat balance* design philosophy—and their implication in terms of the large energy and thermal resource issues. This chapter closes with the summary of arguments, and new findings.

4.2 Heat balance model of a radiant-convective indoor environment

We begin with the *ASHRAE Handbook-Fundamentals* treatment of cooling and heating load as shown in Fig. 4.1. [*4. 9* :18.16] We shall call it the ASHRAE radiant-convective conditioning of air model, or the Air Heat Balance model. It is important to note that the air heat balance model does account for radiative heat exchange among surfaces and their collective interaction with air through convection. What is not explicitly taken into consideration is the mass or mass-substratum of the radiant surfaces.

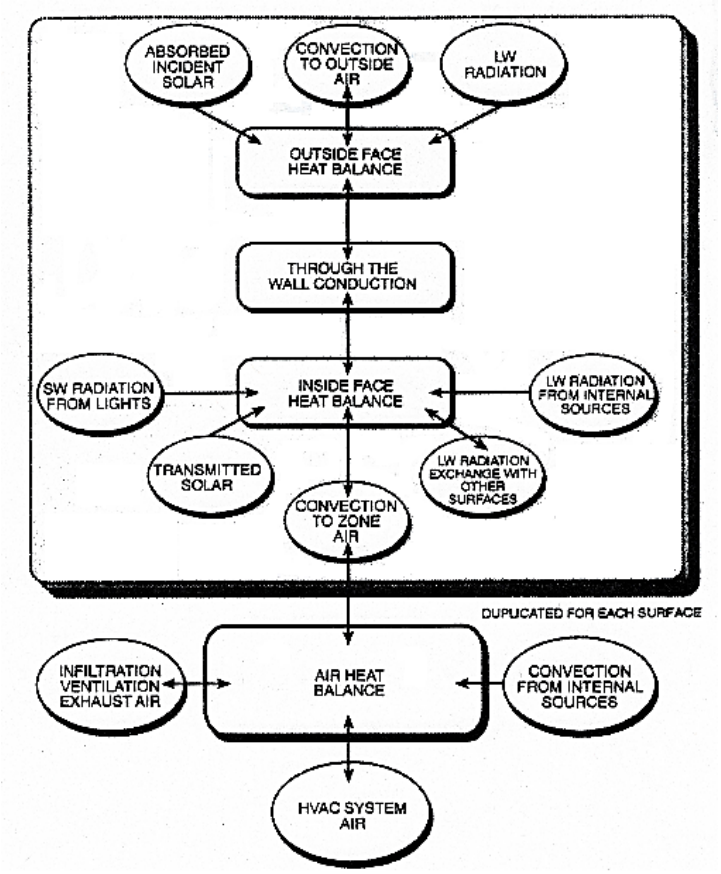

Fig. 4.1. "Schematic of Heat Balance Processes in a Zone." Reproduced from the 2009 *ASHRAE Handbook-Fundamentals* (18.16)

A simplified version of the above "Schematic of Heat Balance Processes in a Zone" Model is shown in Fig. 4.2. The difference in the simplified model from the ASHRAE Schematic is the treatment of the envelope. The ASHRAE's treatment takes detailed heat transfer processes into consideration throughout the configuration of the envelope, including the conduction processes, convective processes on inside and outside surfaces of the envelope, and radiative processes of short-, medium-, and long-wavelength radiation, whereas, our envelope treatment, shown in Fig. 4.2 is a simple overall *R*-value or *U*-value. In addition, the implicit mass behind radiant surfaces of the ASHRAE schematic is shown explicitly in Fig. 4.2.

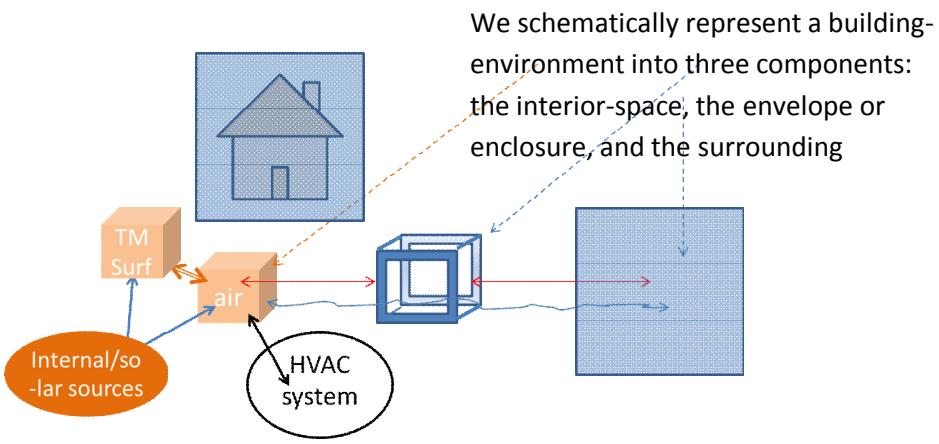

The ASHRAE Air Heat Balance model:

- The material element of the interior space is air and interior TM. A fixed value of dry-bulb *T* (= mean radiant temperature [MRT]) is assumed.
- The envelope is thermally defined by its *R*-value (or *U*-value)—and its CTF
- The surrounding environment is a variable environment seasonally and diurnally.

Fig. 4.2. The ASHRAE Air Heat Balance model, in which the conditioned space is a *static* space

The ASHRAE method does consider the time-dependent interaction on the exterior and interior surfaces of the envelope. Air temperature, however, is kept time-independent or static. The envelope-mass' effect is accounted indirectly through the surface heat interactions, not directly in terms of process through the envelope's internal thermal mass—effect of which impacts only implicitly the surface heat interaction through *conduction transfer function* (CTF) [4.9]. These refinements do not alter the overall load (heat flow) through the envelope, only the distribution of the hourly heat flow.

The simplification made in the model does not change the core fundamental-nature of the ASHRAE model: the treatment of interior space is focused on "AIR HEAT BALANCE" and interior space as air not air and its surroundings. One finds in Ref. [*4.9*:17.3] that, "Typical practice for cooling is to design for indoor conditions of 24 °C db and a maximum of 50 to 65% rh. For heating, 20 °C db and 30% rh are common design values." That is, two *fixed* specified indoor temperatures are chosen, one corresponding to the cooling season, and another to the heating season.

The heat balance of air may be summarized as

$$\dot{Q}_{gain} + \dot{Q}_{env-in} + \dot{m}_{inf} c_p \left(T_{amb} - T_{in}\right) + \dot{Q}_{HVAC-system} = 0 \tag{4.1}$$

The variable $\dot{Q}_{env-in}$ is the rate of heat transmission through the envelope, such that heat in-flow is the positive direction. The variable $\dot{Q}_{HVAC-system}$ is the heating rate of energy required by the HVAC system to maintain the indoor dry-bulb temperature at the designed condition; $\dot{Q}_{HVAC-system}$ is negative when cooling is required.

The general heat equation may be written as

$$\dot{Q}_{gain} + \dot{Q}_{env-in} + \dot{m}_{inf} c_p \left(T_{amb} - T_{in}\right) + \dot{Q}_{HVAC-system} = \left(C_p\right)_{in} \frac{dT_{in}}{dt} \tag{4.2}$$

where $\left(C_p\right)_{in}$ is the heat capacity of the "interior space." The heat balance equation (4.1) is the special case when the indoor space temperature is a fixed value, i.e., $dT_{in}/dt = 0$, and the RHS of equation (4.2) becomes zero regardless of the correct value of $\left(C_p\right)_{in}$,

$$\frac{dT_{in}}{dt} = 0 \Rightarrow \left(C_p\right)_{in} \frac{dT_{in}}{dt} = 0$$

In Section 4.3, we shall show that ASHRAE's implied assumption that the interior space contains only air leads to a paradox. Thus, $\left(C_p\right)_{in}$ cannot be the heat capacity of air alone and must be the heat capacity of air mass *and* other solid-structural mass (and liquid mass if any),

$$\left(C_p\right)_{in} = \left(C_p\right)_{in-air} + \left(C_p\right)_{in-thermal-mass} \tag{4.3}$$

The air heat balance method does not require the correct value of $\left(C_p\right)_{in-thermal-mass}$ as it does not consider the thermal mass explicitly. Without knowledge of the correct heat capacity, however, one cannot investigate the general time-dependent thermal processes of a building.

In the treatment of the envelope the air heat balance model does consider the time dependent term $\dot{Q}_{env-in}$ on both the exterior surface and the interior surface, $\left[\dot{Q}_{env-in}\right]_{ext}$

and $\left[\dot{Q}_{env-in}\right]_{int}$. The exterior $\left[\dot{Q}_{env-in}\right]_{ext}$ is subject to variable ambient condition and is thus the driving force of building time-dependency. The envelope-mass' effect is accounted for indirectly in terms of the CTF. Time-dependency in $\left[\dot{Q}_{env-in}\right]_{ext}$ and $\left[\dot{Q}_{env-in}\right]_{int}$ depends on the ambient condition and envelope CTFs, which are functions of the mass in the envelopes. However, at each instant, $\left[\dot{Q}_{env-in}\right]_{ext}$, $\left[\dot{Q}_{env-in}\right]_{int}$, and the temperatures of all radiant surfaces assume their instantaneous values that are balanced with each other and the air. Each envelope-section is furthermore balanced at the convergence-limit [*4.9*:18.20] of the heat balance calculation

$$\left[\dot{Q}_{env-in}\right]_{ext} = \left[\dot{Q}_{env-in}\right]_{int} \tag{4.4}$$

i.e, there is no gain or loss of heat energy in the wall mass, and no explicit account of wall mass other than the indirect accounting through the CTF. This accounting of envelope mass only determines the heat transmission role of the envelope, with no consideration of its heat storage role.

Air's fixed steady-state value results from its convective interaction with all the inside surfaces, the internal heat (including solar indirectly) gain, and the infiltration enthalpy exchange—and the remaining in-balance, i.e., the load demand, is met by the required $\dot{Q}_{HVAC-system}$ according to equation (4.1). The balance treatment has the simplicity of not having to consider iTM. The HVAC technology gives architects the simplicity and freedom in their architectural creation and mechanical engineers the ready-made solution in their practice; on the other hand, the same technology distances the static indoor built environment from its surroundings devoid of complex interactions between them. Creation of buildings that symbiotically interact with their surroundings necessitates the dynamic or process treatment such as equation (4.2), in which thermal mass is taken into consideration. Otherwise, a paradoxical question arose as Emden first observed.

4.3 The Emden house heating exemplum

While ASHRAE takes building mass into account partially or indirectly in terms of CTF and the radiant surface, most "not-so-informed" laymen have the misconception that building heating and cooling pertains to the air alone. A related common misconception is that indoor thermal comfort depends on convective heat exchange with the air, instead the radiant/convective exchange with the indoor surfaces/air. [4.8]

To highlight the point of overlooking the role of thermal mass behind radiant surfaces, let us imagine a virtual, "mass-less" building in which heating in the winter is solely applied to "air" in a control volume defined by the inside-surface of the building envelope. Assume that the envelope is not air tight so that the air pressure is equal to the ambient air pressure. This is the thought experiment discussed by Emden. [4.10] By posing the question, "Why do we have winter heating?" Emden gave the answer (to argue for an entropy central approach supplanting the conventional energy central approach),

> The layman will answer: "To make the room warmer." The student of thermodynamics will perhaps so express it: "To import the lacking energy." If so, then the layman's answer is right, the scientist's wrong.
>
> We suppose, to correspond to the actual state of affairs, that the pressure of the air in a room always equals that of the external air. In the usual notation, the (inner, thermal) energy is, per unit mass,
>
> $$U = c_V T.$$
>
> (An additive constant may be neglected.) Then the energy content is, per unit volume,
>
> $$u^1 = c_V \rho T,$$
>
> or, taking into account the equation of state,
>
> $$p/\rho = RT,$$
>
> we have
>
> $$u^1 = c_V p/R.$$
>
> For air at atmospheric pressure,

$$u^1 = 0.0604 \text{ cal/cm}^3.$$

The energy content of the room is thus independent of the temperature, solely determined by the state of the barometer. The whole of the energy imported by the heating escapes through the pores of the walls of the room to the outside air.

Emden thus pointed out the paradox of the heating process of a room if it is defined thermally in terms of air alone. Emden's argument may be questioned as to why he neglected any heating of the building mass. One may speculate whether Emden was aware that his wise layman is the same not-so-informed layman who harbors the misconception about building mass and the absence of radiant heating—that he deliberately constructed this ridiculous mass-less (other than the air) room for the purpose of making his larger point supporting an entropy view of the world. The interesting fact is that Emden's short article has been followed up by at least five published books or articles [*4.11,4.12,4.13,4.14,4.15*] revisiting the issue, including a very recent one [*4.15*]. All these train their focus on the air. The most recent one does consider mass other than the air, but it only mentions plasterboard [*4.15*: 75], a small part of total building mass, to conclude (in its main conclusion) that heating of the plasterboard can be neglected in heating a room. Conclusion in Ref. [*4.15*] also includes the line, "[The air] internal energy remains constant, implying that raising the temperature is accompanied by expelling air to the outside and lowering the entropy. Thus, the thermal energy that is transferred to the room is also transferred to the outside where it is wasted," [*4.15*:76] exactly the same conclusion of "energy imported by the heating escapes through the pores of the walls of the room" stated by Emden.

There are two responses to the Emden exemplum: a large lesson to be learnt about what drives the world or what makes the world go round, and a specific lesson about how buildings interact with their surroundings and mechanical equipment. First the second response: The heating process of a real building will certainly have a part of imported energy stored in the building mass corresponding to a higher temperature, which depends

on the energy imported and the heat capacity of the building mass. By neglecting heating of the building mass in a heating process, however, Emden's demonstration exposes that the Air Heat Balance model is only valid as a static model of a conditioned space kept at a fixed temperature.

The absence of quantitatively considering mass in the static model does not mean the absence of mass and its heat capacity. Some quantitative study of the effect of external mass in a building's envelope (eEM) does exist. Experimental result has been reported that the difference lies in the hourly heat transfer rate with a periodic ambient external temperature, not in the total (accumulated over 24 hours) heat transfer rate:

> Measurements proved the following hypothesis. If the climate is cold enough that a building requires heat continuously, then average heating energy requirements depend only on the steady-state thermal resistance of the exterior walls and not on thermal mass. However, if conditions are such that the building interior temperature floats above the heating setpoint for part of the day, then excess energy is required above what a steady-state model would predict. This excess is largest for buildings exhibiting the least thermal damping in the envelope. This excess energy results from the rise in interior temperature above the setpoint, which results in higher thermal losses through the envelope. [*4.16*:182]

That is, the excess is due to the departure of the interior temperature from the static setpoint. Should the interior temperature be kept at the constant setpoint, the thermal mass of the external walls will make no difference in the total heating load.

From the energy central point of view the total heat or cooling load of a building of eEM is the same: This explains why common codes do not make provision for minimum thermal mass in a building envelope. From a practical point of view, the combination of identical total load but different hourly load distribution makes a difference because the whole-sale cost of power required for meeting load is dependent on the hourly distribution: if eEM shifts peak load hours to hours of lower power demand, this peak shaving can save money by lowering the *demand charge* for the same *energy charge*.

Only a dynamic model, by going beyond the limitation of the static air heat balance model, can show the full effect of thermal mass both in the form of iTM and that of eEM.

4.4 Internal thermal mass

In an earlier paper [4.17] we introduced the concept of *neutral* ambient conditions and studied the "dynamics" or thermal manageability of a building under such conditions. In this chapter, as a first step of building conditioning, we allow interior space temperatures to float within a range (≤2 K) regardless of its level. That is, the general heat equation

$$\dot{Q}_{gain} + \dot{Q}_{env-in} + \dot{m}_{inf} c_p \left(T_{amb} - T_{in}\right) + \dot{Q}_{HVAC-system} = \left(C_p\right)_{in} \frac{dT_{in}}{dt} \tag{4.2}$$

is in the first step to be investigated in its special case of

$$\dot{Q}_{gain} + \dot{Q}_{env-in} + \dot{m}_{inf} c_p \left(T_{amb} - T_{in}\right) = \left(C_p\right)_{in} \frac{dT_{in}}{dt} \tag{4.5}$$

The condition of indoor temperature floating within this range without using HVAC is known as the partial manageability of a building, which alone determines the building's structural thermal-mass requirement. This creates more flexible criteria not limited to (or having to wait for) *neutral* ambient conditions for future experimental study. The explicit separation of range determination based on equation (4.5) from the control of level by going back to equation (4.2) also gives full flexibility to engineering solutions for controlling temperature level in the future.

4.4.1 Thermal mass treatment using method developed in TABS investigation

The engineering advance made in TABS makes the analysis of thermal mass possible with or without its hydronic activation. The following is an introduction to the specific assumptions and methods we used for a non-TABS application (i.e., without hydronic activation). In Chapter 3, the TABS-equipped office building located in Zürich

was introduced. Here the characteristics of the building are briefly described again.

The building has two main orientations (south and north) with normal offices along the main façades and corner offices with glazing on two sides at the front faces. It has five stories and each story has 12 normal offices and 4 corner offices. The dimensions of each room in the building are 6m×6m×3m. An RC (resistor-capacitor) model of a south-west corner room in the building is developed. The modeled room will be a benchmark in this chapter.

In the benchmark room, the south- and west-facing walls are exposed to the outdoor air. The ceiling, floor and the other two walls are all considered as iTM. There is no external door, and internal doors are neglected. The room has a large window-to-wall ratio (WWR) of 42%. Thermal resistance of all the windows is *R*-3 hr-ft^2-°F/Btu (0.53 m^2-K/W). The inside surface thermal resistance is *R*-0.7 (0.12); and the outside surface thermal resistance is *R*-0.25 (0.044) in summer and *R*-0.17 (0.030) in winter. The thermal resistance due to ventilation and infiltration/exfiltration is determined to be *R*-8.01 (1.41), which is parallel to the building envelope thermal resistance.

The main materials used in the building are wood, normal-weight (NW) concrete, structural light-weight (LW) concrete and insulation. The external walls consist of 20cm-thick NW concrete. Climate zone 5's thermal resistance requirement is applied to the external walls: constant *U*-0.365 W/m^2-K kept by the insulation outside of the concrete. The total heat capacity of the eEM is 7.70×10^6 J/K. The slabs in the ceiling and floor are 25cm-thick NW concrete, half of which is counted as part of the room. Thus, the total heat capacity of the total mass of the roof and floor slabs is 16.60×10^6 J/K. The internal walls are made of structural LW concrete with thickness of 20 cm. As half of the internal walls are considered part of the room, the total heat capacity is 5.30×10^6 J/K. Other iTM, such as furniture, is considered as wood with dimensions of 6m×6m×0.1m. The total heat capacity of the iTM is 2.54×10^6 J/K. The heat capacity of the windows is neglected. The indoor air has a relatively small heat capacity of 0.14×10^6 J/K.

The heat gains of the room include internal heat gains and solar energy inputs. Internal heat gains are directly put into the indoor air. The solar inputs are calculated from the solar geometry of Zürich, assuming that 8% goes through the windows.

Having described the assumptions and thermal modeling of the building's mass, we shall in the next sub-section, apply the modeling to the building's iTM in order to determine the optimal slab thickness in the building interior. Notice that, in the following sections of this chapter, only one parameter of the benchmark room is varied each time.

4.4.2 The optimal thickness of iTM

Let us first vary the concrete thickness of the ceiling and floor slabs from 0.025 m to 0.800 m. The resulting operative temperature variations ΔT_{op} are listed in Table 4.1. The mean values of the operative temperatures are between 35 ºC and 36 ºC. Here the outdoor mean temperature is 27.10 ºC and the outdoor temperature peak-to-peak amplitudes ΔT_{out} are varied from 2 K to 30 K, with a 4 K increment. From Table 4.1, we find that ΔT_{op} increase almost linearly with the increase of ΔT_{out} for all cases of concrete slab thickness, but increasingly thick concrete slabs cause ΔT_{op} to first decrease and then level off with a small reversing trend eventually. The minimum values occur when the concrete thickness is about 25 cm. The simulation results confirm findings in Refs. [*4.1,4.18,4.19*].

Table 4.2 lists ΔT_{op} when the mean value of the outdoor temperature is 0 ºC, with the assumption that all other factors are the same. The linearity between ΔT_{op} and ΔT_{out} in Table 4.1 is still valid. So in Table 4.2, it only includes ΔT_{op} under the two extreme ΔT_{out} conditions. The maximum deviation in corresponding ΔT_{op} from the summer case is only 0.5%, which means that a building's thermal performance in ΔT_{op} is independent of the outdoor mean temperature. Therefore, we can use any reasonable value of the outdoor air mean temperature to continue the investigation for day-to-day temperature range. Of course, without HVAC heating and cooling for the room [equation (4.5)], the season-to-season operative temperature level changes from 35.6 ºC in summer to 8.4 ºC

in winter.

Table 4.1. Operative temperature variations when concrete thickness of the ceiling and floor slabs is varied (mean T_{op} = 35.56~35.65 ºC)

T_{out} (ºC)		ΔT_{op} (ºC) when concrete thickness of the ceiling and floor slabs is						
Mean	**ΔT_{out}**	**0.025 m**	**0.050 m**	**0.100 m**	**0.200 m**	**0.250 m**	**0.400 m**	**0.800 m**
27.10	2	1.97	1.65	1.36	1.23	1.22	1.23	1.27
	6	2.24	1.87	1.55	1.40	1.39	1.41	1.45
	10	2.52	2.11	1.74	1.58	1.57	1.59	1.64
	14	2.80	2.35	1.94	1.77	1.76	1.78	1.83
	18	3.09	2.59	2.14	1.95	1.94	1.97	2.03
	22	3.38	2.84	2.35	2.14	2.13	2.17	2.23
	26	3.67	3.09	2.56	2.34	2.33	2.36	2.43
	30	3.97	3.33	2.76	2.53	2.52	2.56	2.63

Table 4.2. Operative temperature variations when concrete thickness of the ceiling and floor slabs is varied (mean T_{op} = 8.39~8.48 ºC, mean T_{out} = 0 ºC)

T_{out} (ºC)		ΔT_{op} (ºC) when concrete thickness of the ceiling and floor slabs is						
Mean	**ΔT_{out}**	**0.025 m**	**0.050 m**	**0.100 m**	**0.200 m**	**0.250 m**	**0.400 m**	**0.800 m**
0	2	1.97	1.65	1.36	1.23	1.22	1.23	1.27
	30	3.99	3.35	2.78	2.54	2.53	2.58	2.65

In Table 4.3, the thickness of the structural LW concrete in the internal walls is varied from 0.025 m to 0.800 m. Again, only extreme cases are shown. Relative variation in ΔT_{op} against LW concrete thickness is shown in Table 4.3 to be smaller than the corresponding variations in Table 4.1: the maximum variation is 23.4%, whereas the maximum variation shown in Table 4.1 is 61.5%. This means that the effect of the internal walls on ΔT_{op} is smaller than the effect of the ceiling and floor slabs.

The existence of an optimal thickness for iTM is found; the same thickness is found in the present passive application as that in the standardized practice in hydronically activated TABS application. The investigation of iTM in this section did not consider variation in the external envelope's thermal mass or in its WWR (window-to-wall ratio)—which will be the topic of Section 4.5.

Table 4.3. Operative temperature variations when concrete thickness of internal walls is varied (mean T_{op} = 35.59~35.65 ºC)

T_{out} (ºC)		ΔT_{op} (ºC) when concrete thickness of internal walls is					
Mean	**ΔT_{out}**	**0.025 m**	**0.050 m**	**0.100 m**	**0.200 m**	**0.400 m**	**0.800 m**
27.10	2	1.48	1.40	1.28	1.22	1.24	1.27
	30	3.11	2.94	2.67	2.52	2.58	2.62

4.5 Thermal mass in the external opaque envelope and maximum fenestration WWR

In Section 4.4 the investigation of iTM was made by assuming a constant WWR of 0.42 (42%) and a constant 20cm-thick NW concrete slab in external walls. The same optimal iTM slab thickness was found for all cases and it is hypothesized that the conclusion of optimal slab thickness applies with WWR and external concrete slab thickness different from 0.42 and 20cm. We now direct our attention to investigate the architectural slab thickness requirement in the external walls by varying slab thickness under the constraint of constant thermal resistance for the external wall with WWR as a parameter.

In Table 4.4, the thickness of the NW concrete in the external walls is varied from 0.025 m to 0.800 m. In comparing ΔT_{op} in Table 4.4 to that in Table 4.1, the maximum reduction in ΔT_{op} is 30.4%. In Table 4.5, the insulation placement of the external walls is changed from outside of the concrete to the inside. Clearly, ΔT_{op} in these cases are much larger than that in the outside-insulated cases (the maximum increase is 62.0%). Therefore, it is better to control ΔT_{op} by laying insulation outside the thermal slab mass. In Table 4.6, the thermal mass of the external walls is changed from NW concrete to structural or insulating LW concrete. Notice that, when the insulating LW concrete is very thick, because of its insulating value so that it itself exceeds the constraint of total thermal resistance and the thickness of the insulation layer becomes negative in the

simulation model. No ΔT_{op} value is reported for these cases in Table 4.6.

Table 4.4. Operative temperature variations when thickness of the NW concrete in the external walls is varied (mean T_{op} = 35.59~35.63 ºC; WWR = 0.42)

T_{out} (ºC)		ΔT_{op} (ºC) when concrete thickness of external walls is					
Mean	**ΔT_{out}**	**0.025 m**	**0.050 m**	**0.100 m**	**0.200 m**	**0.400 m**	**0.800 m**
27.10	2	1.37	1.29	1.23	1.22	1.23	1.23
	6	1.60	1.50	1.41	1.39	1.40	1.40
	10	1.83	1.71	1.60	1.57	1.58	1.59
	14	2.08	1.93	1.80	1.76	1.76	1.77
	18	2.32	2.16	2.00	1.94	1.95	1.96
	22	2.57	2.38	2.20	2.13	2.14	2.15
	26	2.82	2.61	2.40	2.33	2.33	2.35
	30	3.08	2.83	2.60	2.52	2.52	2.54

Table 4.5. Operative temperature variations when thickness of the NW concrete in the external walls is varied—inside insulation (mean T_{op} = 35.18~35.28 ºC; WWR = 0.42)

T_{out} (ºC)		ΔT_{op} (ºC) when concrete thickness of external walls is					
Mean	**ΔT_{out}**	**0.025 m**	**0.050 m**	**0.100 m**	**0.200 m**	**0.400 m**	**0.800 m**
27.10	2	1.45	1.47	1.46	1.42	1.37	1.37
	30	4.43	4.46	4.21	3.38	2.76	2.82

Table 4.6. Operative temperature variations when thickness of the structural or insulating LW concrete in the external walls is varied (mean T_{op} = 35.59~35.65 ºC; WWR = 0.42)

T_{out} (ºC)		ΔT_{op} (ºC) when structural LW concrete thickness of external walls is					
Mean	**ΔT_{out}**	**0.025 m**	**0.050 m**	**0.100 m**	**0.200 m**	**0.400 m**	**0.800 m**
27.10	2	1.39	1.33	1.28	1.28	1.28	1.29
	30	3.13	2.92	2.69	2.62	2.64	2.66
		ΔT_{op} (ºC) when insulating LW concrete thickness of external walls is					
27.10	2	1.39	1.35	1.34	1.34	1.35	NA
	30	3.10	2.87	2.74	2.76	2.78	NA

Carefully comparing Table 4.6 with Table 4.4, we find that ΔT_{op} is a weak function of the heat capacity of the exterior envelope mass (eEM): when the eEM is changed to structural and insulating LW concretes, the volumetric specific heats of the eEM slab decrease to 80% and 26%, respectively, of that of the original NW concrete eEM slab.

However, the maximum increases of the corresponding ΔT_{op} are only 4.7% and 9.8%, respectively. This does not mean that the type of material used in the eEM is not important for controlling ΔT_{op}. As shown in the two tables, the variation can be larger than 3 K when ΔT_{out} is large and the amount of the eEM is small. The point is that the effect of the eEM on ΔT_{op} is not as significant as the effect of the iTM.

Until now, we only considered the cases with WWR = 0.42; in the following, the combined effect of thickness of the eEM slab and WWR will be investigated. The fenestration WWR, defined as "the ratio of the transparent glazing area to the outdoor floor-to-floor wall area," [4.9] is an important parameter for controlling ΔT_{op} in a small range. According to Ref. [4.20], "wall" in WWR is defined differently in the *ASHRAE Standard 90.1-2010* and the *2012 IECC*. In *ASHRAE Standard 90.1-2010*, a wall area of both above and below-grade "walls" is the denominator of WWR. Chapter 5 of the *2012 IECC* considers only above-grade walls. Here we follow the definition in the *2012 IECC*. Notice that "the outdoor floor-to-floor wall area" also includes the window area, which means that if the WWR is 100%, there in fact is only window, rather than half window and half wall. Fig. 4.3 gives an intuitive view of the WWR [4.21].

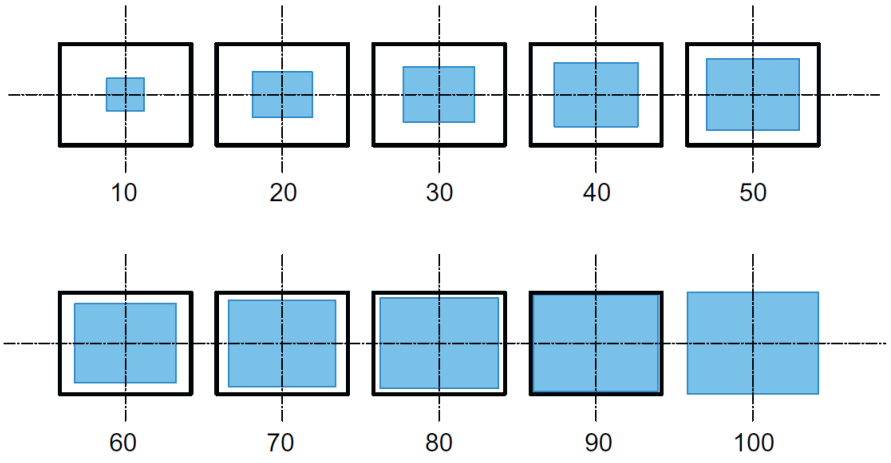

Fig. 4.3. Window-to-Wall area Ratio in percentage

To maintain the maximum ΔT_{op} at or below 2 K, the minimum thicknesses of the NW concrete in the external walls are listed in Table 4.7 and plotted against ΔT_{out} in Fig.

4.4 under different WWRs. The table and figure shows: if the WWR and ΔT_{out} are both large, ΔT_{op} cannot be kept in 2 K regardless of eEM thickness; with decreasing WWR or ΔT_{out}, it is possible to meet the condition with smaller required amounts of eEM; when ΔT_{out} is at or below 10 K, no eEM is needed even with a WWR as high as 0.42, which is in line with the ASHRAE Standards recommendation of a maximum 40% WWR [4.20]. One of our goals is to permit maximum WWR values beyond the *ASHRAE Standard 90.1-2010* and the *2012 IECC* restrictions in buildings at partial homeostasis for the perceived aesthetics of larger fenestration. As seen from Table 4.7 and Fig. 4.4, when ΔT_{out} is not too big, there is no problem to have a 42% WWR with a reasonable amount of eEM (as well as iTM) for controlling ΔT_{op} in a small range.

Table 4.7. Thickness of the NW concrete in the external walls when ΔT_{op} is kept in 2 K

T_{out} (°C)		Concrete thickness (m) of external walls when $\Delta T_{op} \leq 2$ K and WWR=							
Mean	**ΔT_{out}**	**0.60**	**0.50**	**0.42**	**0.30**	**0.20**	**0.15**	**0.10**	**0.05**
	4	0							
	6	0.004							
	8	0.038	0						
	10	0.101	0.024	0					
	12	NA	0.050	0.018					
	14		0.095	0.037	0				
27.10	16		NA	0.061	0.016				
	18			0.099	0.031	0			
	20			NA	0.045	0.016	0		
	22				0.060	0.027	0.014	0	
	24				0.081	0.038	0.025	0.012	0
	26				0.116	0.048	0.034	0.021	0.008
	28				NA	0.059	0.042	0.029	0.018
	30					0.072	0.051	0.037	0.025
	32					0.089	0.061	0.044	0.032
	34					0.113	0.072	0.052	0.038

Fig. 4.4 may be recapitulated into two main guidelines regarding the envelope. In the case of moderate "diurnal outdoor temperature amplitude" ΔT_{out} and/or small WWR, there is no thermal mass requirement for the envelope in consistency with ASHRAE

Standard. In the case of large ΔT_{out} or large WWR, a minimum thermal mass is required; insulation of given thermal resistance should be placed on the outside of the required thermal-mass-structure of the external walls, "wall mass was observed to have a larger effect when it was placed inside the wall insulation than when placed outside the wall insulation." [*4.16*:182] The guideline for the latter case of large ΔT_{out} may be alternatively given as a recommended slab thermal-mass of 0.1 m for external wall inside a continuous insulation layer so that corresponding maximum WWR as a function of ΔT_{out} is allowed as shown in Table 4.8 and Fig. 4.5. Our recommendation is limited to qualitative guidelines; the specific values in the recommendation will need to be further investigated for buildings of different types with different specifications.

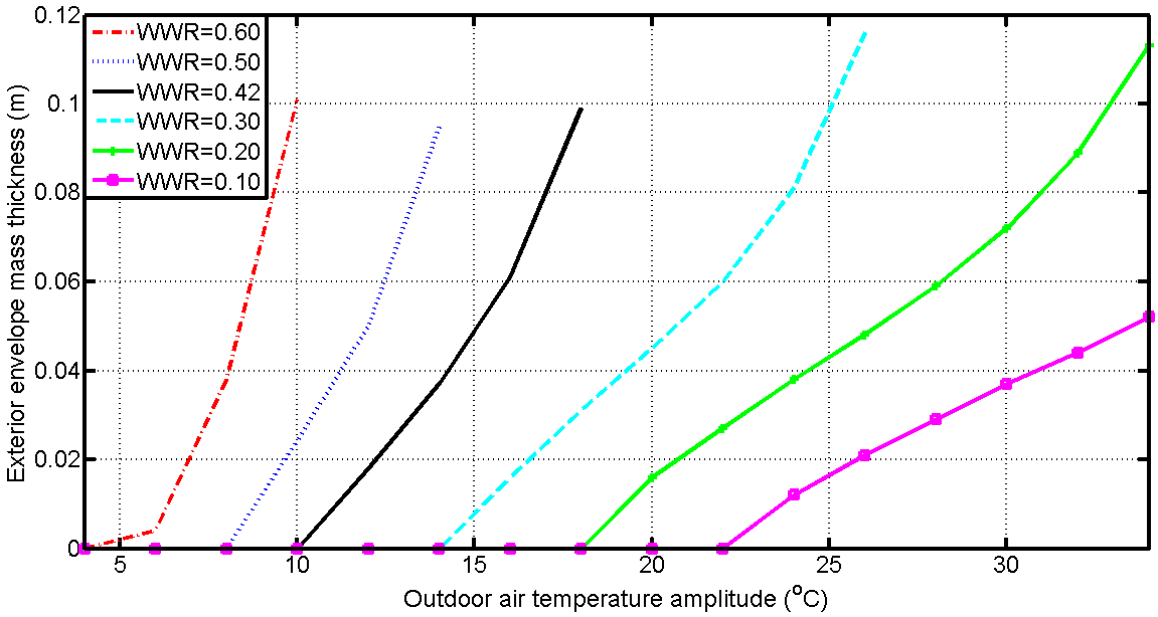

Fig. 4.4. The required envelope mass slab thickness against ΔT_{out} with WWR as parameters

Table 4.8. The recommended maximum WWR as a function of ΔT_{out}

ΔT_{out} (K)	2	4	6	8	10	12	14	16	18
WWR_{max}	0.845	0.777	0.713	0.654	0.599	0.549	0.503	0.460	0.421
ΔT_{out} (K)	20	22	24	26	28	30	32	34	
WWR_{max}	0.384	0.350	0.319	0.289	0.262	0.236	0.212	0.190	

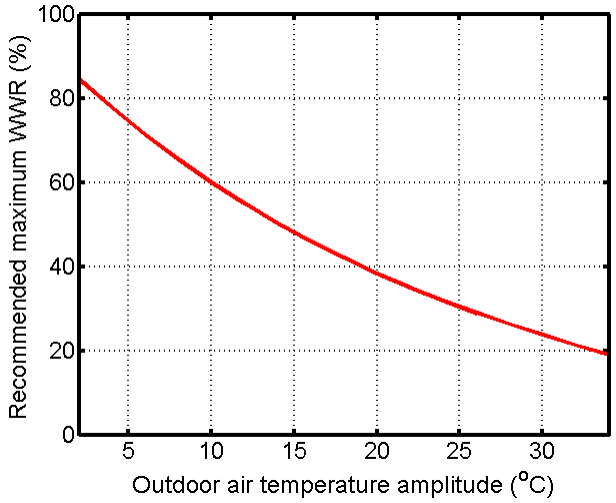

Fig. 4.5. The recommended maximum WWR as a function of ΔT_{out}

4.6 Archi.engineering of buildings

The process design philosophy suggests a two-step process, first step of which is the archi.engineering of a building as capitulated in equation (4.5),

$$\dot{Q}_{gain} + \dot{Q}_{env-in} + \dot{m}_{inf} c_p \left(T_{amb} - T_{in} \right) = \left(C_p \right)_{in} \frac{dT_{in}}{dt} \tag{4.5}$$

in which building design aims for the required indoor temperature range without concern for the control of the indoor temperature level. This first step does not address the issue of energy demand, which will be the topic of the second step when the control of the indoor temperature level is undertaken.

Emden wrote, "In the huge manufactory of natural processes, the principle of entropy occupies the position of manager, for it dictates the manner and method of the whole business, whilst the principle of energy merely does the bookkeeping, balancing credits and debits." [4.10] What is important is not energy per se, but that the Universe exists in a non-equilibrium state; otherwise all the energy in the Universe and in the ocean is of little use. The static conception of a building based on heat balance model

$$\dot{Q}_{gain} + \dot{Q}_{env-in} + \dot{m}_{inf} c_p \left(T_{amb} - T_{in} \right) + \dot{Q}_{HVAC-system} = 0 \tag{4.1}$$

necessarily leads to an energy or energy demand point of view. In contrast, *energy*

demand is not the central focus in the dynamic conception of a building: energy will be used and in some cases the total amount of energy flowing through the building will not be reduced in the second archi.engineering design calculation—as will be capitulated by the integrated form of the general heat equation (4.2)

$$\oint_{cyclic-period} \dot{Q}_{cooling} dt = \oint_{cyclic-period} \left[\dot{Q}_{gain} + \dot{Q}_{total-env-in} \right] dt - \oint_{cyclic-period} \left(C_p \right)_{in} dT_{in} \quad (4.6)$$

which becomes, with T_{in} being recharged back to the same initial temperature at the end of the cyclic-period,

$$\oint_{cyclic-period} \dot{Q}_{cooling} dt = \oint_{cyclic-period} \left[\dot{Q}_{gain} + \dot{Q}_{total-env-in} \right] dt \quad (4.7)$$

Instead of heat balanced at every instant in the heat balance design approach [equation (4.1)], the goal of process design approach can be met with cooling operation (as shown by equation (4.7), the same logic applies for heating as well) during the lowest power cost period or the most favorable natural condition period. That is, the building will be amenable to demand side management, including the harnessing of natural resources. The dynamic conception of a building frees us from the inevitable consumption of energy capital towards the possibility of managing thermal resources in the world—the non-equilibrium systems one finds everywhere around us.

One no longer sees the world in terms of matter and energy alone, but in terms of non-equilibrium existence resulting in irreversibility—as in his autography the physicist Prigogine put this way,

> Among all those perspectives opened by thermodynamics, the one which was to keep my interest was the study of irreversible phenomena, which made so manifest the "arrow of time." From the very start, I always attributed to these processes a constructive role, in opposition to the standard approach, which only saw in these phenomena degradation and loss of useful work. [4.22]

That is, irreversible processes have destructive/constructive duality—a profoundest insight in the history of scientific thought [4.23] discovered originally by Sadi Carnot, which has to be rediscovered by Emden, Prigogine, and in a recent article [4.24].

4.7 Chapter summary

Everyone intuitively knows the importance of a building's envelope resistance and structural mass. Recent advancements in TABS building technology prove the effectiveness of thermal mass. TABS has not, however, been able to challenge the HVAC convention and its balance design philosophy of *engineering building's indoor air to be at a fixed temperature.* Instead of tying thermal mass with hydronic as TABS does, it is argued that the significance of thermal mass in itself can be shown by considering the interior space of a building not as a static object in accordance with the conventional design philosophy, but as a dynamic system based on the process design philosophy of *archi.engineering building's interior to be partially homeostatic within a temperature range.* The proposed design approach takes a new factor, the diurnal temperature variation ΔT_{out} (which is not commonly a parameter in building codes) into consideration. The existence of an optimal slab thickness for iTM is found; the same slab thickness as that for hydronically activated TABS application is found in the present passive application. In the case of large ΔT_{out} or large WWR a recommended thermal mass for eEM is given. The guideline may be alternatively given as a recommended slab thermal-mass of 0.1 m for external wall inside a continuous insulation layer so that corresponding maximum WWR as a function of ΔT_{out} is allowed. While TABS is limited to new construction application, the proposed approach has room for new construction as well as retrofitting application. The archi.engineering of radiant/convectively conditioned building has the passive simplicity of passivhaus and the cooling versatility of TABS. Archi.engineered buildings will be amenable to demand side management, including the full benefits of low cost grid power as well as the harnessing of natural resources.

Reference

[4.1] P. Ma and L.-S. Wang, "Effective heat capacity of interior planar thermal mass (iPTM) subject to periodic heating and cooling," *Energy and Buildings* **47** (2012) 44–52

[4.2] M. Schuler (2010) In FORWARD to *Thermally Active Surfaces in Architecture* by Kiel Moe

[4.3] R.A. Meierhans, "Slab cooling and earth coupling," *ASHRAE Transactions* **99 (2)**: P511-518, (DE-93-02-4), 1993

[4.4] R.A. Meierhans, "Room air conditioning by means of overnight cooling of the concrete ceiling," *ASHRAE Transactions* **102 (1)**: 693-697, (AT-96-08-2), 1996

[4.5] ISO 11855, *Building environmental design—Design, dimensioning, installation and control of embedded radiant heating and cooling systems* (International Organization for Standardization, 2012)

[4.6] ASHRAE Inc., *ANSI/ASHRAE/IES Standard 90.1-2010: Energy Standard for Buildings Except Low-Rise Residential Buildings*, S-I ed., 2010

[4.7] International Code Council (2011). 2012 IECC (distributed by Cengage Learning)

[4.8] D.H. Nall (2013) "Thermally active floors," *ASHRAE Journal* (January 2013, pp.32-xx)

[4.9] ASHRAE, Inc., *2009 ASHRAE Handbook—Fundamentals*, I-P & S-I ed., 2009

[4.10] R. Emden (1938) "Why do we have winter heating?" *Nature* **141**:908-909

[4.11] A. Sommerfeld, (1952) *Thermodynamik und Statistik* (Vorlesungen uber theoretische Physik Band 5)

[4.12] R. Kubo, (1968) *Thermodynamics* (North-Holland Publishing Co.)

[4.13] Z. Bilkadi (1972) "When you heat your house does the thermal energy content increase?" *J. Chem. Educ.* **49**:493-494

[4.14] J.A. Campbell (1973) "Footnote to the house heating exemplum", *J. Chem. Educ.* **50**:365-366

[4.15] H.J. Kreuzer and S.H. Payne (2011) "Thermodynamics of heating a room," *Am J Phys* **79**:74-77

[4.16] B. D. Hunn (editor, 1996) *Fundamentals of Building Energy Dynamics* (The MIT Press) p. 182

[4.17] P. Ma, L.-S. Wang, N. Guo, "Modeling of TABS-based thermally manageable

buildings in Simulink," *Applied Energy* **104** (2013) 791–800

[4.18] P. Ma, *Dynamic Heat Transfer: Effective Heat Capacity of Planar Thermal Mass Subject to Periodic Heating and Cooling*, M.S. Thesis, Stony Brook University, May, 2010

[4.19] P. Ma, L.-S. Wang, "Effective heat capacity of exterior Planar Thermal Mass (ePTM) subject to periodic heating and cooling," *Energy and Buildings* **47** (2012) 394–401

[4.20] E.J. Makela, J.L. Williamson, E.B. Makela, *Comparison of Standard 90.1-2010 and the 2012 IECC with Respect to Commercial Buildings*, Pacific Northwest National Laboratory, Prepared for the U.S. Department of Energy under Contract DE-AC05-76RL01830, September 2011

[4.21] C.E. Ochoa, M.BC. Aries, E.J. van Loenen, J.L.M. Hensen, "Considerations on design optimization criteria for windows providing low energy consumption and high visual comfort," *Applied Energy* **95** (2012) 238 – 245

[4.22] Ilya Prigogine, *Autobiography of Ilya Prigogine*

[4.23] S. F. Mason (1956) *Main Currents of Scientific Thought: A History of the Sciences* (Abelard-Schuman)

[4.24] L.-S. Wang, "Exergy or the entropic drive: Waste heat and free heat," *International J. of Exergy* (in print)

Chapter 5: Full Homeostasis in Buildings — Building cooling with a cooling tower

The previous chapter investigated the passive application of building thermal mass, including interior thermal mass (iTM) and exterior envelope mass (eEM). It found that the operative temperature variation can be controlled in a small range with sufficient amount of both iTM and eEM. However, for a thermally homeostatic building, besides the operative temperature range, another important factor for thermal comfort is the operative temperature level. This chapter will apply a parametric cooling tower in summer to the TABS-equipped room to achieve proper operative temperature level under the cooling condition. Cooling tower is an example of low power equipment (lowPE) driven by *natural energy gradients*—which is a part of the ambient conditions. This chapter will investigate the climatic conditions that are favorable to using the lowPE of cooling tower.

5.1 Building and its ambient conditions

In a Foreword to *Heating, Cooling, Lighting* [5.1] the architect J.M. Fitch wrote, "The central paradox [challenge] of architecture [is] how to provide a stable, predetermined internal environment in an external environment that is in constant flux across time and space…" We want to argue that "an external environment that is in constant flux across time and space" is both a challenge and an opportunity—an opportunity in how a building can harness natural energy temporal gradient and spatial gradient in its interaction with its ambient environment.

One of the main challenges imposed by variable environment is the cooling and heating loads on a building. Conventional HVAC-based cooling and heating aim to meet the imposed loads, which are functions of the internal temperature-range that the designer wants to maintain and the weather temperature conditions. If the HVAC equipment is to guarantee thermal comfort at all time, it must be designed for peak weather conditions. Since any extreme weather condition is a statistical possibility, it would not be practical to aim for the most extreme but transitory condition (which would lead to over-sizing of equipment). The design of equipment is therefore based on a fixed "climatic design [peak] conditions," which for annual cooling according to the *ASHRAE Handbook – Fundamentals* [5.2] is the *design condition for 0.4%* or the *design condition for 1%* or the *design condition for 2%* in annual cumulative frequency of occurrence (exceeding the design condition) in one year. There are 365 × 24 h = 8760 h in one year. The *0.4%*, *1%*, and *2%* design conditions are the three dry-bulb temperatures T_0 values that the instantaneous hourly temperature in the hottest months exceeded the corresponding value for a duration of 35 h (0.4% of 8760 h), 88 h (1%), or 175 h (2%) per year, respectively, for the period of record. For convenience the following discussion will be based on 1% dry-bulb temperatures T_0 or $(T_0)_{design\_1\%}$.

Note that the conventional HVAC-based cooling load for design selection is based on the peak value of hourly temperature T_0, not diurnal average temperature $\overline{T}_0$. (For simplicity in this discussion the conventional load is said to be based on peak hourly value in the steady-state sense. Overlooked below are the various refinements of the conventional load calculations by taking into consideration of the temporal thermal response of a building.) Let the peak-to-peak amplitude of the diurnal temperature variation be ΔT_0, the peak hourly temperature T_0 and the daily mean temperature $\overline{T}_0$ are related as

$$T_0 = \overline{T}_0 + \frac{1}{2}\Delta T_0 \tag{5.1}$$

The peak hourly temperature T_0, which is the determinant of the equipment capacity and the driver (causation) of the irreversible heat transfer process, depends on (and increases with) both the daily mean temperature and its amplitude: both are parts of "external environment that is in constant flux across time and space": high value of $\overline{T}_0$ and high value of ΔT_0 both contribute to the irreversibility in the operation of a building.

This chapter approaches the problem of energy and buildings as a problem informed by thermodynamics as the science of irreversible processes. The central argument of the chapter is that buildings' "external environment that is in constant flux across time and space" represents both a challenge and a driving "force" for buildings' conditioning. This chapter will add a parametric cooling tower to the RC model built in the previous chapter to harness the natural energy gradient driven force for the cooling of the homeostatic building-room. It will also give a discussion of the hypothetical design selection of cooling tower: Instead dependency on the *single* peak hourly temperature T_0, it will be shown that the design conditions are function of *both* the diurnal average temperature of $\overline{T}_0$ *and* the amplitude of the diurnal temperature variation ΔT_0, with quite different functional relationships for the two. At last, how a building function under climatic conditions of different locations will be studied.

5.2 Irreversibility: the management of irreversible ongoing natural energy gradient

The problem of energy and buildings should be understood as a problem informed by thermodynamics as the science of irreversible processes, a brief review of which is given here. Conventional thermodynamics fails to understand irreversibility's dual roles of destruction and construction. Traditionally, irreversibility is identified with irreversible loss, i.e., its destructive role exclusively. The identification of entropy growth (irreversibility) with energy degradation did not, however, come from Carnot, who made

use of dissipation-less "entropy-like" flow as a constructive process. [5.3] It was Kelvin, who, in order to remove the mystery of entropy as being formulated by Clausius, linked its growth to the degradation of energy or the dissipation of exergy. Heuristically, Kelvin's interpretation was a huge success. But, conceptually it was disastrous since the identification led to the disappearance of irreversible processes as a constructive "force," the very notion on which Carnot founded the science of heat. Schrodinger made the first significant move of restoring the constructive role. [5.4] In recent years, the duality of destruction and construction has been successively returned to the core of thermodynamics by the Brussels Thermodynamics School. [5.5]

Kondepudi of the Brussels Thermodynamics School wrote, "Irreversible processes are creators and destroyers of order." [5.6] In his autography, Prigogine, the leader of the School, put the historical origin of the idea this way,

> Among all those perspectives opened by thermodynamics, the one which was to keep my interest was the study of irreversible phenomena, which made so manifest the "arrow of time." From the very start, I always attributed to these processes a constructive role, in opposition to the standard approach, which only saw in these phenomena degradation and loss of useful work. Was it the influence of Bergson's *"L'évolution créatrice"* or the presence in Brussels of a performing school of theoretical biology? The fact is that it appeared to me that living things provided us with striking examples of systems which were highly organized and where irreversible phenomena played an essential role.
>
> Such intellectual connections, although rather vague at the beginning, contributed to the elaboration, in 1945, of the theorem of minimum entropy production, applicable to non-equilibrium stationary states…From the very beginning, I knew that the minimum entropy production was valid only for the linear branch of irreversible phenomena, the one to which the famous reciprocity relations of Onsager are applicable. And, thus, the question was: What about the stationary states far from equilibrium, for

> which Onsager relations are not valid, but which are still in the scope of macroscopic description? Linear relations are very good approximations for the study of transport phenomena (thermal conductivity, thermo-diffusion, etc.), but are generally not valid for the conditions of chemical kinetics…Those problems had confronted us for more than twenty years, between 1947 and 1967, until we finally reached the notion of "dissipative structure." [5.7]

The original insight of Carnot as rediscovered by the Brussels School has been extended in a recent paper [5.3]: In this paper, Wang replaces exergy (suggesting identification) with the *entropic drive* (suggesting duality) and, in addition, stresses the difference between passive, irreversibility driven processes and active (information- or design-directed), irreversibility driven ones. While the former can bring about "dissipative structures," [5.5,5.6] only the latter is capable of *efficient* construction of *stable* NET (non-equilibrium thermodynamics) structures.

There are two kinds of entropic drive or irreversibility-driven processes, latent ones and ongoing ones. Using fossil fuel and fire are latent exergy irreversibility-driven processes, the first kind. Fossil fuel is traditionally regarded as an energy resource and all irreversibility serving only to deprive or diminish the usefulness of the energy resource. This identification of irreversibility as exclusively losses,

Irreversibility = Irreversible loss

is an incorrect notion. The correct understanding is that the same irreversibility can manifest both as destructive irreversible losses and as the constructive entropic drive. The truth is that the irreversibility of fuel→fire→heat is the entropic drive and its active management is what makes it useful by reducing evitable (or avoidable) irreversible losses. It is the strong latent irreversibility (or latent entropic drive) that makes fossil fuel an important resource; better active management of irreversibility makes the resource applications more productive.

The irreversibility of the diurnal variation in a building's surroundings ("external

environment that is in constant flux across time and space") is a second (ongoing) kind of irreversibility: the larger its amplitude, the stronger the irreversibility. Without active management this ongoing entropic drive will eventually be dissipated into pure irreversible losses. With active management, ongoing irreversibility can instead serve for constructive purpose; the larger the amplitude the stronger the constructive role it can play. Making this ongoing irreversibility—this ongoing *natural energy spatial gradient and temporal gradient*—into useful resource necessitates the active management of irreversibility, a concept that has been overlooked in traditional engineering, which think of management only as the management of energy resource, not of irreversibility of either latent kind or ongoing kind.

Thermally homeostatic building is a key to the management of the irreversible natural energy gradient. In the conception of homeostatic buildings, there are two steps. The first step is the design of a TABS-based building with adequate thermal mass and met the requirements of minimum envelope thermal resistance and maximum window-to-wall ratio, so that the building maintain its acceptable operative temperature with no equipment at all. The second step is the selection of equipment, which can be either mechanical ones or lowPE, for maintaining acceptable operative temperature level of a building with any possible external environments. This chapter focuses on the use of lowPE for cooling application. A lowPE requires moderate power for its operation and is by definition driven by natural energy spatial and temporal gradient.

Unlike mechanical equipment which are typically powered directly or indirectly by fossil fuel, lowPE powered by moderate amount of power driven by natural energies (i.e., natural heat and coolness), which are low-T heat and high-(or moderate-)T coolness. Examples of natural energies are: nighttime air's coolness in summer, an example of natural temporal gradient; solar heating in winter and sunlight in summer (as source of power as well as heat source for cooling devices), an example of natural temporal and spatial gradient; heat and coolness of water bodies and geothermal sources, examples of

spatial gradient.

Examples of low-power equipment are cooling tower, active solar thermal (AST) systems and solar PV systems (as well as solar powered cooling systems), water-source heat pump and ground-source heat pump, and possibly many others including Hydronic Solar Wall (HSW) [5.8].

In this chapter only cooling is considered and a hypothetical study of the design selection of cooling tower as an example of lowPE is given. A building with lowPE is driven largely by natural energy gradient and requires little mechanical power, i.e., it is largely autonomous from man-made mechanical power.

5.3 Thermally homeostatic building with cooling tower

The thermally homeostatic building investigated in this dissertation has a TABS and an outdoor cooling tower, as an example of low-power equipment, for harnessing the natural energy gradient driven force in the nighttime, as shown in Fig. 5.1.

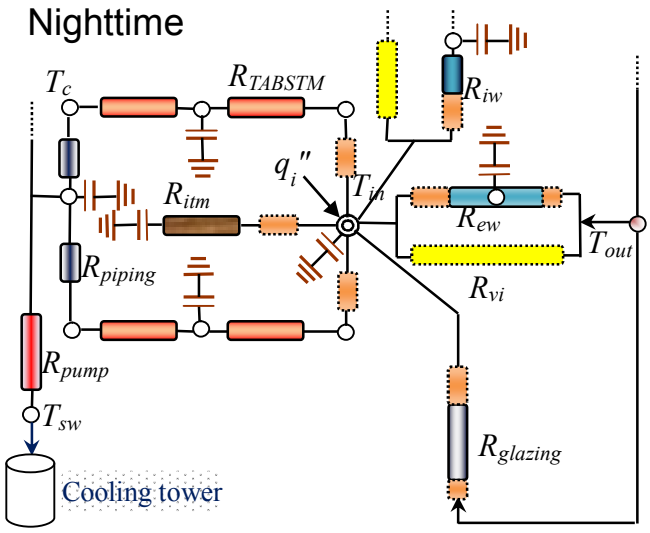

Fig. 5.1. Thermally homeostatic building cooling: nighttime operation

Water pump is on when the outdoor nighttime dry-bulb temperature T_{out} is lower than the water temperature at TABS outlet T_{rw}, which is also the water temperature at cooling tower inlet. In a wet cooling tower, if the climate is not too humid, the supply water temperature T_{sw} can be brought to be near the dew point temperature of outdoor air.

A large volume of literature of the cooling tower application in buildings exists as reviewed in Chapter 2. Here a parametric cooling tower is applied for the cooling of the homeostatic building.

In a dry cooling tower according to Ref. [*5.9*], the heat exchange in an air-water heat exchanger is

$$Q_{water} = C_w \dot{m}_w \left(T_{w1} - T_{w2} \right) \tag{5.2}$$

$$Q_{air} = \alpha \left(\overline{T}_w - T \right) A \tag{5.3}$$

where Q_{water} and Q_{air} are the heat released at the water side and absorbed at the air side of the heat exchangers, respectively; C_w [J/kg-K] is the water heat capacity; $\dot{m}_w$ [kg/s] is the water mass flow rate in the heat exchanger; T_{w1} and T_{w2} are the water inlet and outlet temperatures in the heat exchanger; α [W/m^2-K] is the heat transfer coefficient of the heat exchanger and is related to the airflow velocity through the heat exchanger; $\overline{T}_w$ is the mean water temperature in the heat exchanger; T is the air temperature outside the heat exchanger, A [m^2] is the surface area of the heat exchanger.

Let us simplify the heat exchange process as follows:

$$Q_{water} = Q_{air} \tag{5.4}$$

and

$$\overline{T}_w = \frac{T_{w1} + T_{w2}}{2} \tag{5.5}$$

Then

$$T_{w2} = \left(1 - \frac{2\alpha A}{\alpha A + 2C_w \dot{m}_w} \right) T_{w1} + \frac{2\alpha A}{\alpha A + 2C_w \dot{m}_w} T \tag{5.6}$$

In a [wet, counter-current flow] cooling tower according to Ref. [*5.10*: 661~675], the cooling tower effectiveness, or the cooling tower thermal efficiency, can be defined by analogy to the effectiveness of a simple heat exchanger, if assuming that the heat capacity rate ($\dot{m}\, c_p$) for the cooling tower water is less than that for the air:

$$\varepsilon = \frac{T_{win} - T_{wout}}{T_{win} - T_{wbin}} \tag{5.7}$$

Thus $$T_{wout} = (1-\varepsilon)T_{win} + \varepsilon T_{wbin} \tag{5.8}$$

where T_{win} is the inlet water temperature, T_{wout} is the outlet water temperature, T_{wbin} is the wet-bulb temperature of the inlet air, and ε is the heat exchanger effectiveness

$$\varepsilon = \frac{1-\exp\left[-NTU\left(1-\dot{C}_w/\dot{C}_a\right)\right]}{1-\left(\dot{C}_w/\dot{C}_a\right)\exp\left[-NTU\left(1-\dot{C}_w/\dot{C}_a\right)\right]} \tag{5.9}$$

where $$\dot{C}_w = \dot{m}_w c_{p_w} \quad \text{and} \quad \dot{C}_a = \dot{m}_a \overline{c}_{p_e} \tag{5.10}$$

and NTU is the Number of Transfer Units

$$NTU = UA_e / \dot{C}_w \tag{5.11}$$

In the equations above, $\dot{m}_w$ [kg/s] is the mass flow rate of water, $\dot{m}_a$ [kg/s] is the mass flow rate of air, c_{p_w} [J/kg-K] is the specific heat of water, $\overline{c}_{p_e}$ is the mean specific heat of the moist air treated as an equivalent ideal gas, U [W/m^2-K] is the cooling tower overall heat transfer coefficient, and A_e [m^2] is the equivalent heat transfer surface area

$$A_e = A\overline{c}_{p_e} / c_p \tag{5.12}$$

where A [m^2] is the heat transfer surface area, and c_p [J/kg-K] is the specific heat of moist air.

It is easy to find that equation (5.6) and equation (5.8) have the same form, if in equation (5.6) let

$$\varepsilon = \frac{2\alpha A}{\alpha A + 2C_w \dot{m}_w} \tag{5.13}$$

The cooling tower thermal efficiency ε is between 0 and 1. Ref. [*5.11*] gave an example of the efficiency as a function of air and water flow rates, as shown in Fig. 5.2. In the TABS-equipped room, the mass flow rate of the water in the PEX pipes is 0.12 kg/s. Thus according to Fig. 5.2, the thermal efficiency should be higher. The maximum thermal efficiency is assumed to be 0.8.

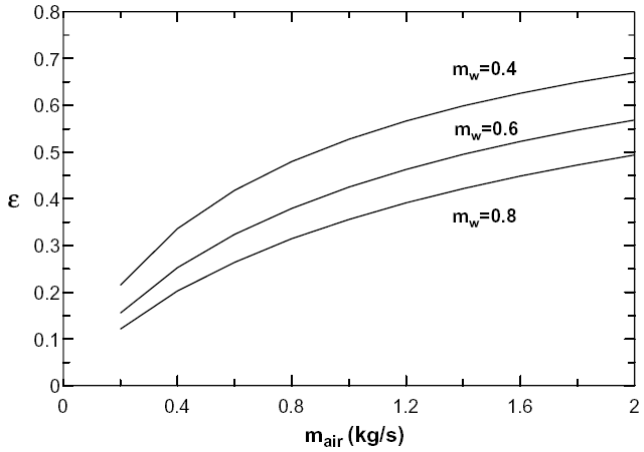

Fig. 5.2. Tower efficiency as a function of air and water flow rate (m_{spray}=1.4 kg/s, T_{wb}=16 °C)

At the room side, according to Chapter 4 in Ref. [*5.12*], the calculation equations are as follows:

$$\left(T_{sw}-T_c\right)/R_t = q''_{room} = \dot{m}_w c_w \left(T_{sw}-T_{rw}\right) \tag{5.14}$$

$$T_{rw} = T_{sw} - q''_{room}/\left(\dot{m}_w c_w\right) \tag{5.15}$$

where T_{sw} is the TABS supply-water temperature, T_c is the TABS slab's core temperature, R_t is the TABS-resistance, q''_{room} [W] is the heat flux from the TABS to the room (negative in the cooling case), $\dot{m}_w$ [kg/s] is the mass flow rate of water in the TABS pipes, c_w [J/kg-K] is the specific heat of water and T_{rw} is the water temperature at the TABS outlet.

From the application point of view, "a wet cooling tower is more effective than a dry tower, because it relies mainly on the wet-bulb temperature of the air and not on the generally higher dry-bulb temperature, as in the case of a dry-cooling tower." [*5.13*] "The ambient wet-bulb temperature of the entering air … is typically 10 °F [5.56 K] to 30 °F [16.67 K] lower than the dry-bulb temperature, depending on the local climate." [*5.14*] In EnergyPlus, cooling tower has two models. In one model, "the nominal capacity is specified for the standard conditions i.e. entering water at 35C (95F), leaving water at 29.44C (85F), entering air at 25.56C (78F) wet-bulb temperature and 35C (95F) dry-bulb

temperature." [5.10: 661] Here the dry-bulb and wet-bulb temperature difference is 9.44 °C (17 °F). Two important parameters determine the wet cooling tower performance: range and approach, as shown in Fig. 5.3. [5.15: 7~8] Their definitions are as follows:

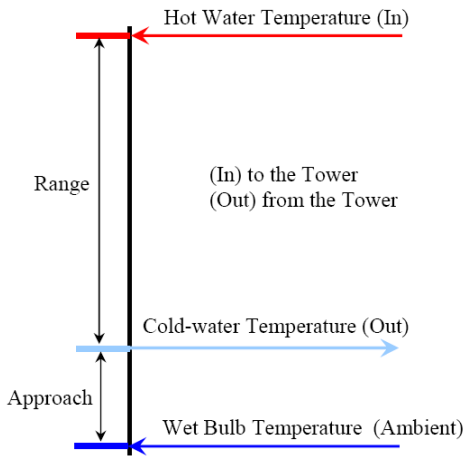

Fig. 5.3. Range and approach of cooling towers

Range: This is the difference between the cooling tower water inlet and outlet temperature. A high CT [cooling tower] Range means that the cooling tower has been able to reduce the water temperature effectively, and is thus performing well.

Approach: This is the difference between the cooling tower outlet cold-water temperature and ambient wet bulb temperature. The lower the approach, the better the cooling tower performance. Although, both range and approach should be monitored, the Approach' is a better indicator of cooling tower performance.

"As a general rule, the closer the approach to the wet bulb, the more expensive the cooling tower due to increased size. Usually a 2.8 °C approach to the design wet bulb is the coldest water temperature that cooling tower manufacturers will guarantee." [5.15: 9]

This dissertation only takes cooling tower as an example of low-power equipment for harnessing natural energy, not focuses on the cooling tower design. Therefore, a parametric cooling tower is added to the RC model of the room. In the following section, a mean value of the outdoor air dry-bulb temperature, which is 27.10 °C, is selected in summer time to investigate the building cooling operation. As in the "Nominal Capacity"

model adopted in EnergyPlus, the dry-bulb and wet-bulb temperature difference is assumed to be 9.44 °C, and thus the mean value of the outdoor air wet-bulb temperature is 17.66 °C. If the guaranteed approach of the cooling tower is 2.8 °C, the mean value of the TABS supply-water temperature should be 20.46 °C, which is lower than the supply-water temperature given in the two basic cases in Chapter 3. Suppose that the cooling tower works from 8:00 PM to 4:00 AM the next day, and in this duration the outdoor air dry-bulb temperature is lower than its mean value. Therefore, combining the information above, there is no doubt that the parametric cooling tower can work effectively.

In the RC model, the heat flux from the TABS to the room q''_{room} and the TABS supply-water temperature T_{sw} are measured; the TABS returned-water temperature T_{rw} can be calculated with equation (5.15) as the mass flow rate of water in the TABS pipes is a known constant; equation (5.8) gives the theoretical outlet water temperature of the cooling tower T_{wout}; a switch controls the operation of the cooling tower; between 8:00 PM and 4:00 AM the next day, the switch is closed and T_{sw} is equal to T_{wout}; from 4:00 AM to 8:00 PM, the switch is opened and temperature of the water in the TABS is free to float. By varying the cooling tower effectiveness, T_{wout} is changed and then T_{sw} is controlled. The model is used to investigate the cooling operations in the following sections in this Chapter.

5.4 Ambient summer conditions of seven US cities

According to the *ASHRAE Handbook* [5.2], the summer months are the months from June through September, a period of (30 + 31 + 31 + 30) × 24 h = 2928 h. In this section, seven US cities will be selected and the ambient summer conditions of the cities will be given. As shown in Fig. 5.4, the cities are: Fullerton, CA; Sacramento, CA; Wilmington, DE; Atlanta, GA; Springfield, IL; Valentine, NE; and Albuquerque, NM. From the figure, it is clear that the distribution of the cities can well present a wide range of ambient

conditions of the United States.

Fig. 5.4. Distribution of the selected seven US cities (made in http://maps.google.com)

For the seven cities, the mean ambient 1% dry-bulb temperatures are between 300.2 K and 300.3 K, and the corresponding mean amplitudes are between 9.5 K (Wilmington) and 18.1 K (Sacramento), as shown in Table 5.1. The reason of the selection is that the seven cities' design 1% daily-mean dry-bulb T may be taken to a constant of 300.25 K (**27.10 °C** or 80.78 °F), as the *design condition for 1%* $(T_0)_{design\_1\%}$. A hypothetical study of the possibility of homeostatic building cooling as a function of available diurnal temperature amplitude can be made on the same base of $(T_0)_{design\_1\%}$.

Table 5.1. Design conditions for the selected US cities (From *2009 ASHRAE Handbook*)

Location	Design 1% hourly dry-bulb temperature ("peak"), $(T_0)_{design\ 1\%}$		Mean daily dry-bulb temperature range, ΔT_0		Design 1% daily-mean dry-bulb temperature, T_0	
	°F	K	°F	K	°F	K
Fullerton, CA	90.1	305.4	19.0	10.6	80.6	**300.2**
Sacramento, CA	97.1	309.3	32.6	18.1	80.8	**300.3**
Wilmington, DE	89.3	305.0	17.1	9.5	80.8	**300.2**
Atlanta, GA	90.7	305.8	19.9	11.1	80.8	**300.2**
Springfield, IL	90.5	305.7	19.3	10.7	80.9	**300.3**
Valentine, NE	94.0	307.6	26.4	14.7	80.8	**300.3**
Albuquerque, NM	92.9	307.0	24.4	13.6	80.7	**300.2**

The real-time hour-by-hour dry-bulb temperatures of the seven cities are in Fig. 5.5. The real-time weather data were requested by email from the website of the US Department of Energy (DOE). [5.16] The data are collected by the National Weather Service (NWS) from weather stations, and are parsed and stored into a local database at the National Renewable Energy Laboratory (NREL). [5.17] Some data in the weather database are missed, and upon request the missing data are exported with interpolated values (for the dew point and the dry bulb temperatures only). If the missing period is less than 6 hours, the data are simply filled linearly; if it is more than 6 hours and less than 48 hours, the data are filled by taking the trend of the first previous day that is valid; if it is more than 48 hours, the program creates a new file where the data starts again. [5.17] In the recent decade, 2007 is the only year that all the four-month summer weather data are in one file, that is, all the missing periods are less than 48 hours. The accumulative hours of missing periods in the four months are from 46 h to 77 h.

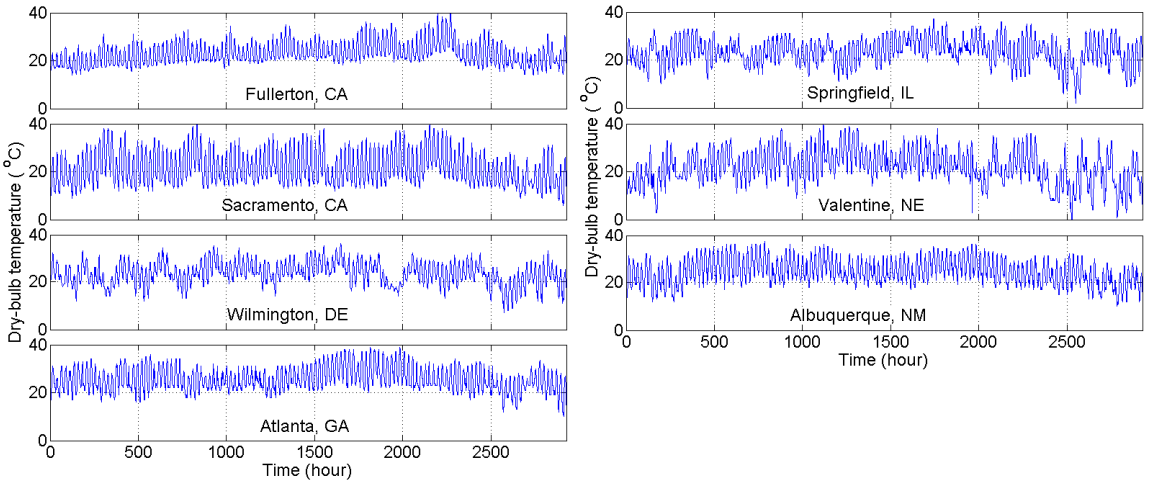

Fig. 5.5. Dry bulb temperatures of the selected seven US cities in the summer of 2007

For each city, the diurnal temperature amplitude is defined by the temperature difference of the maxima and the minima in the duration from midnight to the next midnight. The distribution histograms of the 122 amplitudes of every city are shown in Fig. 5.6. In the figure, if the amplitude is not an integer, it is rounded.

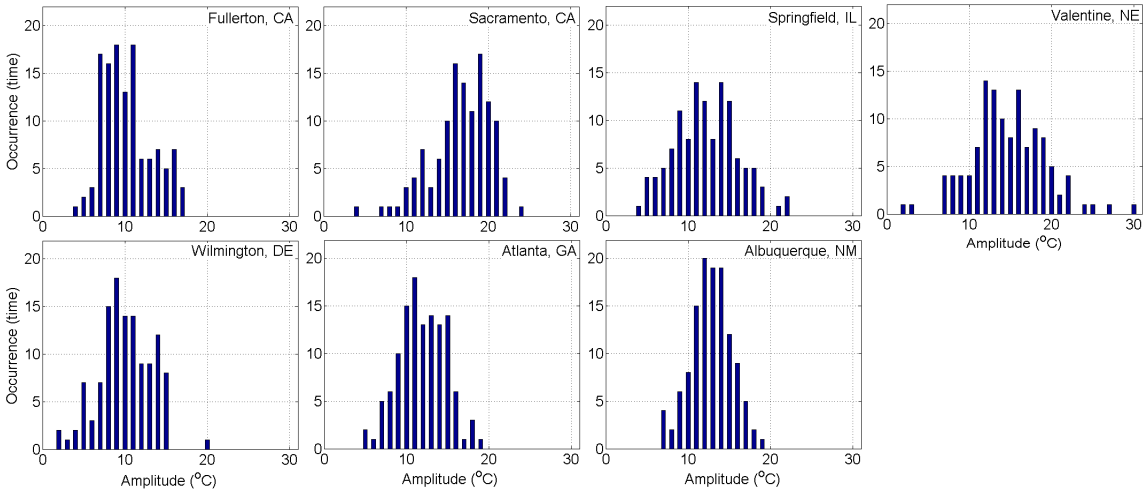

Fig. 5.6. Dry-bulb temperature amplitude distributions of the selected seven US cities in the summer of 2007

From Fig. 5.6, it can be found: (1) most amplitudes are smaller than 20 °C in most cities, except a very small part in Springfield, a small part in Valentine and a moderate part in Sacramento; (2) amplitudes are mainly distributed in the large-amplitude part in Sacramento; (3) in other cities, amplitudes are mainly distributed in the middle- or small-amplitude part.

5.5 Hypothetical example of the maximum $\left(\overline{T}_0\right)_{design}$ by using cooling tower at available ΔT_0

There is considerable variation in the diurnal temperature amplitude ΔT_0 from one climatic region to another one. This diurnal temperature variation is the driving force for building cooling conditioning: although large diurnal variation causes larger operative temperature variation, the same large diurnal temperature variation serves to maintain the proper operative temperature level at higher summer ambient temperature.

The modeling condition and the parameter selection of the investigated homeostatic building-room are as follows:

(1) The mean value of the operative temperature is kept at 25.25 °C for best thermal comfort in summer [5.18];

(2) The ambient temperature amplitudes ΔT_{out} are from 2 K to 34 K with 4 K step;

(3) The maximum cooling tower effectiveness is 0.8;

(4) The external wall NW concrete thickness is 0.10 m, the ceiling and floor NW concrete thickness is 0.25 m, the internal wall LW concrete thickness is 0.20 m, and the interior thermal mass wood thickness is 0.10 m;

(5) The window thermal resistance is 0.53 m^2-K/W and the corresponding thermal conductivity is 1.887 W/m^2-K, which is smaller than the restricted maximum *U*-value (1.99 W/m^2-K) in the *ASHRAE Standard 90.1-2010*;

(6) Three window-to-wall ratios (WWR): 20%, 42% and 60%;

(7) Four *U*-values of the external walls:

***U* = 3.293**: Maximum restriction of nonresidential mass walls (Zone 1 and Zone 2 in *ASHRAE Standard 90.1-2004*; Zone 1 in *ASHRAE Standard 90.1-2007* and *2010*);

***U* = 0.857**: Maximum restriction of nonresidential mass walls (Zone 3 and Zone 4 in *ASHRAE Standard 90.1-2004*; Zone 2 in *ASHRAE Standard 90.1-2007* and *2010*);

***U* = 0.365**: Maximum restriction of nonresidential mass walls (Zone 1 in *ASHRAE Standard 90.1-2004*); Maximum restriction of nonresidential steel-framed walls (Zone 7 and 8 in *ASHRAE Standard 90.1-2004*; Zone 4, 5, 6, 7 and 8 in *ASHRAE Standard 90.1-2007* and *2010*); Maximum restriction of nonresidential wood-framed and other walls (Zone 5 in *ASHRAE Standard 90.1-2007* and *2010*);

***U* = 0.203**: Maximum restriction of nonresidential wood-framed and other walls (Zone 8 in *ASHRAE Standard 90.1-2007* and *2010*).

Notice that Zone 1 and 2 mean very hot and hot climates, respectively, such as Hawaii and Florida. *U* = 3.293 for these two zones is really a high value. Zone 7 and 8 mean very cold and subarctic climates, respectively. All of Alaska is in Zone 7 except for several boroughs in Zone 8. Therefore, *U* = 0.203 is definitely a low value.

Table 5.2 lists the maximum mean value of the ambient temperatures T_{out} that the cooling tower can maintain the most comfortable indoor temperature and the operative

temperature variations ΔT_{op} under the three different window-to-wall ratios and the four different exterior wall thermal conductivities, while the cooling tower effectiveness is 0.8.

Table 5.2. Mean ambient temperatures and operative temperature variations under different window-to-wall ratios and exterior wall thermal resistances when cooling tower ε is 0.8

		WWR = 20%		WWR = 42%		WWR = 60%	
External walls	T_{out} (°C)	T_{out} (°C)	T_{op} (°C)	T_{out} (°C)	T_{op} (°C)	T_{out} (°C)	T_{op} (°C)
U_{ew} (W/m^2 K)	ΔT_{out}	Mean	ΔT_{op}	Mean	ΔT_{op}	Mean	ΔT_{op}
3.293	2	27.29	1.38	26.64	1.77	26.08	2.11
	6	27.96	1.71	27.33	2.11	26.78	2.47
	10	28.63	2.04	28.02	2.46	27.49	2.83
	14	29.30	2.38	28.71	2.81	28.20	3.19
	18	29.98	2.71	29.40	3.16	28.90	3.55
	22	30.65	3.06	30.09	3.51	29.61	3.92
	26	31.31	3.40	30.78	3.86	30.32	4.28
	30	31.98	3.75	31.48	4.21	31.03	4.65
	34	32.65	4.10	32.17	4.57	31.74	5.02
0.857	2	27.91	1.27	26.93	1.69	26.19	2.06
	6	28.79	1.47	27.77	1.94	26.99	2.35
	10	29.66	1.67	28.60	2.18	27.80	2.63
	14	30.54	1.88	29.44	2.43	28.60	2.92
	18	31.42	2.08	30.28	2.68	29.41	3.22
	22	32.30	2.29	31.11	2.94	30.22	3.51
	26	33.17	2.49	31.95	3.19	31.03	3.81
	30	34.05	2.70	32.79	3.44	31.84	4.11
	34	34.93	2.90	33.63	3.70	32.65	4.40
0.365	2	28.18	1.24	27.04	1.67	26.23	2.05
	6	29.15	1.41	27.94	1.89	27.07	2.32
	10	30.11	1.59	28.83	2.12	27.91	2.59
	14	31.08	1.76	29.72	2.35	28.75	2.86
	18	32.05	1.94	30.62	2.58	29.59	3.14
	22	33.01	2.11	31.51	2.81	30.44	3.42
	26	33.98	2.29	32.41	3.04	31.28	3.70
	30	34.95	2.47	33.30	3.27	32.13	3.99
	34	35.92	2.64	34.20	3.51	32.98	4.27
0.203	2	28.30	1.23	27.09	1.66	26.24	2.04
	6	29.30	1.39	28.00	1.88	27.10	2.31
	10	30.30	1.56	28.92	2.10	27.95	2.57
	14	31.31	1.72	29.84	2.32	28.81	2.84
	18	32.31	1.88	30.75	2.54	29.66	3.12
	22	33.31	2.05	31.67	2.76	30.52	3.39
	26	34.32	2.22	32.59	2.99	31.38	3.67
	30	35.33	2.39	33.51	3.22	32.24	3.95
	34	36.33	2.56	34.43	3.44	33.10	4.23

The data in Table 5.2 are plotted in Fig. 5.7 and Fig. 5.8. In the two figures, the ΔT_{op} and the mean T_{out} increase almost linearly with the increase of the ΔT_{out}.

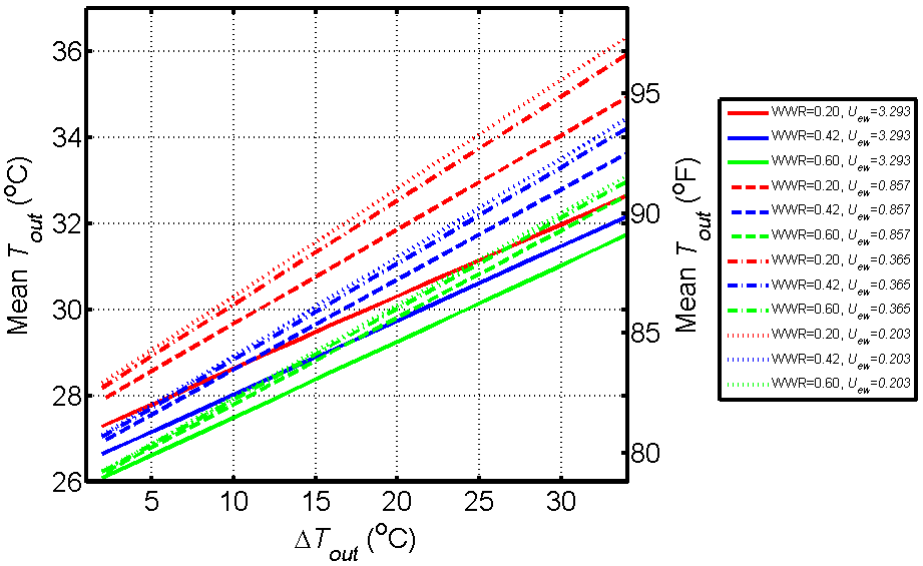

Fig. 5.7. Mean ambient temperatures under different window-to-wall ratios and exterior wall thermal conductivities when cooling tower effectiveness is 0.8

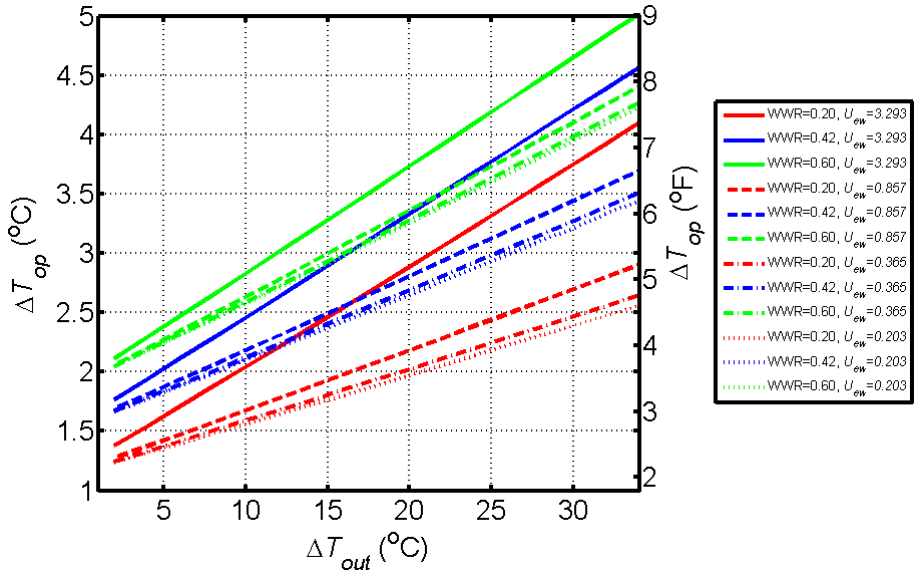

Fig. 5.8. Operative temperature variations under different window-to-wall ratios and exterior wall thermal conductivities when cooling tower effectiveness is 0.8

When the ΔT_{out} is very smaller and the WWR is high, even if the effectiveness is set to the maximum value, the cooling tower alone still cannot keep the mean T_{op} at 25.25 °C, while the mean T_{out} is at the design mean ambient temperature (27.10 °C) of the seven

cities. The maintenance is only possible at mean T_{out} *lower* than the design mean ambient temperature. When the ΔT_{out} is not too small and the WWR is not too high, the cooling tower alone can maintain the mean T_{op} at 25.25 °C, while the mean T_{out} is at the design mean ambient temperature (27.10 °C) of the seven cities.

Clearly, with the increase of the glazing area (larger WWR), the corresponding mean T_{out} decrease and the ΔT_{op} increase, which mean that it is harder for the cooling tower to maintain the desired T_{op} level and range. The reason is obvious: larger glazing area means bigger heat exchange and more solar energy gain through the glazing, and thus the internal thermal environment is harder to be kept stable due to the more influence by the external surrounding.

With the decrease of the external wall thermal conductivity (that is, bigger thermal resistance), the corresponding mean T_{out} increase and the corresponding ΔT_{op} decrease, which mean that for the cooling tower it is easier to maintain the desired T_{op} level and range. The reason is also obvious: smaller thermal conductivity means less heat exchange through the external walls. As the mean indoor temperature is lower than the mean outdoor temperature under the cooling condition, the heat flow through the external walls is net-in to the room in a period (one day), and thus the cooling tower needs to remove less heat from the room due to the bigger thermal resistance.

When the mean ambient temperature is 27.10 °C, the cooling tower effectiveness ε and the operative temperature variations under different exterior wall thermal resistances, window-to-wall ratios and ambient temperature amplitudes are listed in Table 5.3 and plotted in Fig. 5.9 and Fig. 5.10. In this part with the enlargement of the ΔT_{out}, the ΔT_{op} still increase linearly, but the ε decrease nonlinearly. In Table 5.3, some parts are crossed out with oblique lines. The values in these part can be calculated by the RC model; however, since the ε is larger than 0.8, even 1.0, it is not true practically; these values are listed for reference purpose only. The threshold ε = 0.8 is also plotted in Fig. 5.9 and values above the line are considered as meaningless.

Table 5.3. Cooling tower effectiveness and operative temperature variations under different exterior wall thermal resistances, ambient temperature amplitudes and window-to-wall ratios when the mean ambient temperature is 27.10 °C

		WWR = 20%		WWR = 42%		WWR = 60%	
External walls	T_{out}	**CT**	T_{op}	**CT**	T_{op}	**CT**	T_{op}
U_{ew} (W/m^2-K)	ΔT_{out} (K)	ε	ΔT_{op} (K)	ε	ΔT_{op} (K)	ε	ΔT_{op} (K)
3.293	2	0.71	1.36	1.07	1.80	1.52	2.20
	6	0.51	1.64	0.71	2.09	0.94	2.49
	10	0.40	1.92	0.54	2.38	0.68	2.80
	14	0.32	2.20	0.43	2.68	0.53	3.10
	18	0.27	2.48	0.36	2.97	0.44	3.41
	22	0.24	2.77	0.31	3.27	0.37	3.72
	26	0.21	3.05	0.27	3.57	0.32	4.03
	30	0.19	3.33	0.24	3.87	0.29	4.34
	34	0.17	3.62	0.22	4.16	0.26	4.66
0.857	2	0.54	1.24	0.87	1.70	1.30	2.12
	6	0.40	1.40	0.61	1.90	0.84	2.35
	10	0.32	1.56	0.47	2.10	0.62	2.59
	14	0.27	1.72	0.38	2.31	0.49	2.83
	18	0.23	1.88	0.32	2.51	0.41	3.08
	22	0.20	2.05	0.28	2.72	0.35	3.32
	26	0.18	2.21	0.24	2.93	0.30	3.57
	30	0.16	2.38	0.22	3.14	0.27	3.82
	34	0.14	2.54	0.20	3.35	0.24	4.08
0.365	2	0.50	1.21	0.82	1.67	1.25	2.10
	6	0.38	1.34	0.58	1.86	0.81	2.32
	10	0.30	1.48	0.45	2.04	0.60	2.54
	14	0.25	1.62	0.36	2.23	0.48	2.77
	18	0.22	1.76	0.31	2.42	0.40	3.01
	22	0.19	1.90	0.27	2.61	0.34	3.24
	26	0.17	2.04	0.23	2.80	0.30	3.48
	30	0.15	2.18	0.21	2.99	0.26	3.71
	34	0.14	2.32	0.19	3.18	0.24	3.95
0.203	2	0.49	1.20	0.80	1.66	1.23	2.09
	6	0.37	1.32	0.57	1.84	0.80	2.31
	10	0.29	1.45	0.44	2.02	0.60	2.53
	14	0.25	1.58	0.36	2.20	0.48	2.75
	18	0.21	1.71	0.30	2.38	0.40	2.98
	22	0.18	1.85	0.26	2.57	0.34	3.21
	26	0.16	1.98	0.23	2.75	0.30	3.44
	30	0.15	2.11	0.21	2.94	0.26	3.68
	34	0.13	2.25	0.19	3.13	0.24	3.91

In Table 5.3, when the glazing area or the external wall thermal conductivity increases, both the ε and the ΔT_{op} increase, correspondingly. The meanings and the reasons are the same as that of the linear part: the internal thermal environment is harder

to be kept stable due to the more influence by the external surrounding.

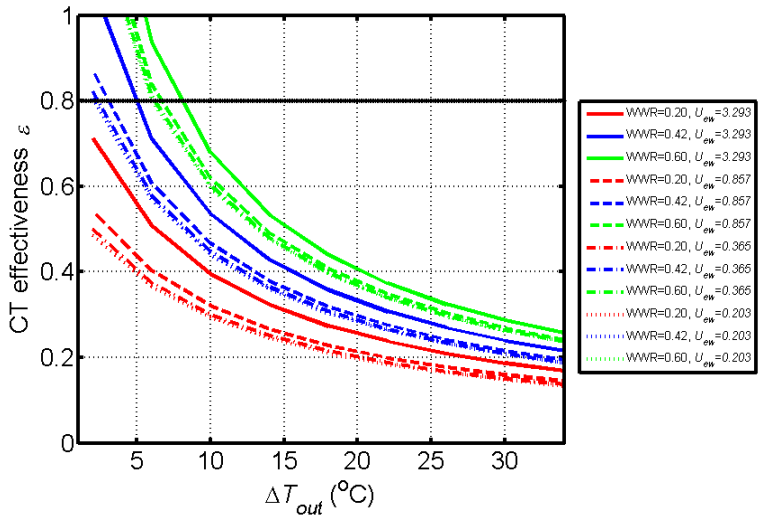

Fig. 5.9. Cooling tower effectiveness under different window-to-wall ratios and exterior wall thermal conductivities when the mean ambient temperature is 27.10 °C

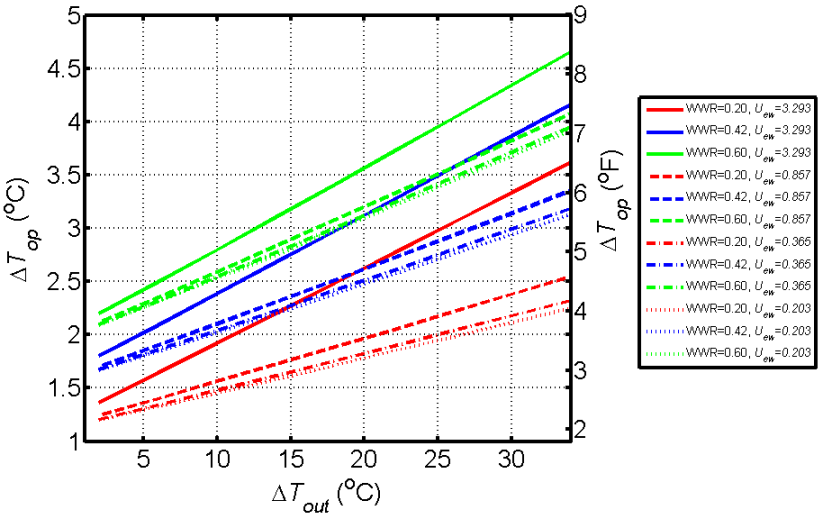

Fig. 5.10. Operative temperature variations under different window-to-wall ratios and exterior wall thermal conductivities when the mean ambient temperature is 27.10 °C

Fig. 5.9 shows that when the ΔT_{out} is relatively small, the ε decrease steeply with the increase of the ΔT_{out}; when the ΔT_{out} becomes very large, the benefit of the big ΔT_{out} becomes insignificant. The reasons are: as both the mean T_{out} and the mean T_{op} are fixed, the amounts of net-flow-in heat through the envelope are almost the same in a period; with fixed solar-internal heat gains, the amounts of heat that need to be removed are

almost the same. So once the nighttime ambient temperature is low enough for the cooling tower to work "normally," even lower ambient temperature is not necessary.

5.6 The possibility of homeostatic building with a constant-size cooling tower in most favorable locations

5.6.1 A building in locations with different micro-climate statistics

Fig. 5.11 shows the daily distribution of dry-bulb temperature mean values vs. amplitudes of the selected seven US cities in the summer of 2007. In this figure, an assumed maximum constant cooling tower effectiveness of 0.8 is used. Each blue cross is one summer day and its position in the plot corresponds to its daily mean temperature vs. temperature amplitude. In each location, the red line separate days that cooling tower with the maximum effectiveness can maintain a 25.25 °C operative temperature level from days that cooling tower cannot: in days below the red line, cooling tower can maintain the optimal operative temperature; in days above the red lines, cooling tower cannot maintain the optimal operative temperature due to high mean ambient temperature or small ambient temperature amplitude, or both.

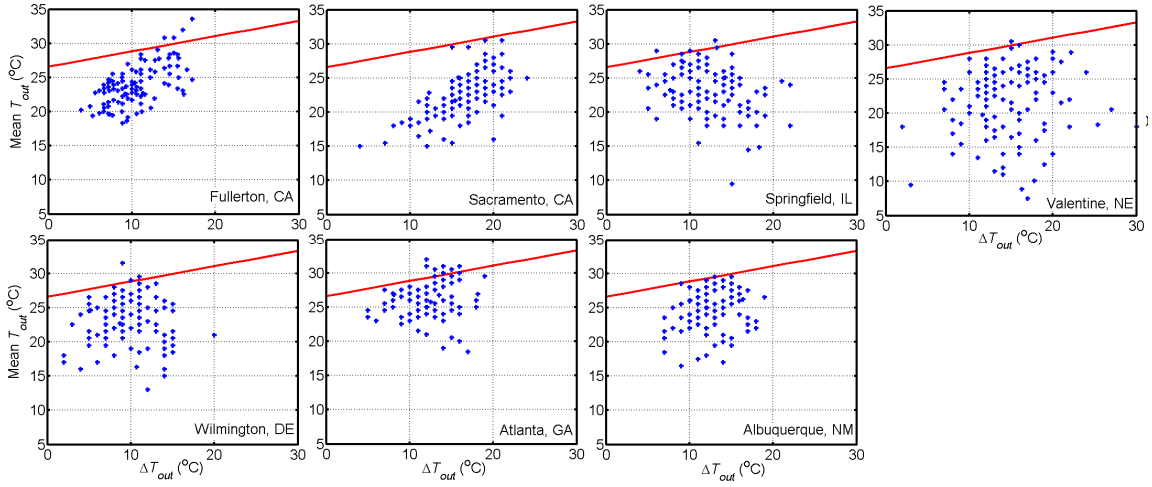

Fig. 5.11. Daily distribution of dry-bulb temperature mean values vs. amplitudes of the selected seven US cities in the summer of 2007

In Table 5.4, days and percentages that cooling tower cannot maintain the optimal operative temperature are given in the second column: in Sacramento, the cooling tower works well enough to maintain a comfortable indoor environment in the whole 4-month summer period; but in Atlanta, there are 12 failure days (9.84%). In the third column, after increasing the mean operative temperature by 1 to 3 K, the failure days drop continuously. The last column gives the mean operatives temperatures when there is no failure day (0% failure day, and it can be called 0% design condition). The mean operative temperature should increase 2.73 K to meet the cooling requirement in Atlanta.

The most striking result is that even though Sacramento has the highest peak hourly temperature of $(T_0)_{design\_1\%}$ = 309.3 K (Table 5.1), it is the easiest location for using cooling tower to maintain its operative temperature level in the whole summer at optimal thermal comfort. In other locations either the thermal comfort has to be partially compromised, or equipment other than pure lowPE (e.g., heat pump) needs to be used for assisting the cooling tower.

Table 5.4. Days that cooling tower cannot meet the cooling requirement in 122 summer days of 2007 and operative temperatures with 0% design condition

Location	CT cannot meet cooling requirement		T_{op} increases			T_{op} with 0% design condition
			1K	2K	3K	
	day	percentage	day	day	day	°C (°F)
Fullerton, CA	4	3.28%	3	1	1	28.42 (83.16)
Sacramento, CA	0	0%	0	0	0	24.91 (76.84)
Wilmington, DE	4	3.28%	1	1	0	28.15 (82.67)
Atlanta, GA	12	9.84%	4	1	0	27.98 (82.36)
Springfield, IL	3	2.46%	2	0	0	26.32 (79.38)
Valentine, NE	1	0.82%	0	0	0	25.81 (78.46)
Albuquerque, NM	1	0.82%	0	0	0	25.26 (77.47)

Using the case of Sacramento as benchmark where all summer days a building can be maintained at 25.25 °C, we determine the possible operative temperatures at the six cities that can be maintained based on this benchmark. The results are shown in Fig. 5.12: in three of the six cities, thermal comfort has to be compromised. Whether a higher indoor operative temperature is acceptable with higher summer outdoor ambient

temperature (i.e., whether human tolerates higher indoor temperature when outdoor temperature is higher) is an interesting possibility. More study is needed to consider such possibility.

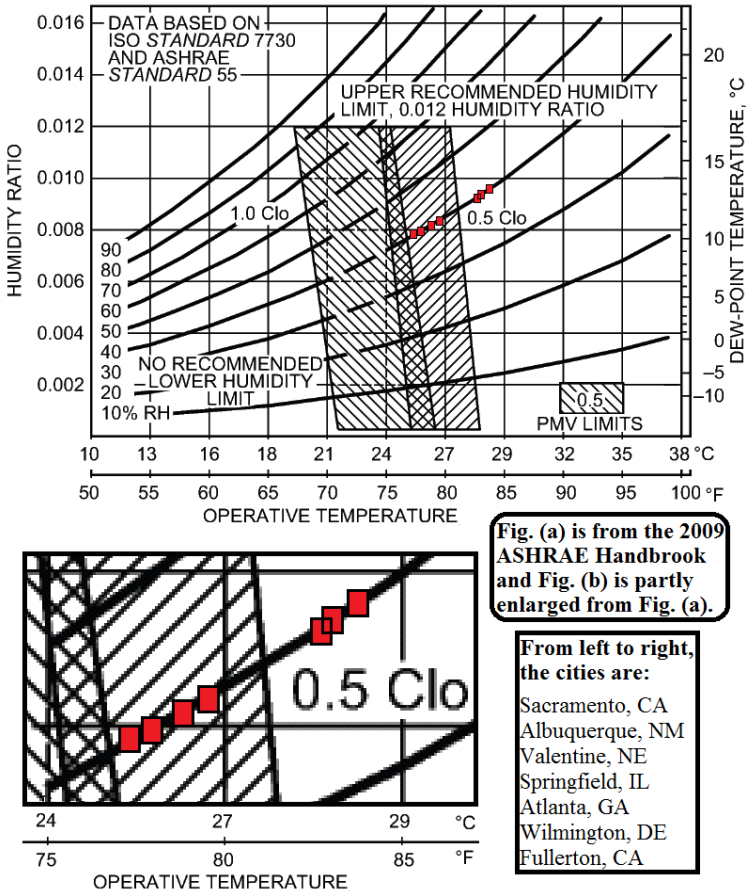

Fig. 5.12. Mean operative temperatures of the selected seven US cities based on 0% design condition on the 40% relative humidity line in the ASHRAE summer and winter comfort zones

The other alternative is the use of equipment other than pure low power ones (e.g., heat pump) to assist the cooling tower for maintaining the acceptable operative temperature level (moving the operative temperature lower into the shaded region in Fig. 5.12). The concept of homeostatic building is a useful one that offers the foundation for multitude pathways of improving lowPE in future and the introduction of new lowPE, as well as the foundation for the experimental test of other kind of equipment such as heat pump.

5.6.2 Most favorable locations and meso-scale climatic process

It is therefore important for moving forward to demonstrate homeostatic buildings first in most favorable locations in North America such as Sacramento. It is interesting to note that the micro-climatic process that creates the condition in Sacramento is that the summer day time high temperature air at Sacramento rises to pull in the sea breeze through Golden Gate strait, and this breeze travels towards Sacramento (see the first two panels of Fig. 5.13) and by the night time it reaches Sacramento resulting in cool nighttime air there (see the last panel of Fig. 5.13). It is the combined result—of solar heating of air generating thermal convection, ocean's moderating temperature effect, and the right distance of the location from ocean for the convective "cool front" to arrive at Sacramento in the nighttime—that creates this natural energy gradient gift. Other locations, especially prevalent in the best wine countries, with the same combination are the upper Napa valley and Paso Robles at the upstream of Salina valley. These are the most favorable locations for experimental testing of homeostatic buildings; these are the places where we can best learn how to managing irreversibility created by sun, air, ocean, and convective sea breeze for homeostatic NET (non-equilibrium thermodynamics) state in radiantly cooled buildings, instead consuming energy from the ground for dissipative-structure-like NET state in traditional buildings.

The big two of renewable energies are wind and the sun. We prefer to call renewable energies as examples of "natural energy gradient," because the term includes all irreversible processes resources beyond those that can be harnessed into energy stock such as power harnessed from PV panel and wind turbine. The physicist and seminal thinker Amory Lovins wrote, "following the remark attributed to General Dwight Eisenhower: 'If a problem cannot be solved, enlarge it'—until its boundaries include the options, synergies, and degrees of freedom that its solution requires." [5.19] We must enlarge the energy problem, as Lovins has been arguing since 1976, beyond the "hard path" of fossil fuel to a "soft path" of renewable energies (along with conservation and

efficiency). We must *also* enlarge the energy problem by thinking in terms of the *irreversibility process* of natural energy gradient, not just *energy stock* in the ground or collected from the sky. Natural energy gradient represents an even bigger world of the enlarged possibilities that Lovins refers to as the *new fire* [5.20]: natural energy gradient of the strong micro-climatic process of *sea breeze* may well be a new, the third kind of, renewable "energy" next to the wind and the solar energy.

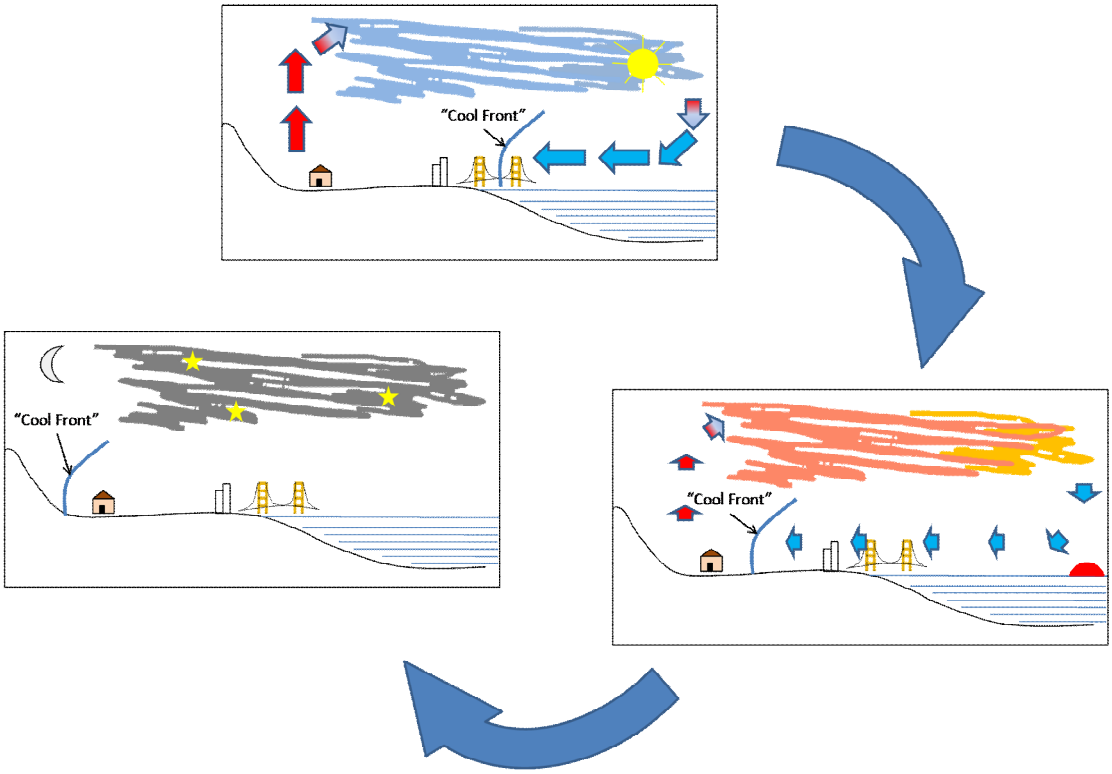

Fig. 5.13. Sea breeze driven by solar heated air current (red) moving the "cool front" (blue), which arrives at the location at the nighttime

5.7 Chapter summary

"Water is 832 times denser than air. Thermally active surfaces [for radiant cooling] are built around this basic principle." [5.21] "Radiant cooling systems are more efficient, more comfortable, more attractive, and more healthful than [conventional HVAC] systems that circulate air." [5.22] Based on TABS, design of homeostatic building can be approached in interdependent but distinguishable two steps: the design of building mass

and envelope for controlling the indoor temperature variation in a small range, and the design of low power equipment from building conditioning. The central thermodynamic argument is that buildings' external natural temporal and spatial gradient represents both a challenge to building's indoor comfort and a driving "force" for buildings' conditioning. Thermally homeostatic buildings overcome this challenge, and in addition harness this driving force for their conditioning. Using cooling tower, it is shown that homeostatic buildings at optimal operative temperature are possible in locations of large diurnal temperature change. In the case of Sacramento we identify its micro-climatic surroundings condition of strong diurnal temperature variation to be derived from strong sea breeze, a meso-scale climatic process. It represents a renewable *thermal* resource in the present case, which is different from sea breeze being a *dynamical* resource for wind farms (e.g., San Gorgonio Pass, CA). We need to think in terms of how to manage irreversibility: while diurnal temperature variation is not usually viewed as a source of energy as wind power is, it is clearly a thermal phenomenon that manifests spatial and temporal irreversible gradient.

Reference

[5.1] N. Lechner (2009), *Heating, Cooling, Lighting,* 3rd ed., (Wiley)

[5.2] ASHRAE Inc, *2009 ASHRAE Handbook – Fundamentals*, SI and I-P Ed. 2009

[5.3] L.-S. Wang, "Exergy or the entropic drive: Waste heat and free heat," *International Journal of Exergy*, (in print; accepted on July 24, 2012)

[5.4] E. Schrodinger, *What is Life?* (1944)

[5.5] I. Prigogine, *From Being to Becoming* (Freedman and Co.) (1980)

[5.6] D. Kondepudi, *Introduction to Modern Thermodynamics*(2008)

[5.7] Ilya Prigogine, *Autobiography of Ilya Prigogine*

[5.8] L.-S. Wang, *US provisional appl. US Patent Office Docket 788-186-PRO*, Dated on Oct. 12, 2011

[5.9] Z. Zhai, S. Fu, "Improving cooling efficiency of dry-cooling towers under cross-wind conditions by using wind-break methods," *Applied Thermal Engineering* **26** (2006) 1008–1017

[5.10] EnergyPlus™, " EnergyPlus Engineering Reference: The Reference to EnergyPlus Calculations," *EnergyPlus Documentation*, Version 7.0 Documentation, Oct. 2011

[5.11] J. Facão, A. Oliveira, " Heat and mass transfer correlations for the design of small indirect contact cooling towers," *Applied Thermal Engineering* **24** (2004) 1969–1978

[5.12] M. Koschenz, B. Lehmann, *Thermoaktive Bauteilsysteme*, EMPA, 2000

[5.13] J. van der Merwe, C.G. du Toit, " Numerical simulation of a wet cooling tower," *R AND D JOURNAL*, Vol. 18, No. 2, July 2002

[5.14] J.W. Furlong, F.T. Morrison, " Optimization of Water-Cooled Chiller – Cooling Tower Combinations," CTI Journal, Vol. 26, No. 1, (2005) 12–19

[5.15] United Nations Environment Programme, *Electrical Energy Equipment: Cooling Towers*, 2006

[5.16] http://apps1.eere.energy.gov/buildings/energyplus/weatherdata_download.cfm (Last access on May 11, 2013)

[5.17] N. Long, *Real-time weather data access guide*, National Renewable Energy Laboratory Contract No.: DE-AC36-99-GO10337. March 2006

[5.18] B. Lehmann, V. Dorer, M. Koschenz, "Application range of thermally activated

building systems tabs," *Energy and Buildings* **39** (2007) 593–598

[5.19] A. Lovins, (2012), Comment on "Opportunities and challenges for a sustainable energy future," *RMI Outlet* (August 28, 2012)

[5.20] A. Lovins (2011), *Reinventing Fire* (Chelsea Green Publishing)

[5.21] K. Moe, *Thermally Active Surfaces in Architecture*, Princeton Architectural Press; 2010

[5.22] Energy Design Resources, *Design Brief: Radiant Cooling*, July 2, 2003

Chapter 6: Design of a Thermally Homeostatic Building in Paso Robles

In this chapter, the special geographical and climatic conditions in Paso Robles, California, are introduced first. Later, a stand-alone, one-story, south-facing small commercial building with large window-to-wall ratio (WWR) located in Paso Robles is designed in detail in the AutoCAD Revit 2013. The existing materials in the Revit are chosen as many as possible to construct the building. The building is designed to meet the partially homeostatic criteria, which is tested by an RC model built in Matlab and Matlab/Simulink. In the RC model, the material properties in the Revit are used.

6.1 Special geographical and climatic conditions of Paso Robles

Paso Robles has large diurnal temperature amplitudes because of the sea breeze from the Monterey Bay, which is critical for homeostatic buildings. This is the main reason that Paso Robles is selected as the building location.

6.1.1 Introduction to Paso Robles

Paso Robles [6.1,6.2] is located at 35°37′36″N and 120°41′24″W, approximately halfway between Los Angeles and San Francisco, as shown in Fig. 6.1 (produced in Google Map). The elevation of Paso Robles ranges from 675 to 1100 ft, while the majority of the main downtown area sits at about 740 ft (230 m) above sea level.

Fig. 6.1. Paso Robles, halfway between Los Angeles and San Francisco

Close to mountains, beaches and deserts, Paso Robles is home to one of the greatest wine growing areas (American Viticulture Area, or AVA) in the United States. The introduction to Paso Robles on the website http://www.pasowine.com is as follows [6.3]:

> Located along California's famed Central Coast, the Paso Robles winegrape growing region's climate is perfect for the production of award-winning premium wines. A long growing season of warm days and cool evenings give rise to vibrantly ripened fruit with dynamic flavor profiles that translate beautifully in your glass of Paso Robles wine.
>
> Traversing the landscape you will find 26,000 vineyard acres, producing more than 40 winegrape varieties - from Spanish to Italian, Bordeaux to Rhône, including the area's heritage variety Zinfandel. The styles of wine are diverse in this very distinct region.
>
> Along your journey through Paso Robles Wine Country, take time to stroll the historic downtown to shop and dine. Boutique stores, wine country cuisine, and tasting rooms fill the blocks surrounding Paso Robles' Downtown City Park. A scene right out of a Norman Rockwell painting, Paso Robles' downtown completes the picture of Paso Robles Wine Country.

6.1.2 Special geographical condition of Paso Robles

Paso Robles contains a total land area of 19.4 square miles (50.3 km^2) according to the US Census Bureau. The Temblor Range (including the San Andreas Fault) lies about 28 miles (45 km) to the east of the city; the Santa Lucia Coastal Range directly rises up from the city's western border. Paso Robles is located at the southern end of the Salinas River Valley, which is a coastal valley in central California, as shown in Fig. 6.2 [6.4].

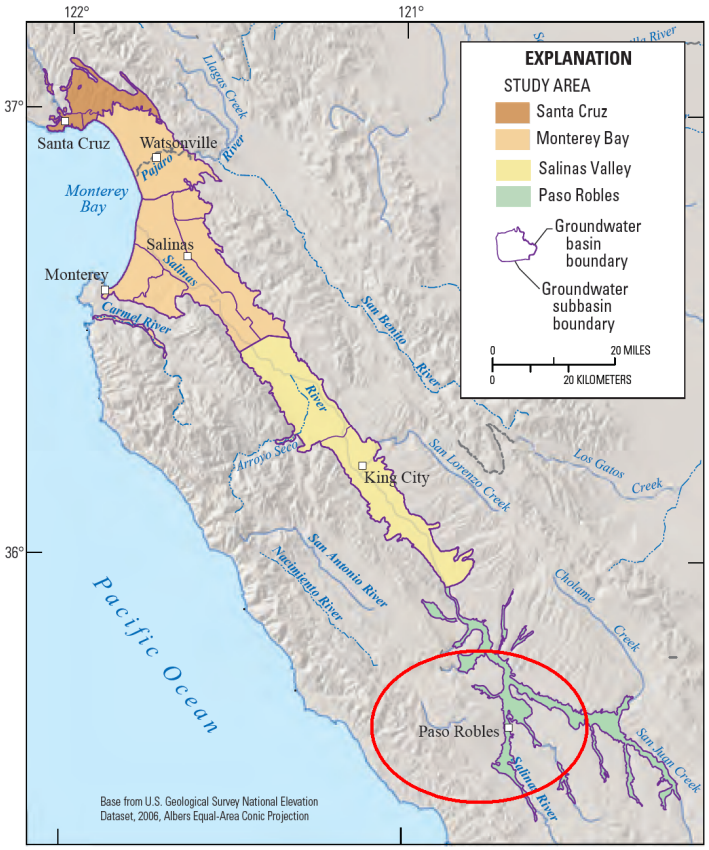

Fig. 6.2. Paso Robles and the Salinas River Valley

According to Ref. [*6.5*], the Salinas River Valley is

approximately 75 km in length and 20-30 km in width, oriented in a NW-SE direction. The valley opens into Monterey Bay on the Pacific coast in the northwest and in the southeast it gradually merges into the coastal mountains. It is bounded by the Gabilan mountain range on the east and Sierra de Salinas Mountain on the west (Fig. 6.3). Elevations

of the surrounding mountains are typically near 900-1000 m above mean sea level. Fremont Peak (960.61 m) is NE of the city of Salinas within a distance of 15 km. Mt. Toro (1056.36 m) is WSW of Salinas within a distance of 10 km. North Chalone Peak (1001.21 m) is SSE of Salinas at a distance of ~40 km.

Typical daytime up-valley and nighttime down-valley winds prevail in the Salinas Valley. However, since it is a coastal valley this diurnal pattern is strongly influenced by the coastal winds and the land and sea breeze systems. During nighttime in the northern part of the valley, the land breeze regime results in the winds descending down the mountain slopes toward the Pacific Ocean. In the middle and southern part of the valley, the down-valley wind blows towards Monterey Bay (Fig. 6.3). However, nighttime meteorological data for the study period shows significant periods of up-valley flows.

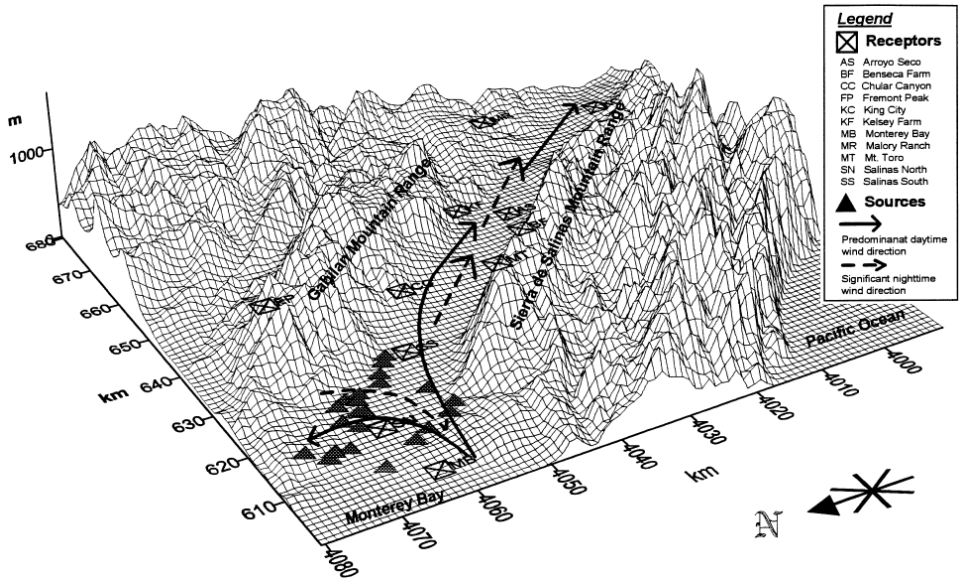

Fig. 6.3. 3D view showing the sources, receptors and the main wind patterns in the Salinas river valley, CA

6.1.3 Special climatic condition of Paso Robles

Due to its special geographical condition, the Paso Robles area actually consists of two different climate types and classifications [6.1]: KCC type *BSk* and KCC type *Csb*. The types are based on the Köppen climate classification (KCC) system. The type *BSk* is

a semi-arid, dry, steppe-type climate, and the type *Csb* is the typical, coastal Californian & "Mediterranean" type. The primary climate of the area is defined by long, hot, dry summers and brief, cool, sometimes rainy winters.

The long-lasting, mild autumns and occasional early springs give Paso Robles a unique climate, which is suitable for growing a variety of crops ranging from primarily grapes, to olives, to almonds and other tree nuts. The average annual rainfall of the city is about 14.71 inches (374 mm), mostly during winter and early spring. Typically, there is no rain falls from May to September in Paso Robles. Summers are usually very hot, with daily temperatures frequently exceeding 100 °F (38 °C) and even exceeding 110 °F (43 °C) occasionally. The diurnal temperature swing in summers of Paso Robles is unusually very large: as much as 50 °F (28 °C). Winters in Paso Robles are often very cool and moist. The lowest temperature can reach to 25 °F (-4 °C).

Recorded monthly outdoor air temperatures around Paso Robles are listed in Table 6.1 with a minimum 30-year record period. [*6.6*]

Table 6.1. Recorded monthly outdoor air temperatures around Paso Robles

Month	Average High	Average Low	Mean	Record High	Record Low
Jan	60°F (16°C)	35°F (2°C)	48°F (9°C)	83°F (28°C) (1976)	12°F (-11°C) (2007)
Feb	62°F (17°C)	38°F (3°C)	50°F (10°C)	83°F (28°C) (1991)	18°F (-8°C) (1971)
Mar	66°F (19°C)	40°F (4°C)	53°F (12°C)	91°F (33°C) (2007)	20°F (-7°C) (1971)
Apr	73°F (23°C)	41°F (5°C)	57°F (14°C)	99°F (37°C) (2004)	27°F (-3°C) (1970)
May	81°F (27°C)	46°F (8°C)	64°F (18°C)	108°F (42°C) (2001)	30°F (-1°C) (1974)
Jun	87°F (31°C)	50°F (10°C)	69°F (21°C)	115°F (46°C) (1961)	36°F (2°C) (1988)
Jul	93°F (34°C)	54°F (12°C)	74°F (23°C)	115°F (46°C) (1961)	41°F (5°C) (1948)
Aug	93°F (34°C)	54°F (12°C)	74°F (23°C)	113°F (45°C) (1996)	40°F (4°C) (1968)
Sep	88°F (31°C)	51°F (11°C)	70°F (21°C)	112°F (44°C) (1955)	34°F (1°C) (1948)
Oct	79°F (26°C)	44°F (7°C)	62°F (17°C)	106°F (41°C) (1980)	20°F (-7°C) (1971)
Nov	67°F (19°C)	38°F (3°C)	53°F (12°C)	98°F (37°C) (1966)	18°F (-8°C) (1958)
Dec	59°F (15°C)	34°F (1°C)	47°F (8°C)	83°F (28°C) (1958)	8°F (-13°C) (1990)

Extending the record period, according to Ref. [*6.7*], the all-time record high temperature was 117 °F (47 °C) on August 13, 1933, and the record low temperature was

0 °F (-18 °C) on January 6, 1913. On average, there are 81.0 days with high temperatures of 90 °F (32 °C) or higher and 64.0 days with low temperatures of 32 °F (0 °C) or lower. The daily temperature averages and extremes in Paso Robles are shown in Fig. 6.4. At the Paso Robles FAA Airport [6.8], the record high temperature was 115°F (46 °C) on June 15, 1961 and July 20, 1960, and the record low temperature was 8 °F (-13 °C) on December 22, 1990. There is an average of 86.7 days with highs of 90 °F (32 °C) or higher and an average of 53.6 days with lows of 32 °F (0 °C) or lower.

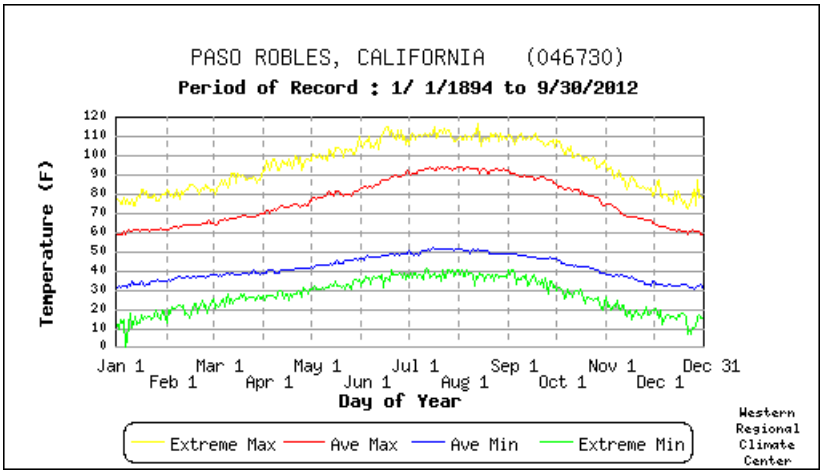

Fig. 6.4. Daily temperature averages and extremes in Paso Robles

- Extreme Max. is the maximum of all daily maximum temperatures recorded for the day of the year.
- Ave. Max. is the average of all daily maximum temperatures recorded for the day of the year.
- Ave. Min. is the average of all daily minimum temperatures recorded for the day of the year.
- Extreme Min. is the minimum of all daily minimum temperatures recorded for the day of the year.

6.2 Design of a homeostatic building

6.2.1 Dimensions

The stand-alone homeostatic building is a one-story south-facing small commercial building located in Paso Robles, California. Fig. 6.5 shows the main dimensions of the building. It has a large lobby, a waiting room, a reception room, three offices and two restrooms. The total cooled and heated floor area is 2310 ft^2 (214.6 m^2). The building can

be divided into two zones: the front zone (consisting of the lobby, the waiting room, the reception room and the two restrooms) and the office zone (consisting of the three offices). In the exterior walls of the front zone, large curtain walls are installed, which means that this zone is transparent to the outdoor environment.

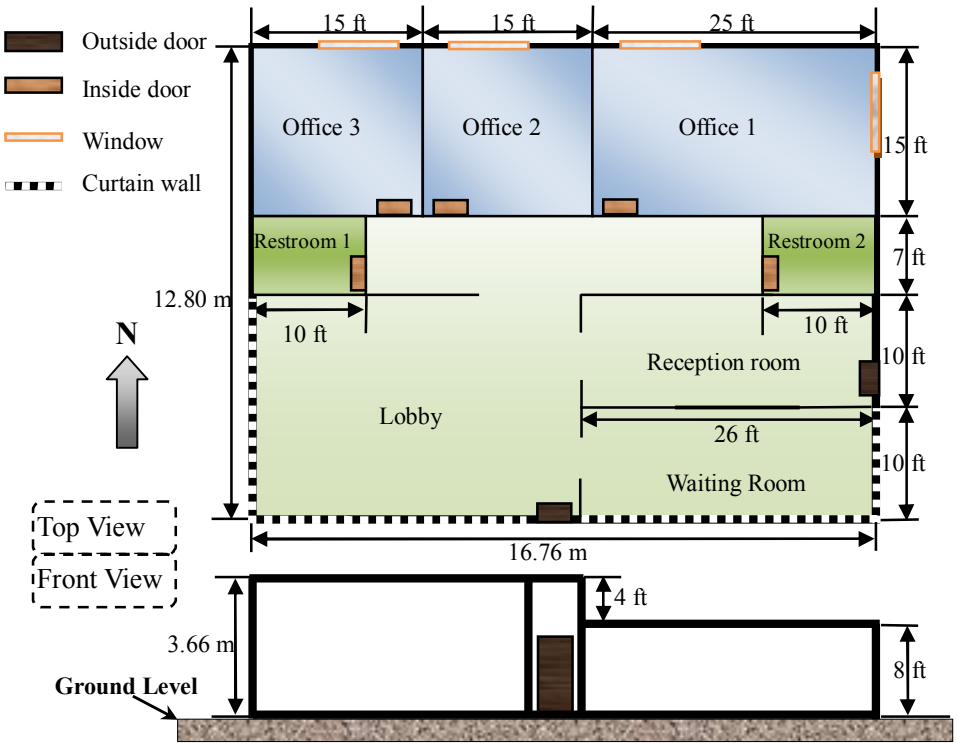

Fig. 6.5. Schematic of the small commercial building

6.2.2 Configurations

Exterior walls:

The exterior walls are selected as "Basic Wall: CW 102-85-100p." The *U*-value of this kind of wall is 0.3463 W/m^2-K (corresponding *R*-value is 2.8877 m^2-K/W), which meets the climate zone 5's requirement (maximum 0.365 W/m^2-K). The thickness of the concrete in the walls is 0.100 m, which is exactly the recommended thickness for exterior walls in Chapter 4. From exterior side to interior side, the exterior walls consist: 0.102m common brick, 0.050m air, 0.035m cavity fill, vapour retarder membrane layer, 0.100m

concrete masonry units, and 0.012m gypsum wall board. The total thickness of the walls is 0.299m.

Floor:

Below the ground level, the floor is selected as "Floor: Concrete Domestic 425mm 2." However, there are two problems: the *U*-value is 0.6084 W/m^2-K, which does not meet the climate zone 5's requirement (maximum 0.420 W/m^2-K for mass floors), and the concrete thickness is 0.225m while it is expected to be 0.250m for a TABS-equipped building.

Therefore, three modifications are made for the floor: first, the cast-in-situ concrete layer is changed from 0.175m to 0.200m; second a carpet with an *R*-value of 0.125 m2-K/W is added to the surface of the floor; and last the rigid insulation layer is thickened from 0.050m to 0.071m.

As a result, the *U*-value of the new type of floor becomes 0.4180 W/m^2-K (corresponding *R*-value is 2.3926 m^2-K/W). The new floor type is renamed as "Floor: Concrete Domestic 478.5mm 2." It consists: 0.0075m carpet, 0.050m sand/cement screed concrete, 0.200m cast-in-situ concrete, damp-proofing membrane layer, 0.071m rigid insulation, and 0.150m site-hardcore.

For thermal protection purpose, the exterior walls are extended to the bottom of the floor, which is 0.4785m deep measured from the ground level.

Foundation walls:

Below the exterior walls, there are 3 ft (0.914 m) depth foundation walls, which are selected as "Basic Wall: Foundation - 300mm Concrete." As its name implies, the walls are constructed by 0.300m-thick cast-in-situ concrete. The thermal resistance of the concrete is 0.2868 m^2-K/W.

Roofs:

There are two roofs in the building: the upper level roof, which covers the lobby area, and the lower level roof, which covers other areas of the building. The two roofs

have a 2 ft (0.610 m) extension from the outside surface of the exterior walls. The roofs have the same roof type—"Basic Roof: Warm Roof - Concrete." The *U*-value of this roof type is 0.5861 W/m^2-K, which does not meet the climate zone 5's requirement (maximum 0.273 W/m^2-K for insulation entirely above deck roofs). The concrete thickness is 0.225m but is expected to be 0.250m for a TABS-equipped building.

Two modifications are made: the cast-in-situ concrete layer is changed from 0.175m to 0.200m; and the rigid insulation layer is thickened from 0.050m to 0.118m.

Now the *U*-value of the new roof type becomes 0.2723 W/m^2-K (corresponding *R*-value is 3.6731 m^2-K/W). The new roof type is renamed as "Basic Roof: Warm Roof – Concrete 250mm." It consists: 0.038m tile roofing, 0.118m rigid insulation, 0.020m asphalt-bitumen, roofing felt membrane layer, 0.050m sand/cement screed concrete, and 0.200m cast-in-situ concrete.

Interior walls:

The type of the interior walls is selected as "Basic Wall: Interior – Blockwork 190," which is made of 0.190m concrete masonry units with 0.012m gypsum wall board on both sides.

Doors:

There are two exterior doors (south and east) and five interior doors in the building. All the doors are selected as "M_Single-Flush 0915 × 2134 mm," whose *U*-value is 3.7021 W/m^2-K (zone 5's requirement is maximum *U*-3.975 for swinging opaque doors).

Windows:

In the office zone, there are four exterior windows (three in the north wall and one in the east wall). All the windows are the type "M_Fixed 2134 × 1524 mm 2," which is modified from the basic "M_Fixed" window type. The glazed panels are "Double glazing - 1/4 in thick - clear/low-E (e = 0.05) glass," whose *U*-value is 1.9873 W/m^2-K (zone 5's requirement is maximum *U*-1.99 for all nonmetal framing vertical glazing), solar heat gain coefficient is 0.26, and visual light transmittance is 0.42.

Curtain walls:

In Revit, no detailed thermal properties of the curtain wall type are presented. According to Ref. [*6.9*], "A standard clear insulated double glazing unit has a *U*-factor of 2.76 W/m^2-K at center-of-glass. When the edge-of-glass and frame are taken into account, the overall *U*-factor will become even higher." Comparing to other building components, curtain wall has a much higher *U*-value, which may "lead to a number of potential problems, such as high-energy consumption, thermal discomfort to occupant in the perimeter zones, and condensation risk." [*6.9*] However, "the typically large continuous span of glazing in curtain walls can provide occupants with pleasant view, contact with outdoors and natural lighting." [*6.9*] Many architects prefer large glazing in their designs. In the design of the homeostatic building, the zone 5's requirement of metal framing curtain wall is met: *U*-2.56 W/m^2-K (corresponding *R*-value is 0.391 m^2-K/W). The glazed panels of the curtain walls are selected as "Low-E double glazing SC = 0.3" glass, whose *U*-value is 2.1030 W/m^2-K (corresponding *R*-value is 0.4755 m^2-K/W), solar heat gain coefficient is 0.31, and visual light transmittance is 0.57.

Under the lower level roof, the length of the east-facing curtain wall is 3.048 m and the length of the south-facing curtain wall is 7.925 m; under the upper level roof, the south-facing curtain wall is 7.315 m and the west-facing curtain wall is 6.096 m. Therefore, including the windows and the curtain walls, the total WWR is 45.1% (27.7% east, 89.2% south, 38.5% west and 18.9% north).

Roof support column:

Because the curtain walls cannot support the roofs, five roof support columns are added between the foundation and the roofs: four columns supporting the upper level roof are at the corners of the roof and one column supporting the lower level roof is at the southeast corner of the building. The columns are selected as "M_Rectangular Column 610 × 610 mm" and the material is sand/cement screed concrete.

Some thermal and physical properties of the materials used in the small commercial

building are summarized in Table 6.2.

Table 6.2. Thermal properties of materials in the small commercial building

Category	Material	Thermal conductivity k (W/m-K)	Specific heat c_p (kJ/kg-K)	Density ρ (kg/m^3)
Brick	Common brick	0.540	0.840	1550
Concrete	Concrete masonry units	1.300	0.840	1800
	Sand/cement screed concrete	1.046	0.657	2300
	Cast-in-situ concrete	1.046	0.657	2300
Insulation	Rigid insulation	0.035	1.470	23
Membrane	Vapour retarder	0.167	1.674	1500
	Damp-proofing	1.150	0.840	2330
	Roofing felt	0.500	1.000	1700
Curtain wall		0.391	—	—
Miscellaneous	Gypsum wall board	0.650	0.840	1100
	Carpet	0.060	1.360	190
	Tile roofing	0.840	0.800	1900
	Asphalt-bitumen	1.150	0.840	2330
	Cavity fill	0.058	0.840	350
	Air	0.025	0.001	1.2
	Site-hardcore	No thermal properties are presented in Revit.		

6.2.3 Modeling

The small commercial building is modeled by the RC method in Matlab and Matlab/Simulink, as shown in Fig. 6.6. In the figure, the building envelope (including the roofs, the exterior walls, the windows, the curtain walls and the doors) is connected to the outdoor and indoor air with surface thermal resistors; the floor is connected to the indoor air and the earth; inside of the building, there are internal walls and other interior thermal mass (assumed as wood with dimensions of 0.1m×floor area); the indoor air is considered as a small capacitor; the internal heat gain is put into the indoor air directly; solar energy gain is calculated according to the solar geometry in July 15 in Paso Robles, and its distribution is 80% on the floor surface and 20% on the upward surface of other interior thermal mass; the outdoor air mean temperature is 23 °C with the peak-to-peak amplitude of 22 K; the simulation time step is still 60 seconds.

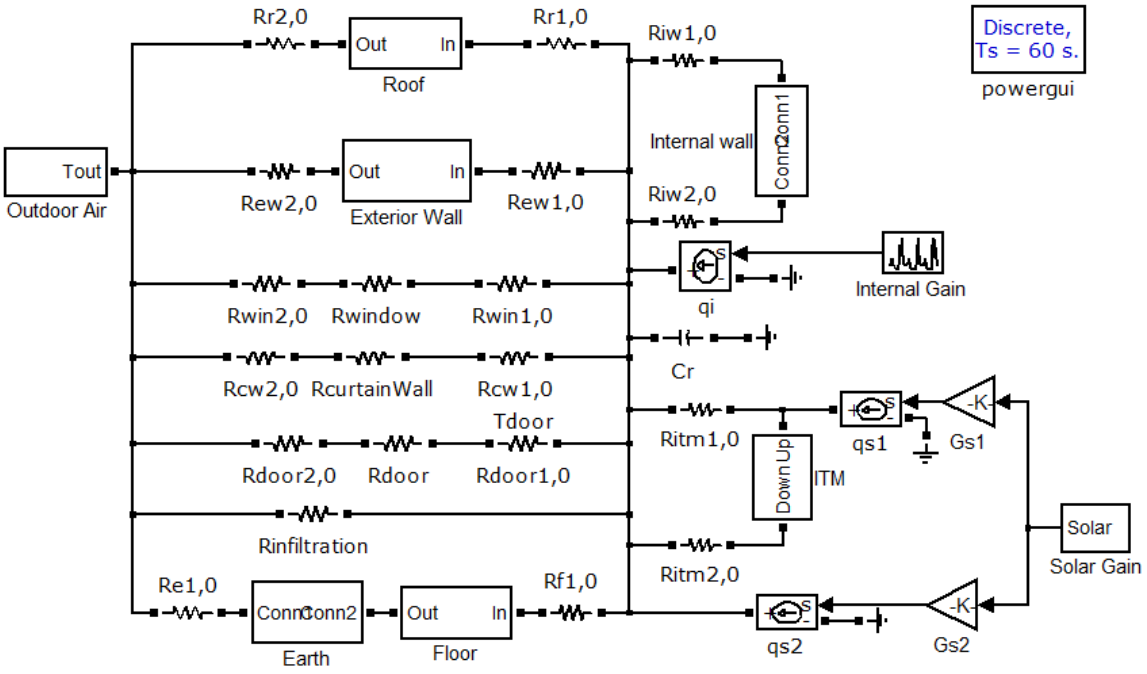

Fig. 6.6. Model of the homeostatic small commercial building in Simulink

As assumed in previous chapters, all the windows and curtain walls have good shading devices and only 8% of solar energy goes into the building. Then the operative temperature variation of the building is only 1.56 K (the mean value is 28.71 °C). Even there are no shading devices, the operative temperature variation just increase to 2.59 K (the mean value increases to 34.92 °C). With good shading devices, the outdoor air temperature amplitude can be increased to 30 K, if the operative temperature variation is kept in 2 K. Therefore, the designed small commercial building is a perfect partially homeostatic building.

6.2.4 Final drawing

The final floor plan of the small commercial building is shown in Fig. 6.7. Different views of the building are shown in Fig. 6.8.

Fig. 6.7. Floor plan of the homeostatic small commercial building

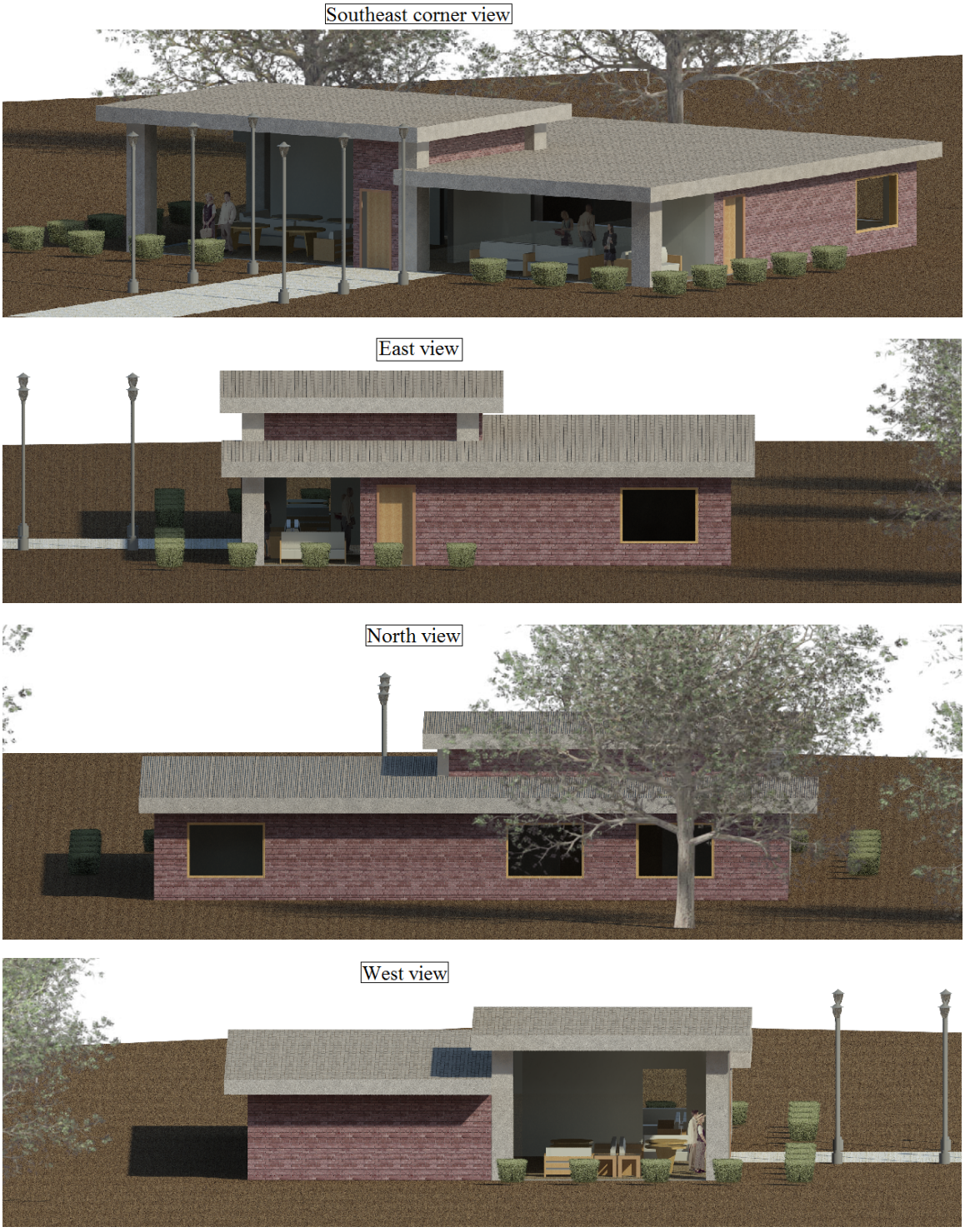

Fig. 6.8. Different views of the homeostatic small commercial building

6.3 Chapter summary

Because of its special geographical condition, Paso Robles has large diurnal temperature variations (as much as 28 K) in summer time, which makes it one of the most favorable locations of using cooling tower for homeostatic buildings. This chapter designs a stand-alone, one-story, south-facing small commercial homeostatic building in Paso Robles in the AutoCAD Revit 2013. The building has a front zone (a large lobby, a waiting room, a reception room and two restrooms) and an office zone (three offices). In the front zone, large curtain walls are used as part of the building envelope. Therefore, the building has a high window-to-wall ratio (WWR) of 45.1% (27.7% east, 89.2% south, 38.5% west and 18.9% north) and people outside of the building can see most of the front zone through the curtain walls. Later, a resistor-capacitor model of the building is built in Matlab and Matlab/Simulink. Simulation shows that even with such a high WWR, the operative temperature variation of the building is only 1.56 K under typical weather conditions, which means that the designed small commercial building is a good partially homeostatic building.

Reference

[6.1] See: http://en.wikipedia.org/wiki/Paso_Robles,_California (Last access on May 11, 2013)

[6.2] See: http://www.prcity.com (Last access on May 11, 2013)

[6.3] See: http://www.pasowine.com/pasorobles (Last access on May 11, 2013)

[6.4] U.S. Geological Survey and the California State Water Resources Control Board, *Groundwater Quality in the Monterey Bay and Salinas Valley Groundwater Basins, California*, Fact Sheet 2011–3089, July 2011

[6.5] P.S. Honaganahalli, J.N. Seiber, "Measured and predicted airshed concentrations of methyl bromide in an agricultural valley and applications to exposure assessment," *Atmospheric Environment* **34 (21)** (2000) 3511-3523

[6.6] See: http://www.weather.com/weather/climatology/monthly/USCA0842 (Last access on May 11, 2013)

[6.7] See: http://www.wrcc.dri.edu/cgi-bin/cliMAIN.pl?ca6730 (Last access on May 11, 2013)

[6.8] See: http://www.wrcc.dri.edu/cgi-bin/cliMAIN.pl?ca6742 (Last access on May 11, 2013)

[6.9] Hua Ge, *Study on overall thermal performance of metal curtain walls*, PhD thesis, Concordia University, October 2002

Chapter 7: Conclusions and Recommendations

The ASHRAE's heat balance design philosophy of buildings is *engineering building's indoor air to be at a fixed temperature*. This dissertation proposed a new process design philosophy called the Thermal Homeostasis in Buildings (THiB). The design of homeostatic buildings is approached in two steps: *archi.engineering building's indoor air-mass partially homeostatic to be within an acceptable temperature range* without equipment, and *maintaining the building fully homeostatic to be at a comfortable temperature level* with low-power equipment or off-peak mechanical equipment.

Main conclusions are summarized as follows:

(1) By employing hydronic radiant conditioning systems, thermally homeostatic buildings have lower energy consumption, higher indoor air quality, more comfortable internal environment, lower initial cost and much lower life-cycle cost;

(2) Using an RC (resistor-capacitor) model built in Matlab and Simulink, the time-dependent temperatures of the indoor air and the surfaces of each element in a building can be calculated;

(3) The ASHRAE's heat balance design model is replaced by the process design model of the systematic study of building's structural thermal mass requirement;

(4) With adequate thermal mass, both interior and exterior, the indoor temperature of a homeostatic building can be kept within a small range;

(5) An optimal slab thickness for interior thermal mass is found, which is the same as that for hydronically activated TABS application in the present passive application;

(6) In the case of large diurnal temperature variation or large window-to-wall ratio, a recommended thermal mass for exterior envelope is given;

(7) In summer time by harnessing natural energy gradient with cooling tower, the

indoor temperature can be maintained at a comfortable level in locations with large diurnal temperature variation;

(8) By identifying the strong micro-climatic process of sea breeze as the driven force of the large diurnal temperature variation, it proposes that the meso-scale climatic process can be a new kind of renewable resources alongside wind and the sun;

(9) Large fenestration that higher than 40% is permitted in homeostatic buildings for aesthetics, natural lighting and solar gain;

(10) A stand-alone small commercial building located in Paso Robles is designed to meet the partially homeostatic criteria in the AutoCAD Revit 2013, which is confirmed by simulation to be partially homeostatic even with a large window-to-wall ratio of 45.1%.

Proposed innovations in this dissertation are in the following:

(1) A dynamic definition of envelope: Partial homeostasis depends on the combined use of internal (TABS) mass' thermal capacity and of envelope's heat transfer property that is based on both the resistance (+ air tightness) and the thermal mass of the envelope. While envelope resistance requirement is predominantly a function of design peak hourly temperature according to standard design guide's recommendation, envelope thermal mass requirement is a parametric function of design diurnal temperature amplitude with parameter window-to-wall ratio;

(2) A different kind of renewable "energy": "Natural cooling" (homeostasis in summer) of a partially homeostatic building is facilitated by large diurnal temperature variation that, for instance, prevails in Sacramento, CA, which is derived from strong sea breeze process a building can harness. This is an example of a renewable thermal resource in the present case, which is different from sea breeze being a renewable dynamical power resource for wind farms;

(3) A new paradigm of man-made thing—the true meaning of organic architecture: Machines are man-made things whereas living organisms are natural things. One of

features that demarcates living things from machines is “homeostasis,” which, however, is a feature within the realm of man-made things. This dissertation articulates the creation of homeostatic systems of TABS-based building as a historical opportunity in making a difference in contributing to a sustainable future.

Some suggestions of future work are:

(1) Investigate the heating operation of thermally homeostatic buildings;

(2) Add the dedicated outdoor air systems for air-quality and moisture controlling;

(3) Investigate the possibility of using heating and cooling panels in building retrofitting to achieve thermal homeostasis;

(4) Build a homeostatic building in Paso Robles for testing and measuring to validate the proposed design philosophy.

Appendix

Appendix A

Detailed drawings of the designed homeostatic building in Paso Robles

Homeostatic Building in Paso Robles

Southwest corner view

Southeast corner view

TABLE OF CONTENTS

Stony Brook University

www.stonybrook.edu

No.	Description	Date

Homeostatic Building in Paso Robles

Coversheet

Project number	SBUME2013.05
Date	May 20, 2013
Drawn by	P. Ma
Checked by	L.-S. Wang

G101

Scale

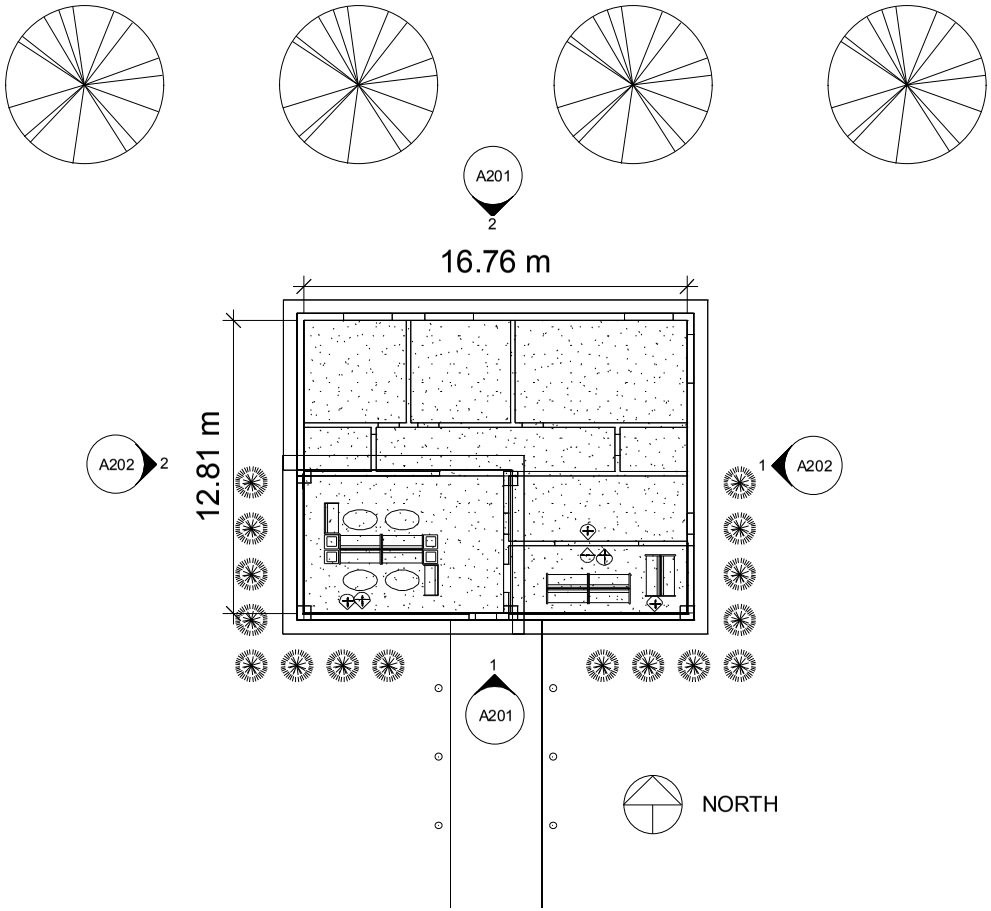

1 Site

1 : 200

Stony Brook University

www.stonybrook.edu

No.	Description	Date

Homeostatic Building in Paso Robles

Site Plan

Project number	SBUME2013.05
Date	May 20, 2013
Drawn by	P. Ma
Checked by	L.-S. Wang

AS101

Scale 1 : 200

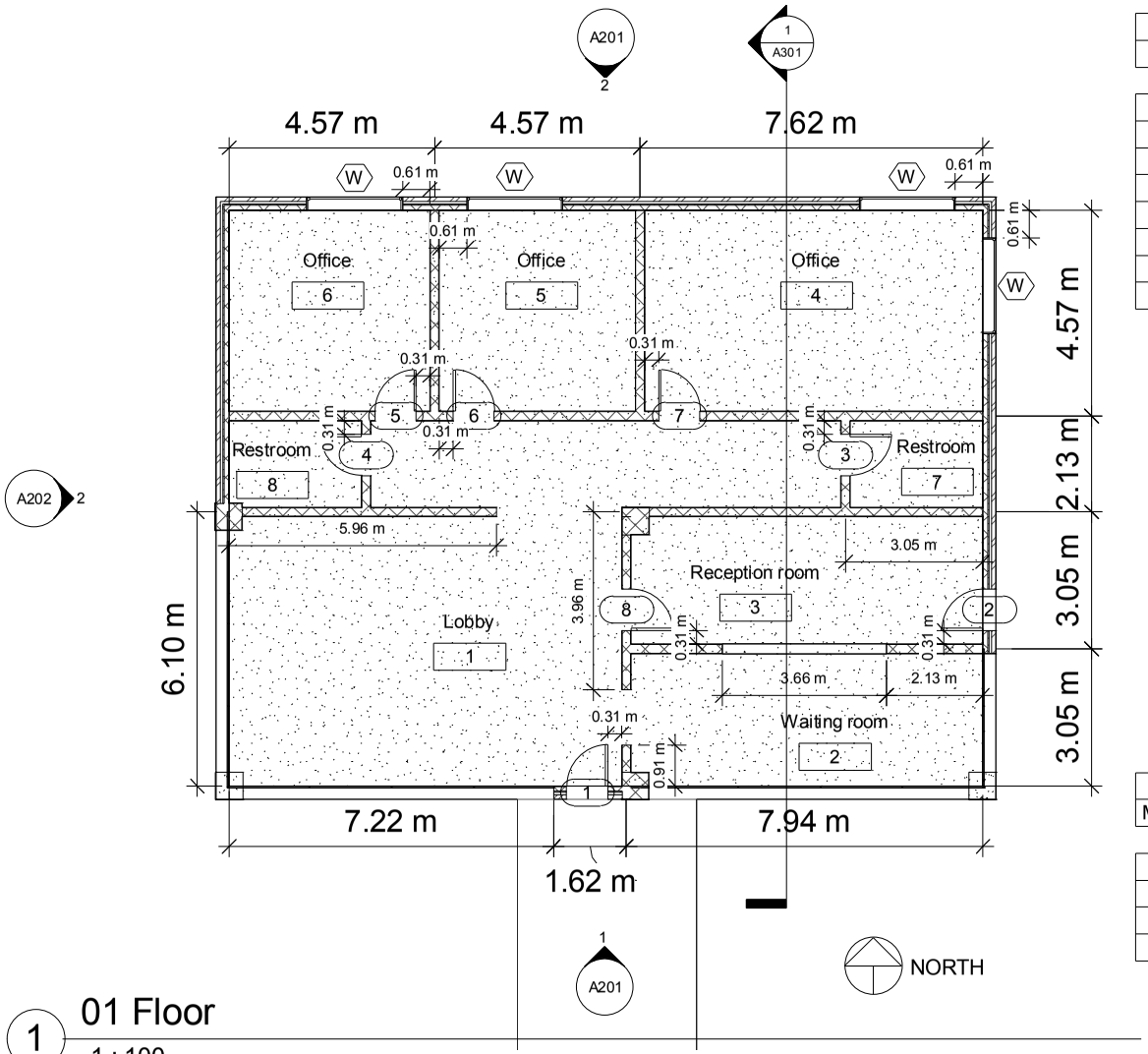

1 01 Floor

1 : 100

Door Schedule		
Mark	Family and Type	Thermal Resistance (R)
1	M_Single-Flush: 0915 x 2134mm	0.2701 (m²·K)/W
2	M_Single-Flush: 0915 x 2134mm	0.2701 (m²·K)/W
5	M_Single-Flush: 0915 x 2134mm	0.2701 (m²·K)/W
4	M_Single-Flush: 0915 x 2134mm	0.2701 (m²·K)/W
3	M_Single-Flush: 0915 x 2134mm	0.2701 (m²·K)/W
6	M_Single-Flush: 0915 x 2134mm	0.2701 (m²·K)/W
7	M_Single-Flush: 0915 x 2134mm	0.2701 (m²·K)/W
8	M_Single-Flush: 0915 x 2134mm	0.2701 (m²·K)/W

Room Schedule		
Number	Name	Area
1	Lobby	72.91 m²
2	Waiting room	22.91 m²
3	Reception room	21.99 m²
4	Office	33.55 m²
5	Office	19.46 m²
6	Office	19.94 m²
7	Restroom	5.65 m²
8	Restroom	5.62 m²

Window Schedule			
Mark	Family and Type	Thermal Resistance (R)	SHGC
1	M_Fixed: 2134 x 1524mm 2	0.5032 (m²·K)/W	0.26
2	M_Fixed: 2134 x 1524mm 2	0.5032 (m²·K)/W	0.26
3	M_Fixed: 2134 x 1524mm 2	0.5032 (m²·K)/W	0.26
4	M_Fixed: 2134 x 1524mm 2	0.5032 (m²·K)/W	0.26

Stony Brook University

www.stonybrook.edu

No.	Description	Date

Homeostatic Building in Paso Robles

Floor Plan

Project number	SBUME2013.05
Date	May 20, 2013
Drawn by	P. Ma
Checked by	L.-S. Wang

A101

Scale 1 : 100

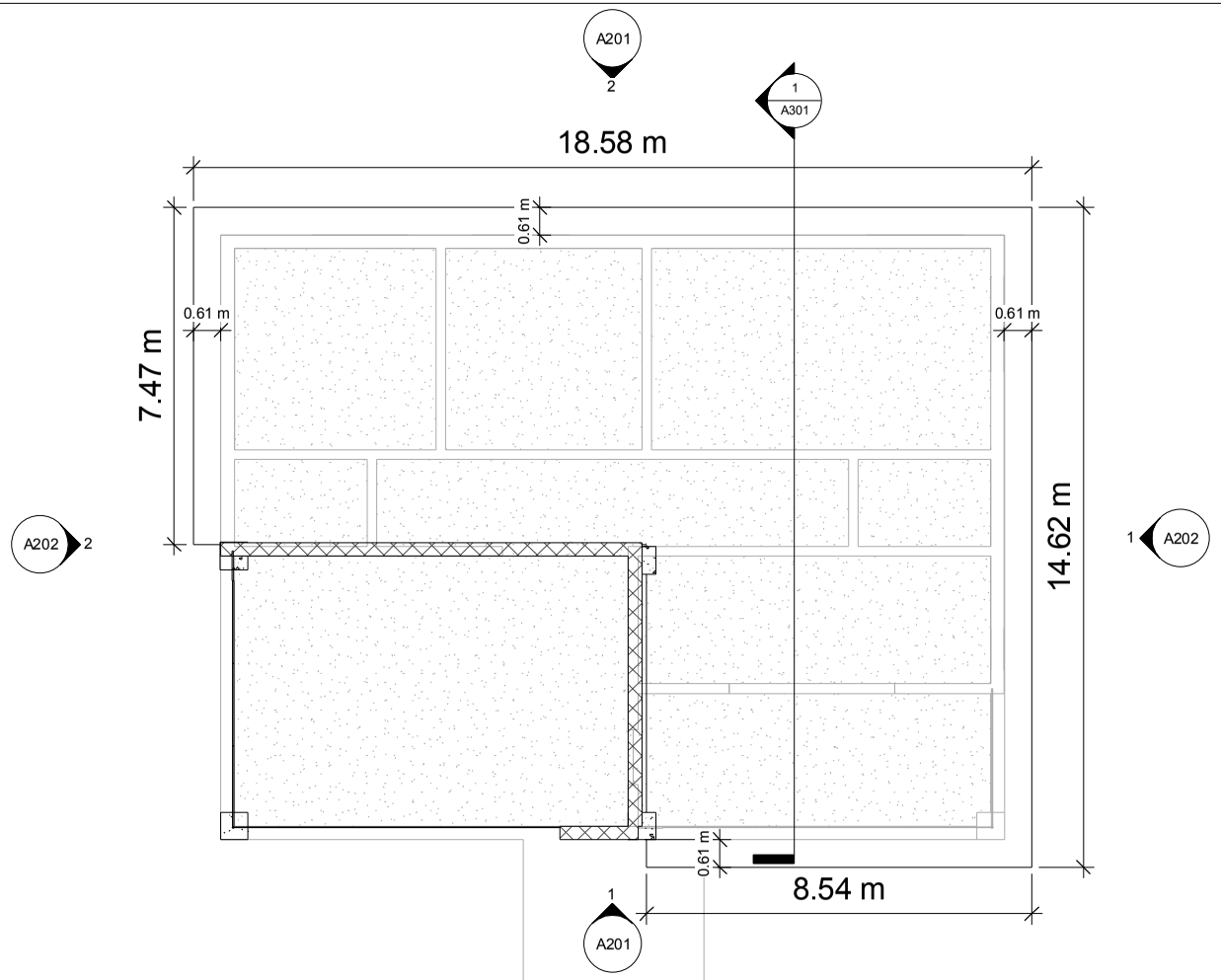

1 02 Lower roof

1 : 100

Stony Brook University

www.stonybrook.edu

No.	Description	Date

Homeostatic Building in Paso Robles

Lower Roof Plan

Project number	SBUME2013.05
Date	May 20, 2013
Drawn by	P. Ma
Checked by	L.-S. Wang

A102

Scale 1 : 100

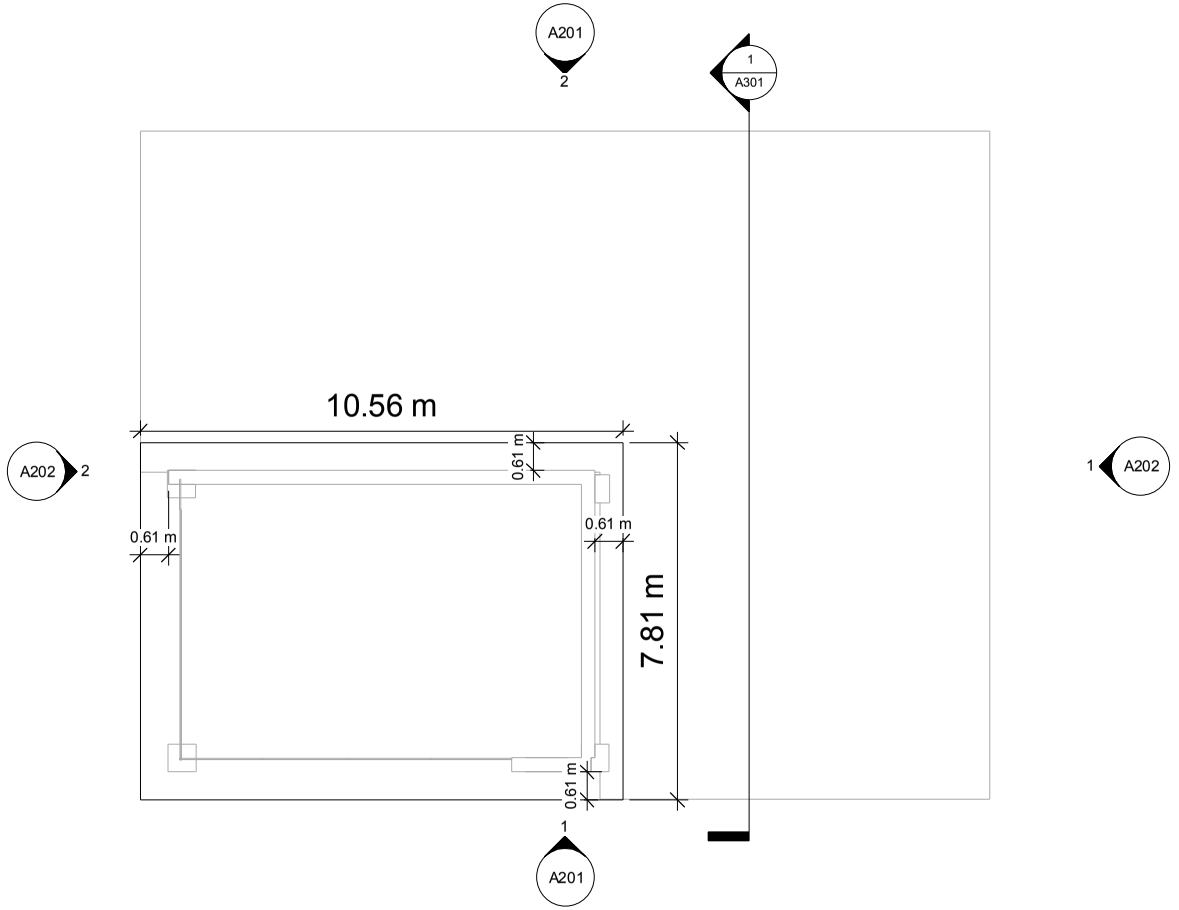

1 03 Upper roof

1 : 100

Stony Brook University

www.stonybrook.edu

No.	Description	Date

Homeostatic Building in Paso Robles

Upper Roof Plan

Project number	SBUME2013.05
Date	May 20, 2013
Drawn by	P. Ma
Checked by	L.-S. Wang

A103

Scale 1 : 100

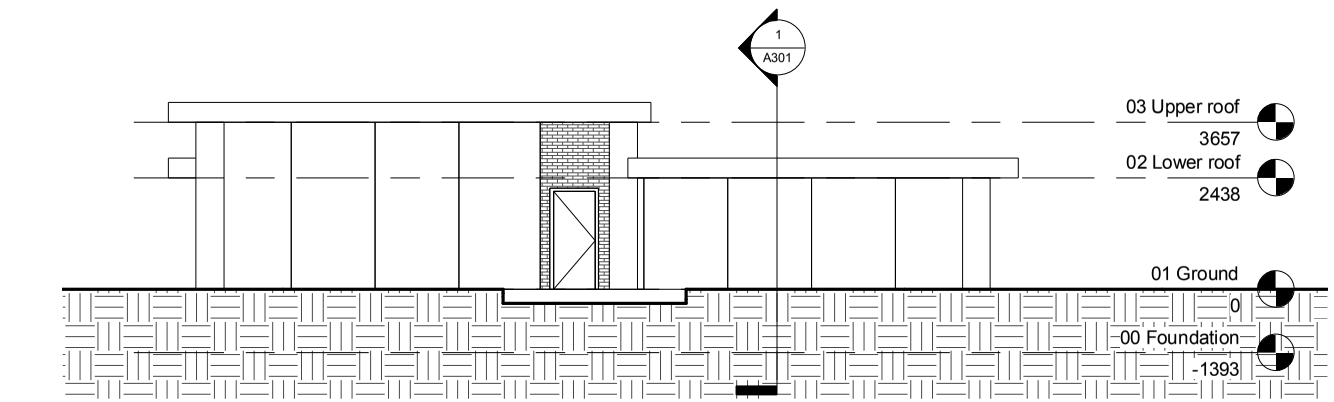

1 South

1 : 100

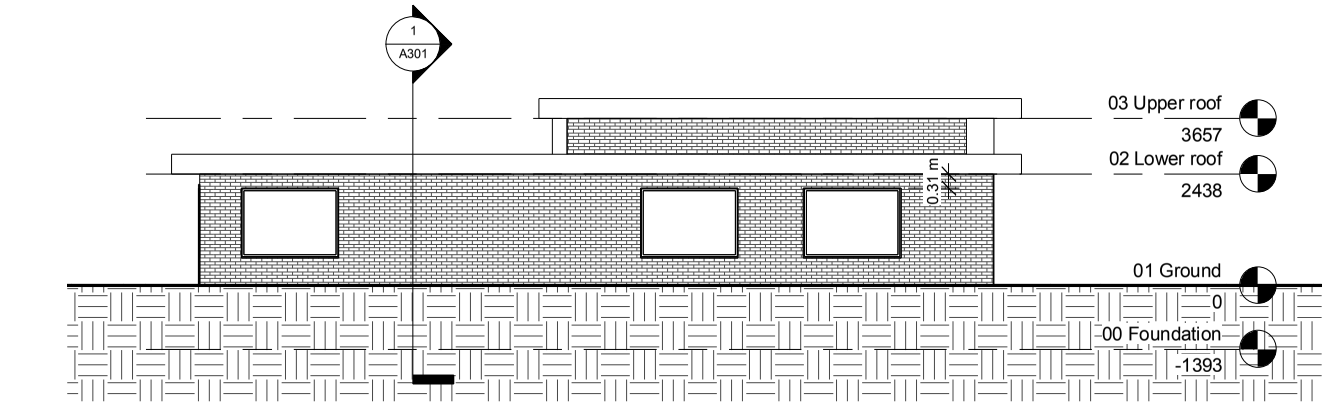

2 North

1 : 100

Stony Brook University				
www.stonybrook.edu				

No.	Description	Date

Homeostatic Building in Paso Robles

South & North Elevation

Project number	SBUME2013.05
Date	May 20, 2013
Drawn by	P. Ma
Checked by	L.-S. Wang

A201

Scale 1 : 100

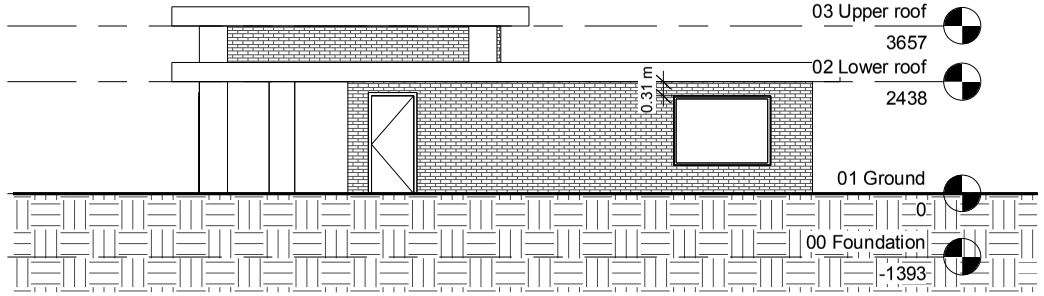

1 East

1 : 100

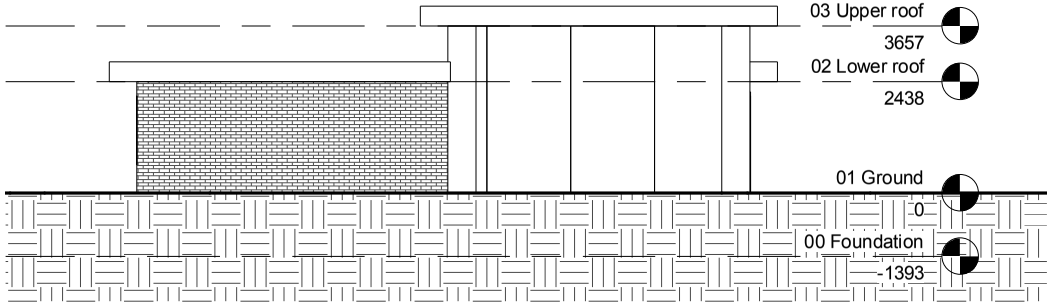

2 West

1 : 100

Stony Brook University

www.stonybrook.edu

No.	Description	Date

Homeostatic Building in Paso Robles

East & West Elevation

Project number	SBUME2013.05
Date	May 20, 2013
Drawn by	P. Ma
Checked by	L.-S. Wang

A202

Scale 1 : 100

Basic Roof:
Warm Roof -
Concrete 250mm

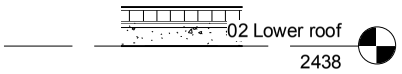

7 Roof
1 : 50

Basic Wall:
Interior -
Blockwork 190

6 Internal wall
1 : 50

Basic Wall:
CW 102-85-100p

2 External wall
1 : 50

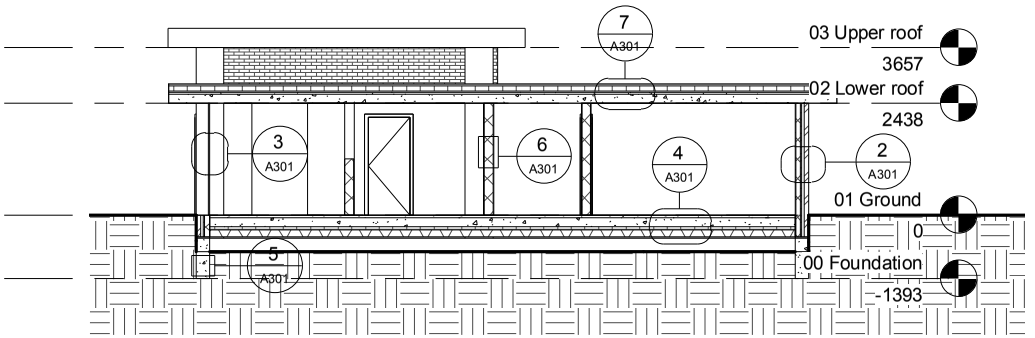

1 Building section
1 : 100

Curtain Wall with "Low-E double glazing SC=0.3" glass
M_Rectangular Column 610 x 610 mm

3 Curtain wall and Roof support column
1 : 50

Basic Wall:
Foundation -
300mm Concrete

5 Foundation wall
1 : 50

Floor:
Concrete Domestic 478.5mm 2

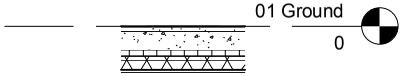

4 Floor
1 : 50

Stony Brook University

www.stonybrook.edu

No.	Description	Date

Homeostatic Building in Paso Robles

Building Section

Project number	SBUME2013.05
Date	May 20, 2013
Drawn by	Author
Checked by	Checker
Scale	As indicated

A301

1 Winter Solstice

Stony Brook University					
www.stonybrook.edu					

No.	Description	Date

Homeostatic Building in Paso Robles	Winter Solstice	
	Project number SBUME2013.05	A401
	Date May 20, 2013	
	Drawn by Author	
	Checked by Checker	Scale

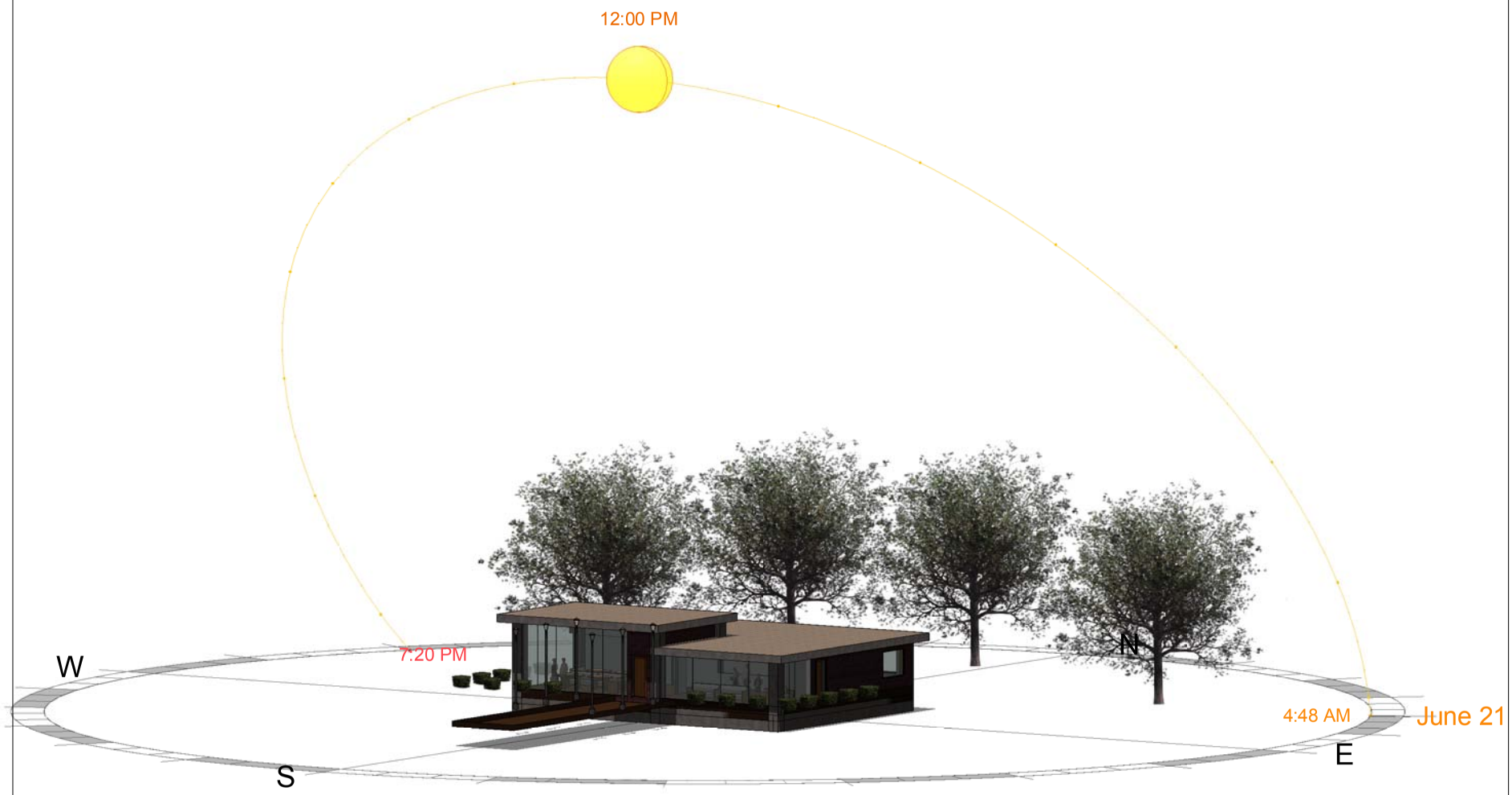

1 Summer Solstice

Stony Brook University

www.stonybrook.edu

No.	Description	Date

Homeostatic Building in Paso Robles

Summer Solstice

Project number	SBUME2013.05
Date	May 20, 2013
Drawn by	P. Ma
Checked by	L.-S. Wang

A402

Scale